POWER DISTRIBUTION SYSTEM PROTECTION METHODOLOGIES WITH INVERTER-BASED RESOURCES INTEGRATED MICROGRIDS

by

Bilkis Banu

A dissertation submitted to the faculty of
The University of North Carolina at Charlotte
in partial fulfillment of the requirements
for the degree of Doctor of Philosophy in
Electrical Engineering

Charlotte

2022

Approved by:

_____
Dr. Sukumar Kamalasadan

_____
Dr. Michael Smith

_____
Dr. Valentina Cecchi

_____
Dr. Churlzu Lim

ABSTRACT

BILKIS BANU. Power Distribution System Protection Methodologies With Inverter-Based Resources Integrated Microgrids. (Under the direction of DR. SUKUMAR KAMALASADAN and DR. MICHAEL SMITH)

This work presents new protection methods for addressing challenges related to integrating a fully inverter-based generation resource microgrid into the power distribution system. Renewable-energy-sourced microgrids offer promise in providing sustainable energy solutions to meet energy needs. Most of the widely used renewable resources and energy storage systems are interfaced with the power grid through power electronic devices, such as inverters. Diverse expertise is required for the design, construction, and operation of an inverter-based microgrid (IBMG). First, this dissertation provides a comprehensive overview of IBMG characteristics and highlights key obstacles in the design of these systems. The difference between the response of inverter-based resources and synchronous machine-based resources and the dependency of inverter response on its control modes are discussed. Second, a method for distribution system short circuit study considering inverter-based distributed generation is designed. Third, an Electromagnetic Transient (EMT) based inverter modeling for grid following and grid forming mode for both balanced and unbalanced distribution systems is proposed. Fourth, a method is proposed for controlling transient overvoltage in a microgrid-integrated power distribution system. Finally, a new protection method for detecting faults in an IBMG system helps to address the well-known issue of microgrid protection sensitivity and selectivity. The effectiveness of the overall framework is tested with small test systems and large IEEE test systems with relevant data sets. The studies show that the proposed approaches can improve the IBMG system design and increase the reliability of such systems.

ACKNOWLEDGEMENTS

TABLE OF CONTENTS

LIST OF TABLES

LIST OF FIGURES

LIST OF ABBREVIATIONS

C&I Commercial and Industrial.

CCI Current-controlled Inverter.

CT   Current Transformer.

DDSRF-PLL Decoupled Double Synchronous-Reference Frame PLL.

DER Distributed Energy Resource.

DOE Department of Energy.

DSOGI-PLL Dual Second-Order Generalized Integrator PLL.

EI   Electrical Inertia.

EMT Electromagnetic Transient.

EMTP Electromagnetic Transients Program.

FPNSC Flexible Positive and Negative Sequence Control.

GC   grid following.

GF   Grid Forming.

GFI Grid Forming Inverter.

GFOV Ground Fault Overvoltage.

HIL   Hardware-in-the-Loop.

IBMG Inverter-Based Microgrid.

IBR Inverter-Based Resource.

IDG Inverter-Based Distributed Generation.

IEEE Institute of Electrical and Electronics Engineers.

IIDG Inverter-Interfaced Distributed Generator.

LL   Line-to-Line.

LLG   Line-to-Line-to-Ground.

LLL   Line-to-Line-to-Line.

LLLG Line-to-Line-to-Line-to-Ground.

LROV Load Rejection Overvoltage.

MG   Microgrid.

MV   Medium Voltage.

OC   Over Current.

PCC   Point of Common Coupling.

PD   Protection Device.

PI   Proportional-Integral.

PLL   Phase-Locked Loop.

PPA   Power Purchase Agreement.

PR   Proportional-Resonant.

PT   Potential Transformer.

PV   Solar Photovoltaic.

SG   Synchronous Generator.

SLG   Single-Line-to-Ground.

SPIDERS Smart Power Infrastructure Demonstration for Energy Reliability and Security.

TOV Transient Overvoltage.

U.S. United States.

USA United States of America.

UV Under-Voltage.

VSC Voltage Source Converter.

VT Voltage Transformer.

CHAPTER 1: INTRODUCTION

Conventional generation sources (e.g., fossil fuels) are currently being phased out and replaced by cleaner energy sources (e.g., low-carbon or zero-emission electricity sources, such as nuclear energy) and more sustainable energy sources (e.g., renewable energy sources, such as solar, wind, hydropower, biomass, and geothermal resources, etc.). Sustainable solutions are needed that enable supply of robust and reliable power, while also satisfying regulations and environmental goals. Towards this target, the distribution system has seen a rapid increase in the penetration of distributed energy resources (DERs), which are typically smaller scale generation sources such as wind and solar that are usually located close to load centers, since they can improve power system reliability and resiliency in those locations. However, compared to synchronous generation, the operational characteristics of these renewable energy inverted-based generation sources requires additional considerations to achieve performance requirements, because of the stochastic behavior of the energy source and the electrical power characteristics of inverted-based generation (e.g., reactive power).

The purpose of the work detailed in this dissertation is to offer new effective methods of addressing the challenges related to integrating a fully inverter-based generation resource microgrid with the power distribution system. A comprehensive overview of inverter-based microgrid (IBMG) design characteristics is provided and key obstacles in the design of these systems are highlighted. This work shows the differences between the response characteristics of inverter-based resources and those of synchronous machine-based resources and emphasizes that the inverter response is dependent on its control modes. A method for controlling transient overvoltage in a microgrid is presented, which is a very important, but often overlooked, consider-

ation in the design of microgrids. This work also presents a new protection method for detecting faults in an IBMG system, which helps to address the well-known issue of microgrid protection sensitivity and selectivity. The effectiveness of the overall framework is tested with small test systems and large Institute of Electrical and Electronics Engineers (IEEE) test systems with relevant data sets and test cases. Test results validate the proposed methods and show that these approaches can improve the IBMG system design and increase the reliability of such systems.

For an introduction to the work, CHAPTER 1 is organized as follows:

- Section 1.1 provides a general introductory overview of microgrids.

- Section 1.2 provides recent trends with microgrids.

- Section 1.3 details common microgrid applications (e.g., Commercial / Industrial, Institutional / Campus, Community, Military, and Overview of Utility Microgrids that are Inverter Only Sourced)

- Section 1.4. discussed the dissertation objectives, key contributions, intellectual merit and broader impact, and the organization of the dissertation.

As detailed in Section 1.4, the rest of the dissertation develops the proposed methods, presents test results to validate the methods, provides discussion regarding the key findings, before concluding and offering areas for future work.

1.1 Microgrid Overview

The most technically advanced distributed energy resource (DER) solution currently on the market is a microgrid, which can meet the electricity demand of a remote community as well as ensure grid reliability and resilience. A microgrid is a group of interconnected loads and distributed energy resources within clearly defined electrical boundaries that functions as a single, controllable entity in relation to the grid, according to the United States (U.S.) Department of Energy (DOE). To

enable it to function in both island mode and grid-connected mode, a microgrid can connect to and disconnect from the grid [8, 9, 10]. Solar photovoltaic (PV) systems, combined heat and power units, advanced batteries, and building load control are among the resources that make up a typical grid combine of DERs in a microgrid cite8416171,8408955. A microgrid controller actively manages these systems and adjusts to changing loads and generation operational characteristics. In most cases, microgrids operate in parallel with the utility grid, but in the event of a power outage, they can operate independently of the main utility grid (island mode). Tolerance for power outages has significantly decreased as society's reliance on technology has increased in all spheres, while the United States' vulnerability to power outages has increased as a result of aging grid infrastructure and cyber and physical threats. Because of this, many customers are more likely to choose a microgrid over other less advanced DER solutions if they can seamlessly disconnect from the utility grid during a power outage. Reduced emissions, less volatile energy costs, and reduced energy costs are additional benefits for customers.

Microgrids are not commonplace in the electric grid and there are many unique variations. They have most often appeared on campuses, in public institutions, and at critical load facilities [11]. Expanding microgrid deployment trends involve; difficult to serve areas of the grid [12], customers with renewable and energy storage resources and communities seeking higher reliability and a measure of self-sufficiency [13, 14]. Figure 1.1 illustrates electrical boundaries of different sizes and types of microgrid's in distribution circuits. Individual customer microgrids are normally behind the meter while utility-owned and government research demonstrations have involved entire MV feeders. There is also a possibility for microgrids to operate with adjustable or dynamic boundaries.

A variety of microgrid implementations and ownership structures exist [15]. The operational states of a microgrid can generally be classified as grid-connected or is-
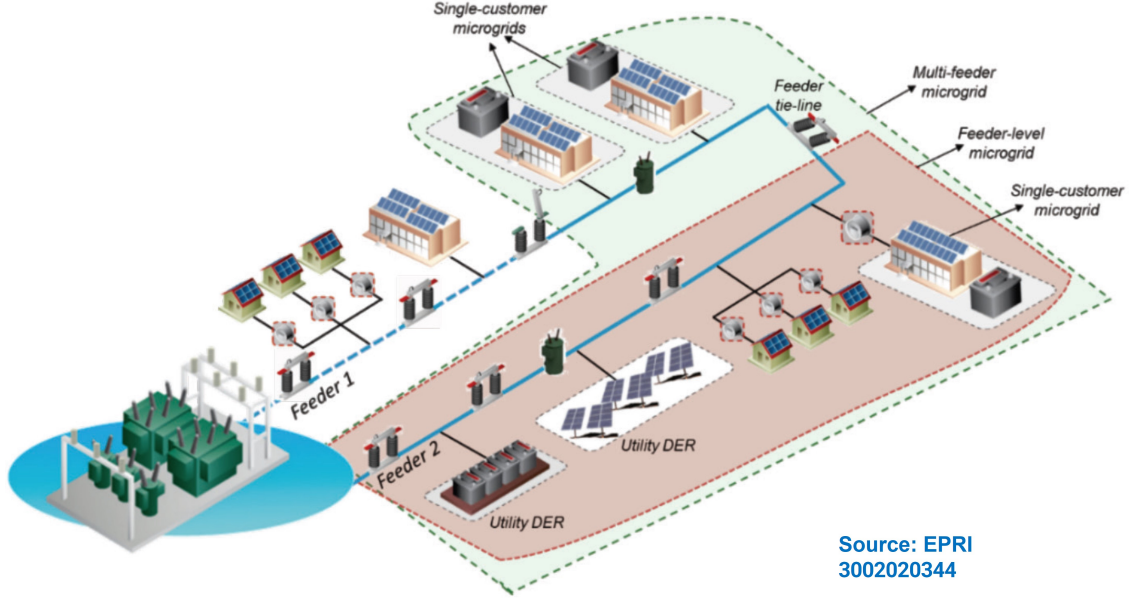
Figure 1.1: Different Types of Microgrids [1].

landed [16]. Microgrids can transition between operating states or cease to energize (shut down), as shown in Figure 1.2. While grid-connected, microgrid DER resources may serve the local load, exchange power with the grid or both. In addition, local load control typically needed for microgrid off grid operation may also be actively used to manage demand when grid following. Transitions between the grid and island states are typically infrequent and only account for a small portion of a microgrid's operational lifetime. They can be accomplished as open transition via protection equipment such as with a break, or as closed transition, without any interruption. These transition options, although simply stated, add a significant degree of complexity to the design, interconnection and operation of microgrids. Transitioning microgrids on and off grid requires specific steps, sequence and timing. These requirements are not well defined in standards, however recently IEEE is taking this particular area in consideration and coming up with more standards. As one example, there are nuances in the criteria for intended compared to unintended microgrid islands. In the following sections, microgrid operation and transition processes are discussed. Gaps in standards related to communication and executing transitions are identified [17]. These

are best clarified using the standard terminology used in defining distributed energy resource interconnections.
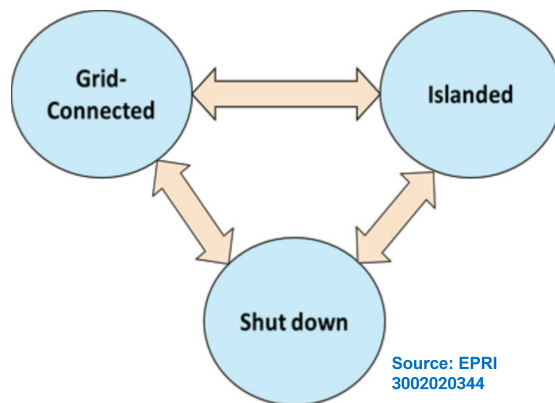
Figure 1.2: Microgrid Operating States [1].

1.2 Microgrid Recent Trends

Microgrids are a worldwide phenomenon, as depicted in Figure 1.3. Everyone is attempting to adopt this wonderful solution to make the power system more timely. With 41.3 percent of the total microgrid revenue, Asia-Pacific will dominate. It is anticipated that North America will hold 32.5 percent of the global market share. By 2024, it is anticipated that total microgrid asset value will account for 164.8 billion dollars in cumulative revenue. According to Navigant Research data, the current base of microgrids in use in the United States prior to 2015 was slightly more than 1,000 MW. A total of 71 microgrids (approximately 592 MW), with an estimated value of 1.7 billion, were installed between January 2015 and June 2016. Figure 1.4, which depicts regional concentrations as well as generation sources, is an illustration of research analysis [2] regarding microgrid deployments in the United States. High utility costs, regulatory incentives, and a greater susceptibility to grid outages are the geographic drivers.

Many of the current state-level programs supporting the adoption of microgrids in several U.S. states are based on increased resilience. Regulators are beginning to broaden their view of the benefits microgrids can provide to society as it becomes
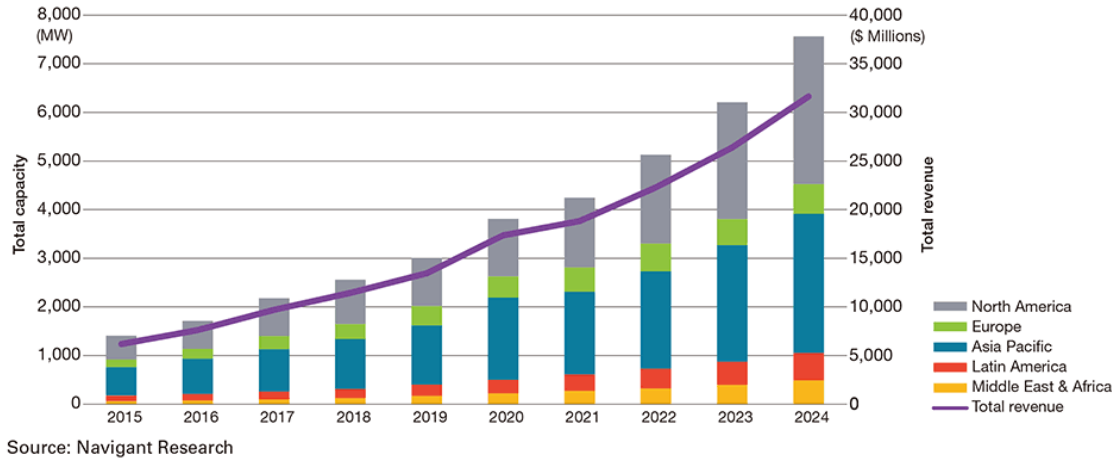
Figure 1.3: Regional Revenue and Microgrid Capacity in World Markets from 2015-2024 [2].

clearer that they are one of a suite of DER solutions that are available to utilities to achieve a variety of goals, including the following, However, resilience was the initial driver for much of the current state-level policy support.

- Supporting distribution operations vulnerable to stability issues stemming from high renewable energy penetration.

- Supplying a non-wires alternative for regions with rising electricity demand.

- Delaying or supporting projects for capital improvements.

1.3 Microgrid Applications

Microgrids have a wide range of customer applications, including providing greener, more reliable energy to universities and commercial industrial sites and powering mission-critical functions in cities and military bases (see Figure 1.5 for additional details [2]).

1.3.1 Commercial and Industrial Microgrid Applications

Customers' reluctance to consider alternatives to conventional backup generation or redundant utility feeds, as well as difficulties in the value proposition related to return
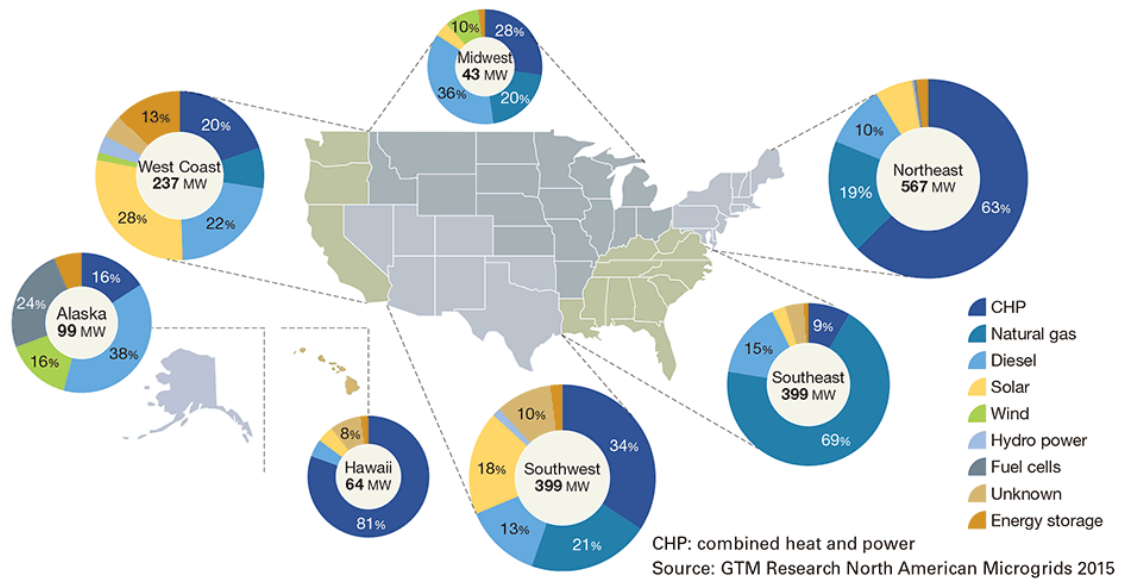
Figure 1.4: USA Microgrid Deployments [2].
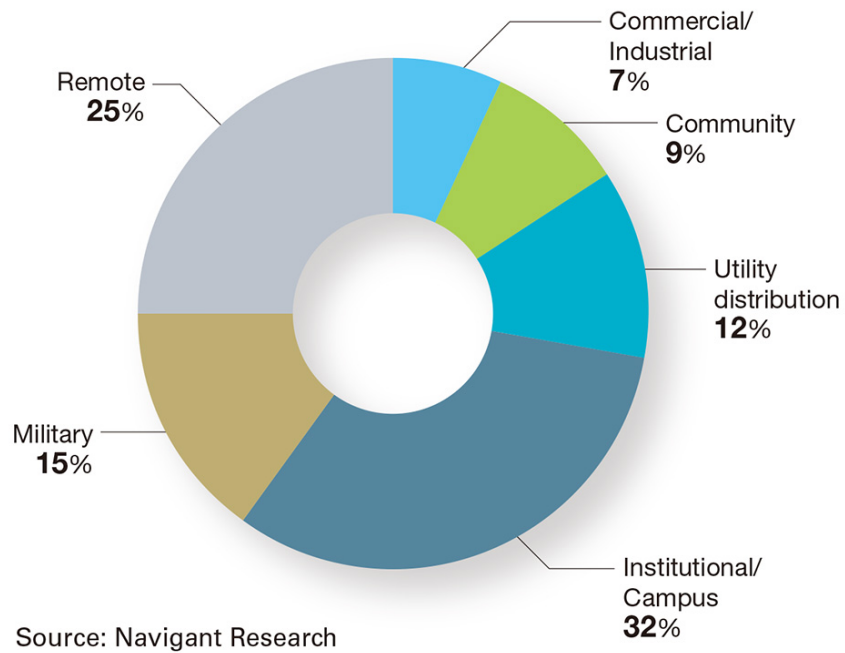
Figure 1.5: Microgrid Applications [2].

on investment, have slowed the commercial and industrial (C&I) segment's growth the most. However, an increase in C&I adoption is being driven by new vendor business models that, through power purchase agreements (PPAs), enable customer adoption without requiring capital expenditure. The fact that backup generators

are dependent on fuel delivery, which can be difficult during major weather events, makes the fact that microgrids can provide an indefinite supply of power during a prolonged grid outage an increasingly important consideration for C&I customers in North America.

1.3.2   Institutional and Campus Microgrid Applications

In terms of annual capacity and revenue from this customer segment, North America ranks highest of all other global regions. In 2015, total capacity was 219.7 MW, and by 2024, it is expected to rise to almost 1.2 GW per year. North American revenue for this segment is expected to reach 4.2 billion U.S. dollars per year by 2024. Due to their large electric and heating loads, college and university campuses are particularly appealing candidates for a microgrid. Additionally, they typically have their own electric and thermal infrastructure and only a few points of interconnection with the utility, making projects technically simpler and less costly. Universities have discovered that many fee-paying parents in the United States place a high value on maintaining power supply during a grid outage. In addition, it is important to take into account the microgrids' ability to support the ambitious sustainability goals that many colleges and universities have set, as well as their use as educational and research platforms. The University of California, San Diego; New York City College; Fairfield College; as well as Princeton University are institutional and campus microgrid examples.

1.3.3   Community Microgrid Applications

Microgrids have become more widely known as a viable option for achieving community resilience objectives thanks to state-sponsored microgrid programs. In the event of a major storm, energy resilience for critical facilities is typically the primary focus of community microgrids. Communities in the eastern United States have been without power for several days at a time as a result of an increase in the magnitude

and frequency of hurricanes and ice storms (see Figure 1.6 and Figure 1.7). Residents have difficulty evacuating from many places. Residents can shelter in place while still having access to essential services like police, fire, medical, pharmacy, shelter, gasoline, and food thanks to microgrids. To guarantee the continuity of essential municipal services, numerous cities are considering microgrids. Compared to community microgrids, which involve multiple participants and off-takers (e.g., hospitals, city hall, fire stations, grocery stores, etc.), a single municipal customer is simpler. From a technical, business model, and financing perspective, these microgrids are the most difficult. However, many state regulators appear determined to eliminate these obstacles. For instance, the New York Prize Program supported the design and feasibility of 83 community microgrids. In June and July 2016, Hitachi delivered feasibility studies to its partner communities and received 12 of these awards. [2]
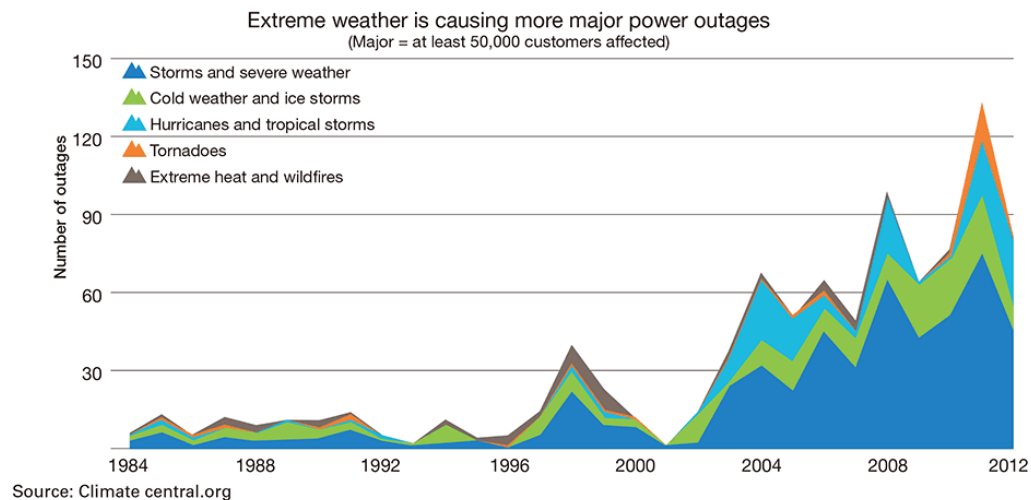
Figure 1.6: Power Outages Caused by Major Weather Events 1994-2012 [2].

1.3.4   Military Microgrid Applications

The Smart Power Infrastructure Demonstration for Energy Reliability and Security (SPIDERS) program initiative is run by the U.S. military. The aim of this program is to use microgrids to supply mission-critical facilities with power in the event of a utility grid failure or attack. The solution's integration of energy storage and solar

Power Outages by Month
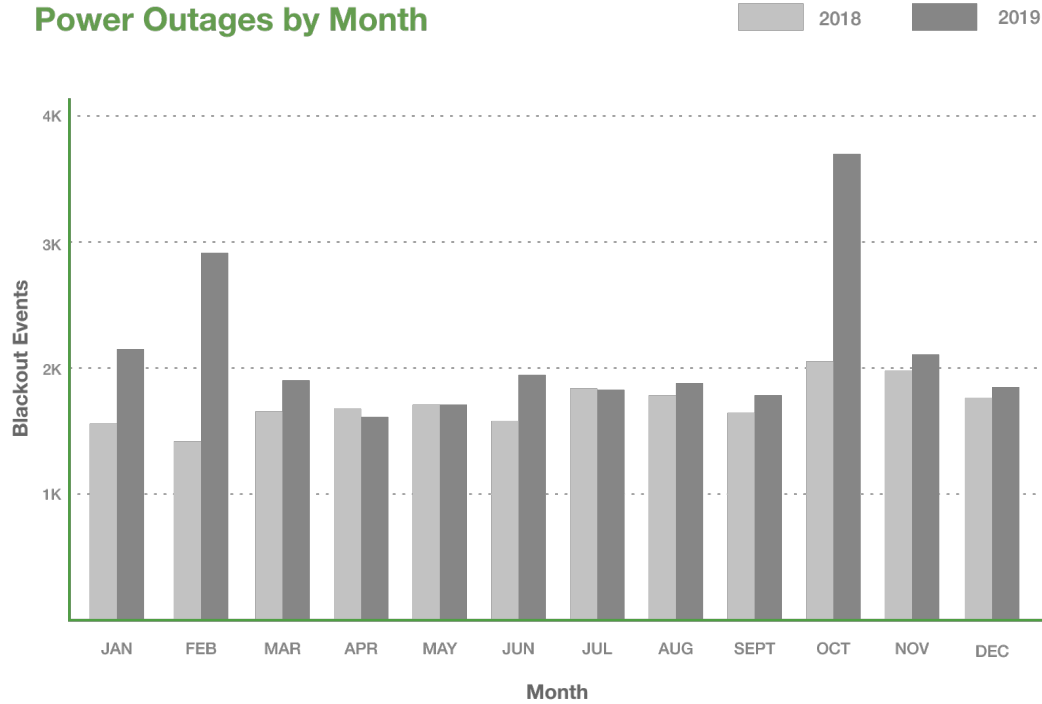
Figure 1.7: Power Outages by month 2018-2019 [3].

PV into the existing diesel backup generators provides a portfolio of diverse fuel sources, allowing for a solution with a longer lifespan and a reduced carbon footprint than conventional backup generators. So far, there have been a few demonstration projects [2].

1.3.5 Utility Microgrid Applications

Microgrids are being investigated by utilities as a potential new revenue stream, an infrastructure and operational resource, and a potential Hitachi customer or rival. Microgrids can assist distribution utilities in addressing a variety of operational objectives and challenges as an infrastructure resource. In order to better serve their current customers, a number of non-regulated utilities have entered the microgrid market. San Diego Gas & Electric's Borrego Springs Microgrid, Duke Energy's Mount Holly Microgrid, National Grid's Potsdam Microgrid, and Hot Springs Microgrid are examples of utility microgrid projects [2].

1.3.6 Overview of Fully Inverter Sourced Microgrids

Based on decades of experience with the physical properties and control responses of large synchronous generators, today's electric power systems are managed for stability. The electric power systems of today are rapidly moving toward having an increasing proportion of generation come from energy storage devices like batteries and nontraditional sources like wind and solar, among others [18]. These newer sources are interconnected throughout the electric grid, both from within the distribution system and directly to the high-voltage transmission system, and they range in size from residential-scale rooftop systems to utility-scale power plants. This is in addition to the variable nature of many renewable generation sources due to the weather-driven nature of their fuel supply. Most importantly for our purposes, power electronic inverters connect many of these new resources to the power system. These resources are collectively referred to as inverter-based resources. Maintaining the grid's dependability and stability is crucial as the electric power system is being transformed by the rapid deployment of renewable technologies [19].
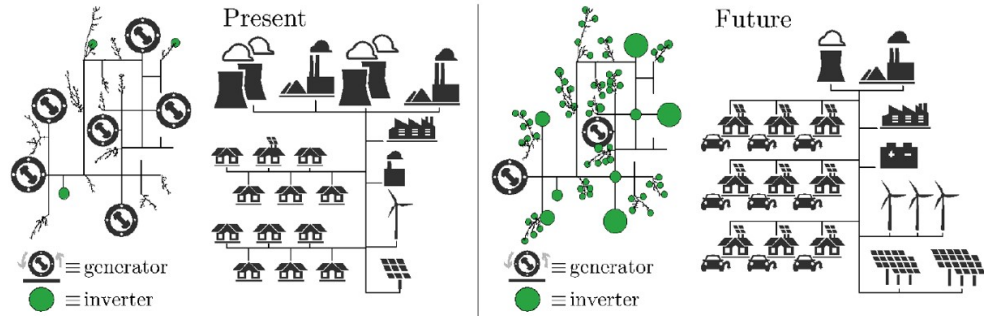
Figure 1.8: Present and Future Power Systems Compared: (left) Historically, synchronous generators with a large rotational inertia have dominated current power systems. (right) Inverter-based generation resources will make up a significant portion of future power systems [4].

The U.S. DOE's grid-forming inverter roadmap [4] acknowledges that inverter-based resources will include both grid-forming resources and other kinds of control, like grid-following resources. Future power systems must operate based on the phys-

ical properties and control responses of numerous inverter-based resources, in addition to those of traditional, large synchronous generators [20] (see Figure 1.8). This makes the transition to a grid with more inverter-based resources extremely challenging. Recognizing that there is no established body of experience for operating hybrid power systems with significant inverter-based resources on the scale of today's North American interconnections is the source of these difficulties.

1.4   Dissertation Objectives, Motivation and Contribution

This section describes the main objectives of this dissertation along with motivation behind the work. It also outlines the main contribution.

1.4.1   Objectives

This research work has the following objectives:

- Study and investigate the challenges of integrating fully inverter-based resource (IBR) sourced microgrids in power distribution system. The challenges are summarized in CHAPTER 3, CHAPTER 5, and CHAPTER 6.

- Implementation of protection devices modeling in electro-magnetic transient (EMT) simulation software PSCAD®. This is discussed in CHAPTER 3.

- Methodologies for performing steady state short circuit studies with inverter-based resources. This is discussed in CHAPTER 4.

- Study the ground fault overvoltage (GFOV) phenomenon in microgrids and develop possible mitigation options with inverter controls. This work is described in CHAPTER 5.

- Study the fault detection challenges in microgrids and develop possible mitigation options through advanced protection algorithms. The results of this work are presented in CHAPTER 6.

- Develop an integrated framework for distribution system connected microgrids that helps mitigate the grid impacts and microgrid design challenges. The results and findings of CHAPTER 5 and CHAPTER 6 help to create the integrated microgrid design framework.

1.4.2   Contributions

The main contribution of this dissertation is to help address the integration challenges of fully inverter-based distribution microgrids as follows.

- Study and evaluation of the methods for performing distribution system short circuit studies with inverter-based resources. The main advantages of the study are: (a) it provides a complete understanding of the distribution system feeder protection philosophy; (b) it implements how protective devices can be modeled in EMT software; (c) it provides theoretical background on how to perform short circuit studies with inverter-based resources using a sequence network, and (d) it highlights the difference between the response characteristics of inverter-based resources and synchronous machine based resources.

- Investigation and evaluation of the control methods and functionalities of IBRs. The main advantages of the study are: (a) it helps to develop an inverter model that closely matches the response of commercially available large inverters; (b) it provides details about inverter controls in the grid following mode; (c) it provides a detailed summary of inverter controls in a grid forming mode, and (d) it also includes a detailed list of inverter onboard protection functionalities.

- Transient overvoltage (TOV) phenomenon is studied for fully inverter-based microgrids and a new method is proposed that can help mitigate TOV in microgrids using inverter controls. The main advantages of the proposed work are: (a) For inverter machine-based microgrids, it provides expressions for phase overvoltage and investigation of the TOV, when the inverters operate in grid

forming mode; (b) it controls inverter negative sequence impedance to mitigate the phase overvoltage and voltage unbalance observed in the microgrid, and (c) it provides a comparison of the overvoltage results for different inverter control modes and transformer configurations.

- A new method for fault detection and protection is proposed for a fully inverter-based distribution microgrid. The main advantages of the proposed work are: (a) it provides a study regarding how the addition of an IDG to a distribution system affects the sensitivity and selectivity of protection devices (PDs) for both grids tied and grid-forming modes of operation of IDGs; (b) it outlines of the challenges associated with overcurrent protection schemes for fully inverter-based resource microgrids, and (c) it proposes new microgrid protection scheme that overcomes the challenges of typical distribution system overcurrent protection for fully inverter sourced distribution microgrids.

1.4.3   Intellectual Merit and Broader Impact

The intellectual merit of the work is highlighted as follows:

- This dissertation provides a comprehensive overview of fully inverter-based distribution microgrids and highlights the integration challenges of such microgrids with the modern power system. This will help in increasing the understanding of such microgrid systems and accelerates it's adaptation.

- The proposed work uses inverter controls to mitigate TOV in fully inverter-based microgrids. The proposed work helps to increase design margins in IBMG designs and provides increased reliability with reduced costs.

- One of the limitations of fully inverter-based microgrids is fault detection and protection because of limited fault current contribution from power electronic-based generating resources. This dissertation proposes a fault detection method

that helps eliminate the limitation of conventional overcurrent-based fault detection used in distribution microgrids.

The broader impact of the research work presented in this work can be summarized as follows:

- This dissertation proposes a methodology of inverter control that does not only applies for microgrids but to other power systems applications where grid-forming inverter technologies are used.

- The proposed method increases the understanding of renewable energy-resourced microgrids and these types of systems will be implemented a lot in the future to increase power system reliability and resiliency.

- This research work will enable more and more renewable energy resources like battery storage and solar to be incorporated into the distribution system.

- The proposed control technique facilitates increased penetration of renewable energy, thus helping to achieve the goal of utilizing cleaner sources of energy to meet our energy needs and reduce emissions to meet environmental goals. Also, any of the societal benefits that can be associated with increased penetration of renewable energy can be attributed to this research as the work performed here helps to enhance the adaptation of renewable energy-based microgrids and helps increase power system reliability and resiliency.

1.4.4   Dissertation Organization

The dissertation chapters are organized as follows:

- CHAPTER 1 provides an introduction to microgrids and various types of microgrids. The objectives, motivation, and contribution of the dissertation are presented in this chapter.

- CHAPTER 2 introduces the challenges associated with integrating fully inverter-based microgrids with power systems.

- CHAPTER 3 discusses the design of conventional distribution system protection and how short circuit studies can be performed with inverter-based resources.

- CHAPTER 4 discusses the control modes and functionality of inverter-based resources.

- CHAPTER 5 presents a new method for mitigating ground fault overvoltage using inverter control.

- CHAPTER 6 introduces the protection challenges of inverter-based microgrids and proposes a new method for detecting fault in inverter-based microgrids.

- CHAPTER 7 discusses the conclusions and offers suggestions for future work.

CHAPTER 2: LITERATURE REVIEW

The definition of a microgrid does not restrict its size or topology. This would indicate that it is difficult to come up with a generalized protection architecture that could economically be used for an arbitrary microgrid of any size [21]. Assuming that most microgrids will evolve from existing distribution feeders, the cost of retrofitting will vary widely depending on the existing protection architecture on the feeders. For example, urban feeders may be easier to retrofit economically than rural ones. The choice of protection architecture will be influenced by the size, type, and interconnection of the DERs supplying a microgrid and will have to adapt to widely varying magnitudes of fault currents during grid-interconnected and grid-isolated modes of operation.

2.1   Chapter Introduction

It is important to make sure that the protection schemes can detect and respond to faults inside and outside of the microgrid and maintain coordination between protective devices in both grid-interconnected and grid-isolated modes and in the presence of varying numbers and types of sources [22]. Finally, it is also important to define the zones of protection in an economical fashion. A wide range of protection schemes have been proposed in literature [23, 24], each assuming certain topologies, operating conditions, and source types. Some proposed protection schemes have used principles including overcurrent (IEEE devices 50, 51, 67), undervoltage (IEEE device 27), voltage restrained or voltage controlled overcurrent (IEEE devices 51VR or 51VC), active or reactive power (IEEE devices 32, 32Q), distance (IEEE device 21), current differential (IEEE device 87), over- or under-frequency (IEEE devices 81O, 81U),

harmonic-content, and traveling waves, many of them using varying complexities of communication infrastructure. Summaries of many proposed schemes can be found in reference [25] .

2.2   Microgrid System Design Considerations

Careful selection of protective equipment must be considered to assure that the microgrid can operate in a dependable and secure manner. Protective equipment that may be dependable with the high short-circuit levels of a strong utility source may not provide the same level of dependability when applied in a microgrid environment with varying and bi-directional fault contributions from various source levels due to grid-interconnected or grid-isolated operation . Protective equipment designed to dependably detect faults while islanded may not be secure while grid interconnected.

2.2.1   System Studies for Microgrid Design

During the conceptual design phase of a microgrid, system impact studies, including short circuit analyses/equipment duty, overcurrent coordination studies, and transient stability studies should be performed to have a thorough understanding of the system's protection requirements for different operating conditions. These studies need to be performed prior to the completion of designs to avoid protection deficiencies. Additionally, the capabilities of the software tools should be thoroughly evaluated to make sure that the requirements of the studies can be achieved and that results are realistic. Inverter-interfaced DERs are commonly included in microgrid systems. The inverter-interfaced DERs have different fault characteristics than traditional generation sources and they typically act as voltage dependent current sources, unlike the Thevenin equivalent circuits representing generators, as conventionally used in electric power system analysis software. Inverter-interfaced DERs must be modeled correctly in the software tools during the protection studies to get accurate results from the studies. When appropriate, detailed EMTP and/or Alternative Transients

Program (ATP) type models can be considered in the simulation studies to accurately represent the source fault characteristics in the time-domain. To test the designed protection scheme under various operating conditions and with different microgrid topologies, hardware-in-the-loop testing combined with relays or virtual protection models can be beneficial.

2.2.1.1   Distribution System Short Circuit Studies with Inverter-Based Resources

The majority of microgrids are made up of distributed generators that are primarily powered by photovoltaic and wind energy [26]. As a result of the fact that these prime movers are unable to directly deliver electricity at the nominal magnitude and frequency, inverters are required to serve as an interface between the prime movers and the microgrid [27, 28]. This suggests the term "inverter-interfaced distributed generators" (IIDG), which is frequently used in the context of microgrids. Grid-forming and grid-feeding (sometimes referred to as grid-following) inverters are two distinct categories of inverters with distinct control objectives [29]. Grid-feeding inverters inject the required active and reactive power into the grid at the inverter terminals, whereas grid-forming inverters maintain the nominal voltage magnitude and frequency at the inverter terminals as their control objective. At least one grid-forming inverter is required for an autonomous microgrid to function, establishing the nominal voltage magnitude and frequency. The grid-feeding inverters are then connected to the Point of Common Coupling (PCC), which has already been energized by the grid-forming inverter, in order to inject the active and reactive power that loads in the microgrid require. Because they establish a voltage of the nominal magnitude and frequency required by the microgrid [30, 31], grid-forming inverters play a similar role to synchronous generators (SG) [32] in this sense. For power flow and short-circuit analysis, the equivalent models of electric equipment in the sequence domain are necessary [33]. It is important to keep in mind that short-circuit analysis requires all zero-sequence, positive-sequence, and positive-sequence models, whereas

power flow analysis only requires positive sequence models [34, 35, 36]. The characteristics of grid-forming inverters have not yet been described by a practical model. The fact that the inverter controllers are quick enough to participate during fault time is a fundamental principle that leads us to re-define equivalent models for these generators [37]. In other words, the inverter's control system can regulate the sequence components of output voltage and output current within a short time of a fault [38] thanks to the high bandwidth of control loops [39] and inertia-less power electronic devices. In contrast, SGs can be adequately defined by their electric characteristics during that brief time period [40], which resulted in long-known sub-transient, transient, and stationary periods between the onset of a fault and the time before it goes out of step [41, 42, 43]. Small-signal models, such as those in [40] that can be used for power flow studies [44], make up the majority of inverter modeling efforts. The model that Ramasubramanian and Vittal [45, 46] aims to model converter-interfaced synchronous generators in the positive sequence is one more illustration. Because they assume that the inverter voltages are balanced and that they are operating at their nominal value, these models cannot be used in fault analysis. There have been a few published attempts to describe the fault response of IIDGs, such as [47, 48, 49]. "However, during faults, they primarily addressed the control strategy's mechanism. The positive-sequence output impedance of inverters under normal operating conditions was examined by Zhong and Zeng [50]. In protective relaying, the primary concern-namely, the output impedance during a fault-is not addressed. In contrast, Shen et al. The response of IIDGs to various control strategies was examined in [51]. Even though the work is more in-depth than other works of a similar nature, suggested models cannot be used in power systems with faults because they do not take into account the characteristics of comparable models. Guo and Mu [52] proposed per-phase models of an inverter during a fault in a similar work, but these models are not tangible because the sequence domain is not taken into account. The work

in [52] proposed an equivalent model of inverters under symmetrical fault conditions, separating grid-forming from gridfeeding inverters. The proposed models still include control loops, indicating that the effects of the controllers were not fully translated to fundamental electrical elements, resulting in a complex model for fault analysis of large-scale power systems, even though the current limiting is carefully considered. "They [inverters] are often incapable of providing sufficient fault current and their controllers play a principal role in the DG behavior," according to Haj-Ahmed and Illindala in [53]. While the first feature has been extensively discussed in numerous research publications, such as [54], the second feature has not yet been fully comprehended. In particular, the magnitude and phase angle of inverter sequence output impedances have not been thoroughly investigated. The translation of fault characteristics of inverters to practical equivalent models is typically the flaw in existing works. As a result, there is still no universal model of IIDGs under fault conditions that places an emphasis on system aspects. This means that the proper sequence-domain modeling of grid-forming inverters, which can be useful for both small and large-scale power systems, is the focus of the current work. Due to the authors' belief that grid-feeding and grid-forming inverters should be modeled in distinct ways due to their distinct control strategies, the current manuscript focuses solely on the modeling of grid-forming inverters in the sequence domain. The work in [55, 56] can be considered for additional details regarding typical grid-feeding inverter modeling.

2.2.1.2 Inverter Control System Design

The loss of directly grid-coupled mass inertia comes with the ongoing transition of power systems from conventional generation dominated by inverters to generation dominated by synchronous machines. Consequently, the requirement for inverter-coupled power units to contribute inertia becomes clear. In addition, inverters ought to play a role in the process of forming the grid voltage, which is currently carried out by synchronous generators in interconnected power systems. Grid-forming

inverters are available products that have been demonstrated to be suitable for island systems [57]. These grid-forming inverters, in contrast to conventional current-controlled inverters, produce a voltage phasor with some autonomy but still operates synchronously with the grid voltage. The inverter can also deliver instantaneous reserve by reversing the voltage phasor with the right control. Inverters' ability to form a grid can be determined by looking at how the voltage phasor is activated. In [58, 59], the concept of providing inertial response with inverters in the event of frequency deviations to support angle stability or frequency stability in interconnected grids was presented. In the meantime, a number of grid-forming control ideas for inverters are presented in [60]. Although some of them were made specifically for use in island grid applications, they might also be useful in interconnected systems in the future. The goal of this chapter is to compare and contrast various approaches and provide an overview of various control schemes. The switched dc-link voltage, which is achieved by the switching pattern of the converter legs, is the manipulated value in voltage source converters (VSC). Consequently, a controlled voltage source behind a filter inductor is assumed to be the converter itself. The short-term voltage source controlling discussed here refers to the voltage source's immediate behavior following an event at the PCC. It is possible to add additional control loops that are independent of the specific grid-forming control approach, such as overlaid control loops or resonance damping loops. The relevant terms inertia, grid-forming, and grid-following inverters are first defined. The ideas for grid-forming voltage sources are then discussed. For both the voltage angle and the voltage amplitude, the provided voltage phasor's dynamic behavior is examined. Grid-forming control strategies with their voltage phasor dynamics are deduced by starting with the dynamics of synchronous machines. The deduced dynamical transfer function takes as an input either the output power or an equivalent quantity, such as current.

2.2.1.3   Inverter Terminology

For clarity and to avoid possible confusion, some pertinent inverter terms are explained in the following discussion because various terms are used in the literature in ways that are either partially misleading or contradictory in the wrong context.

A power system's electrical inertia, or EI, is traditionally determined by the mechanical inertia of rotating machines in a synchronous area. Due to the kinetic energy stored in the rotor, a generator's mechanical inertia allows it to electrically smooth frequency deviations. From a technical standpoint, the ability to instantly respond to a change in the voltage phase angle at the point of connection with a power response is referred to as EI. This is because the generator's voltage phasor reacts slowly. EI can also be provided by power-electronic devices that use appropriate control algorithms, such as grid-forming control. EI is typically not offered by conventionally current-controlled inverters.

The term "grid-forming inverter," or GFI, refers to an inverter with a control strategy that enables it to directly control the terminal voltage and solely form the grid voltage using inverters taking into account the reserve and storage capacity that is required. These inverters may be able to provide EI by default. The term "grid-forming" was first used in the work in [61] and has since gained traction in both academia and industry. As a result, this chapter makes use of it as well.

In contrast to GFI, the term "current-controlled inverter" (CCI) or "grid-following inverter" refers to an inverter with a control strategy that regulates the injection of current based on the measurement of terminal voltage in order to achieve a particular power set point. The inverter can function as a grid-feeding inverter, injecting power regardless of voltage or frequency deviations at the terminal, thanks to the determination of the power set point. Reactive and active power set points can be adjusted with grid-supporting inverters when voltage or frequency deviations occur. Even though they can quickly adjust their power response to frequency deviations or

even frequency derivatives, conventional CCIs do not provide EI. Their active power injection is generally delayed in comparison to the active power response of devices with EI capability due to delays in active power set point determination following angle or frequency changes (e.g., due to frequency measurement).

2.2.2 System Grounding Considerations

System grounding of the microgrid must be thoroughly evaluated to assure safe operation, making certain that protective relaying will function properly and insulation integrity is maintained. Ideally, it would be desirable to have the microgrid system grounding the same whether grid-connected or grid-isolated. For example, consider a microgrid with a high-voltage PCC that is interconnected with a system that is normally operated solidly-grounded. If the microgrid DERs are interconnected through a transformer with a solidly-grounded wye connection on the PCC side and delta connection on the DER side, the microgrid system will be solidly grounded while operating grid-isolated. Alternatively, if each of the microgrid DERs are interconnected through a transformer with a delta winding on the PCC side and there is no other grounding transformer, the microgrid system will not be solidly grounded while operating grid-isolated. To maintain a solidly-grounded microgrid system while operating grid-isolated, transformers with a low-impedance zero-sequence path (e.g., a grounding transformer) may be utilized. Maintaining an effectively grounded system for a DER unit is necessary so that overvoltage is not excessive during line to ground faults and ground relaying operates as intended. If the DER unit has a step-up transformer that has a low voltage delta winding and high voltage solidly-grounded wye, a low impedance path for ground current can result. Assuring that the step-up transformer is effectively grounded but the zero-sequence impedance is not excessively low may require that a neutral reactor be installed to limit ground current supplied by the DER installation. Alternatively, the main power transformer may be left ungrounded (using either a delta winding or an ungrounded wye) and a smaller grounding bank

may be added to the installation to provide a sufficiently low zero-sequence path to limit overvoltage during line to ground faults. The interconnection requirements of the utility should dictate system grounding in addition to primary equipment and protection.

2.2.3 Communication System

A reliable communication system for the microgrid is essential for a variety of functions, including generator dispatch and protection communications. Communication between the utility substation's circuit breaker, the circuit breaker at the PCC, and the DER circuit breakers internal to the microgrid is often valuable; ideally, the communication system would interface with other protective devices of the microgrid as well. Communications protocols, media, and infrastructure must be considered to ensure that the system operates at appropriate speeds for the required protection operations. At the same time, the communication path redundancy and the security of the communication system should be taken into consideration. For protection purposes, the communication between the feeder relay and the microgrid protection systems is generally binary information. This means that communication circuits can use any of the commercially available communication technologies, such as power line carrier, spread spectrum radio and two-way pager, as well as available communication media, such as transmission lines, telephone lines, fiber optic cables and air for radio communications. The criteria for choosing the correct medium includes availability, operating speed, maximum latency, reliability, cybersecurity, redundancy and path failover, susceptibility to electromagnetic interference, ownership, maintainability, and cost.

2.2.4 Protective Equipment

The microgrid protection scheme must detect balanced and unbalanced faults in the microgrid, abnormal frequencies, and abnormal voltages. In the grid-interconnected

mode, it should also be able to detect faults on the utility side and islanding conditions. Detecting abnormal frequencies or voltages and islanding conditions can be achieved by using conventional methods. However, fault detection and protection coordination in a microgrid is more challenging [62, 63]. The typical application of distribution fuses may not be adequate in a microgrid due to the possibility of low fault currents. To detect faults while grid-isolated additional reclosers or fault interrupters with microprocessor-based relays or controllers may be required. The distribution transformers that step down to utilization voltage are typically protected with high-side fuses, and protection deficiencies that could occur under grid-isolated conditions need to be thoroughly evaluated. On the utilization voltage systems, fault current levels may be too low for reliable operation of typical overcurrent devices. Additional over/undervoltage sensing may be required that could provide a transfer trip signal to the microgrid grid-isolating device. Additional protection elements, including elements based on travelling wave technology, are also under investigation.

2.3   Temporary Overvoltage Challenges for Microgrids

When connecting inverter-based generation resources to a four-wire distribution system, TOV is an important design consideration. Photovoltaic (PV) inverters operating in a grid-following mode of operation were the subject of previous research into temporary overvoltage caused by GFOV and load rejection overvoltage (LROV). Due to its contribution to improving the resilience of the power system, the grid-forming mode of operation of inverters has received increased attention. The overvoltage observed in the system during an unbalanced ground fault can be affected by the control methodology of an inverter, which determines how it responds to faults. To help reduce the risk of transient overvoltage, a method for controlling the negative sequence impedance during a ground fault is proposed. PSCAD$^®$ is used to run a small system-level electromagnetic transient simulation to verify the inverter's characteristics and the method's efficacy. Microgrid implementation has garnered interest

in recent grid advancements and the incorporation of renewable energy generation [64].Not only can a microgrid serve a remote community or a critical load [65], but it can also boost the system's resilience and dependability. The work in [19, 66] point to the potential for utility energy efficiency and cost savings from microgrids as a key component of resilient distribution systems. Although a microgrid can have multiple generating resources, renewable energy (RE) based microgrids provide resiliency and more energy and cost savings than diesel generators based microgrids [19]. Several utilities in North America are implementing only RE-based microgrids that are going to provide more reliable and resilient electric power to their ratepayers [66]. Deploying RE based microgrid also helps states to meet their 100% renewable and zero-carbon electricity goals (e.g., California's SB 100).

A power electronic interfaced converter connects numerous renewable resources to the grid. Coordination among protective devices, transformer configuration for interconnection, and load rejection overvoltage are just a few of the difficulties associated with an IBR microgrid. A power electronic interfaced converter connects numerous renewable resources to the grid. Reverse power flow and multiple injection points of fault current, loss of coordination between protective devices, relay desensitization, transfer trip strategies, anti-islanding detection, open phase detection, interconnection transformer winding configuration and grounding, and load rejection overvoltage are just a few of the difficulties associated with an IBR microgrid. Because they offered multiple stacked value streams, IBR microgrids are becoming increasingly common. The design of a system for distribution integration presents a significant obstacle in the form of TOV. TOV is caused by a number of factors, including ferroresonance, generation to load ratio, and a single line to ground fault. Overvoltage can be significant in an electric power system that is supplied by an ungrounded source through a single line to ground fault. Overvoltage can be significant in an electric power system that is supplied by an unground source during a single line to ground

fault in other healthy phases. TOV poses a serious threat to the power system's safe and dependable operation [67] and the catastrophic failure of surge arresters.

For the single-phase to ground fault or double line to ground fault on the distribution system, all phases to ground connected equipment on unfaulted phases will experience overvoltage up to 173 percent. This overvoltage has the capability to damage not only the utility side protection devices but also residential equipment. In 1971, as a result of GFOV, a large chapter mill experienced generator failure. Moreover, this overvoltage can cause severe public protection phenomenon.

Per the IEEE standard, C62.92.1 [68], the system needs to be designed to ensure effective grounding for all operating scenarios. Effective grounding limits the overvoltage to 125-138% of nominal voltage depending on utility system configurations and requirements. Effectively grounded systems quickly respond to ground faults by introducing a low impedance return path.

Effective grounding criteria for synchronous machine based generations are well defined [69] and systems are designed to meet the following criteria for zero sequence reactance, resistance and positive sequence reactance: $0 < \frac{X_0}{X_1} < 3$ and $0 < \frac{R_0}{X_1} < 1$. However, per IEEE standard C62.92.6 [70], the GFOV mechanism is different for current regulated resources, like an inverter and varies depending on the inverter control topology.

One of the important design consideration for interconnecting inverter based generating resources to a four wire distribution system is the potential of temporary overvoltage (TOV). Past studies investigated temporary overvoltage due to GFOV and load rejection overvoltage (LROV) for photovoltaic (PV) inverters in grid following mode of operation. In recent times, grid forming mode of operation for inverters have gained increased attention as it helps to increase power system resiliency. Several electric utilities in North America is developing only IBR microgrid projects. Inverter's response during a faults depends on it's control methodology and hence ef-

fects the overvoltage observed in the system during an unbalanced ground fault. This chapter presents a theoretical comparison of temporary overvoltage observed in an ungrounded distribution system for IBR and conventional synchronous machine based resources. It also shows the impact of grid following mode and grid forming mode of operation on inverter negative sequence impedance and TOV. A control methodology is proposed to control the negative sequence impedance during a ground fault to mitigate the potential of transient overvoltage. A Electromagnetic Transient Simulation is performed using PSCAD® on a small system to show the inverter characteristics and effectiveness of the proposed method.

2.4   Protection Challenges for Only Inverter-Based Microgrids

Traditionally, power flow from substations to loads has been the goal of distribution systems. There are a number of protection issues that arise when a DER is integrated with these distribution systems [71]. Utility radial systems, for instance, may need to be upgraded or redesigned because they were typically intended for short-circuit sensing and unidirectional current flow. It may be necessary to replace relays without directional power flow sensing. Relays may not be able to detect some reverse-direction short-circuits, have insufficient sensitivity to detect them, and DER protection must work with the utility auto-reclosing scheme, among other things.

Microgrids pose additional challenges due to the nature of their operation and the incorporation of DERs within them [72]. These challenges are in addition to those that independently connected DERs pose to their respective utility or grid systems. When operated in an island or grid-tied mode, for instance, microgrids are likely to have significantly different and varying short-circuit levels. They might only contribute a small amount of short-circuit current, especially from DERs that mostly use inverters (e.g., photovoltaics, battery-based energy storage, full-converter-based wind turbine generators, etc.). Microgrid feeders may have a power flow in both directions depending on how the generation, load, and circuit topology are different. During and after

the microgrid's transition from grid-tied to island operation, a normally grounded distribution system may lose a relatively low-impedance zero-sequence path. It might be hard to find a utility source that has gone missing. Adapting microgrid protection systems to a new generation, circuit topology, or load should be carefully planned. When a microgrid moves from an island to a normal grid-tied mode, the process of resynchronizing it with its utility grid can cause issues like excessive inrush current, voltage and frequency disturbances, transient stability, and other issues.

Moving to a new topology (e.g., operating the microgrid in a grid-tied or island mode, etc.) can alter the operating conditions of the microgrid. The use of adaptive mechanisms, for example, is one way that a microgrid protection system must always guarantee the safety of the microgrid system, connected equipment, and personnel. Additionally, a false operation of a microgrid protection system, such as responding to a utility or grid event that does not warrant its operation, must never occur. During microgrid transition periods, many different kinds of protective relays may become temporarily inoperable or enter an indeterminate state while their settings are changed or adapted. As a result, the microgrid is susceptible to inadequate protection [72].

Protective elements that are utilized in microgrid systems that include voltage sensing include under-voltage (UV, IEEE device 27), over-voltage (OV, IEEE device 59), directional over-current (OC, IEEE device 67), voltage-restrained OC, IEEE device 51V, and voltage-controlled OC. As a result, if a voltage transformer (VT) fuse blows and causes a voltage input loss to a relay, plans for microgrid protection can be significantly impacted. Voltage-restrained or voltage-controlled OC elements may accidentally operate [73] if a fuse blows on a set of VTs. UV elements may also operate unintentionally on a set of VTs with a blown fuse [71]. If a voltage sensing function is absent, directional OC elements may malfunction or cease to function when required [71]. For microgrid protection schemes, these and other anticipated

effects of a voltage input loss must be taken into account. Because they do not require voltage sensing, current differential and non-directional OC protection, two types of protection, cannot completely replace voltage controlled and voltage restrained OC protection [71]. The differential current scheme requires measurement inputs from remote terminals of the protected circuit elements, whereas the non-directional OC scheme lacks the sensitivity of the directional OC, voltage controlled, and voltage restrained OC schemes.

2.5   Chapter Summary

In this chapter, a review of the microgrid system design considerations is provided. The main considerations for microgrid design, distribution system short circuit studies with inverter-based resources, inverter control system design, system grounding considerations, overvoltage challenges in the microgrid, communication system design, and protection challenges in the fully inverter-based microgrid are discussed. In the next Chapter, a method for distribution system short circuit study considering inverter-based distributed generation is discussed.

CHAPTER 3: METHOD FOR DISTRIBUTION SYSTEM PROTECTION STUDY CONSIDERING INVERTER BASED DISTRIBUTED GENERATION

Power system protection is an essential consideration for the reliable operation of the electric power system [74]. Protection systems are necessary for ensuring equipment and human safety. Several protection schemes are used in practice, and these schemes vary depending on their location purpose and the components they are intended to protect [75].One of the key steps of developing protection scheme is to perform short circuit studies. Conventionally, synchronous machine based generating resources (SMGR) are modeled as a voltage source behind resistance. But, the modeling of Inverter based resources (IBR) are not as simple as modeling synchronous machine based generating resources (SMGR). The models of IBRs vary with the control mode of operation of the inverter. In grid following mode of operation because of the controls it is modeled as a control source and in grid forming mode of operation it is modeled as a voltage source behind variable resistance. It is also important to model the protection devices correctly in electromagnetic transient platform like PSCAD®. This chapter discusses how the protection devices are modeled and how short circuit studies are performed with inverter based resources.

3.1 Chapter Introduction

This chapter mainly focuses on load flow and short circuit study considering distribution network protection components and schemes. Main protection devices for distribution networks are fuses, recloser, relay, sectionaliser, and circuit breakers. The primary purpose of this chapter is to understand the protection devices in the distribution side and their functionality. Underlying mathematical models of these

protection devices are studied, and then models are developed for simulation. Then their functionalities are tested in simulation. For simulation, PSCAD® was used, since it is an EMTP software that can characterize the transient behavior of the system well. For protection analysis, it is crucial to observe the transient response of the system and take the necessary step for any abnormal situation. In PSCAD®, two small size distribution systems, along with protection devices, were modeled. Load flow and short circuit studies were performed for both the system theoretically and simulation wise. Load flow and short circuit play a vital role in choosing the rating of the electrical components as well as protection components in the system. Load flow and short circuit are mandatory for setting up the coordination between the protection components. All the protection devices are appropriately coordinated in both the PSCAD® model. To understand the operations of these protection devices, faults are applied at different locations, and operations of associated protection devices are observed and analyzed.

The main contributions of this chapter are:

- Modeling of protections devices in the electromagnetic transient platform PSCAD®.

- Method of modeling inverter based resources for short circuit studies.

- Studying the impact of inverter based resources on existing distribution protection coordination.

The rest of the chapter is organized as following; section 3.2 shows the load flow and short circuit analysis for two simple models and the results from PSCAD® is validated with hand calculation. Section 3.3 outlines the details of how each protection devices like relay, recloser,fuse, sectionalizer can be modeled in PSCAD®. Section 3.4 shows how the operation of distribution circuit with protection devices. Section 3.5 describes how to perform short circuit studies for synchronous machine based microgrids. And, the inverter machine based microgrid short circuit studies are covered in section 3.6.

Section 3.7 highlights the impact of inverter based resources on existing distribution system protection coordination practices. Finally, section 3.8 concludes the chapter and outlines future work.

3.2   Distribution System Short Circuit Study and Protection Modeling

In this section discuss how a typical distribution system short circuit study perform. Also thoroughly discuss on distribution system protection devices modeling.

3.2.1   Objectives

The main objective is modeling a distribution system in PSCAD along with all the protective devices of distribution system.

- Modeling of distribution system with protection devices in PSCAD$^{\circledR}$.

- Understanding the functionalities and settings of different protection devices.

- Understanding the protection device selectivity and sensitivity.

- Understanding the overall distribution system protection philosophy which includes the following

    - Minimize the number of consumers affected by the fault

    - Eliminates safety hazards as fast as possible

    - Minimize the service failure to the smallest possible branch in the distribution system

    - To discriminate between overloading and short circuit.

3.2.2   Distribution Circuit Models and Settings

Two models are considered for the study. Model 1 is a radial system without recloser and sectionalizer and model 2 is a radial system with recloser and sectionalizer

3.2.2.1   Model 1 Description

Figure 3.1 shows a 115-kV radial distribution system in which the substation resistance value is 13.92 ohm. There is a step-down transformer right after the substation, and the substation is feeding 9MVA load (Total 3 loads, each 3MVA). The voltage rating of the transformer is 115kV/13.2kV. The winding configuration of the transformer is Y-Y. The transformer power rating is 25MVA, and positive sequence leakage reactance is 0.048 pu. There are three bus bars (Bus A, Bus B, Bus C) between substations and load. Line impedance value between Bus B and Bus C is 1.125ohm.
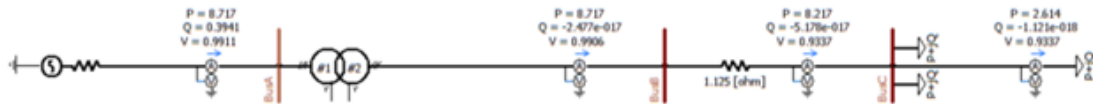
Figure 3.1: Single line diagram of model 1.

3.2.2.2   Load Flow Analysis

It is essential to do load flow analysis (voltage, active power, reactive power, line losses) to design a new power system network. Moreover, load flow studies determine if system voltage remains within specified limits under normal or emergency operating conditions. Load flow also helps to analyze system equipment such as transformers and conductors are overloaded or not. Due to the source resistance, there is a voltage drop inside the source, and the voltage magnitude at Bus A is 0.9911 pu instead of 1. Only the transformer in the circuit consumes reactive power; for that reason, there is a small amount of MVAR flowing from the substation at Bus 1, and there is no other reactive power flow downstream. The voltage magnitude of Bus B is less than 1 because of the transformer reactance. Between Bus B and Bus C there is

Table 3.1: Load flow of model 1

Bus Number	Voltage Magnitude (PU)	Voltage Angle (radian)	Active Power (MW)	Reactive Power (MVAR)
Bus A	0.9911	0.000158072	8.717	0.3941
Bus B	0.9906	-0.01690277	8.717	0
Bus C	0.9337	-0.01690272	8.217	0

line impedance which causing the voltage magnitude at Bus C is smaller than Bus B. Power always flows from higher voltage angle to lower voltage angle since it is a radial distribution system, voltage angle at Bus A should be higher than Bus B. Similarly, voltage angle should be higher at Bus B compare to Bus C

3.2.2.3   Short Circuit Analysis

Short circuit analysis is fundamental to determine the rating of the electrical equipment to withstand the thermal and electromagnetic effects of the short-circuit current as well as to determine the setting of protection equipment and coordination.

In the distribution, three phase balanced fault information is used to select and set phase relay so an LLLG fault applied at each of the buses. LLLG fault is most severe among all types of fault. If we derive the total fault current equation using sequence network for different types of fault (SLG, LL, LLG, LLL, LLLG) the amount of impedance for LLLG is less then compare to other types of fault. Since the impedance is less, the fault current will be higher.

Formula for fault current calculation:

Total fault current for LLLG fault,

$$I_f = \frac{V_f}{Z_{ff} + Z_f} \tag{3.1}$$

Here, V_f= Prefault bus voltage (we can get prefault bus voltage by doing load flow).

Z_{ff} = Thevenin impedance viewed from the faulted bus.

Z_f= Value of fault impedance.

Total fault current for SLG fault,

$$I_a = \frac{3E_a}{Z^1 + Z^2 + Z^0 + 3Z_f}$$ (3.2)

Here, E_a = Source Voltage.

Z^1 = Positive sequence impedance.

Z^2 = Negative sequence impedance.

Z^0= Zero sequence impedance.

Z_f = Value of fault impedance.

Table 3.2: Short Circuit Analysis of model 1

| Bus Number | Fault Type | Short Circuit Current (A) | | Error Percentage |
		PSCAD® Model Value	Hand Calculation Value	
Bus A	LLLG	4395.9	4769.8	-7.838
	LLG	3494.3	NA	NA
	LL	2985.2	NA	NA
	LG	2361.6	NA	NA
Bus B	LLLG	18170.739	14714.8	23.486
	LLG	14835.469	NA	NA
	LL	12237.257	NA	NA
	LG	9972.406	NA	NA
Bus C	LLLG	5170	4640	11.422
	LLG	4161	NA	NA
	LL	3517	NA	NA
	LG	2790	NA	NA

For LLLG fault at bus A, the theoretical value is closer to the simulation value. Due to the transformer voltage rating (115kV/13.2kV), the short circuit current is higher in the Bus B. The percentage of error at Bus B between theoretical calculation and PSCAD® is high. Even though in the simulation exactly same reactance value of the transformer used (which is given in theory). The reason of this phenomenon

could be theoretical value of the reactance of the transformer is not appropriate for simulation.

3.2.2.4   Model 2 Description

In figure 3.2 shows a portion of a radial distribution system single line diagram. For reliability, a recloser and a sectionaliser setup in the downstream of the system. Recloser has two fast and two delayed operations capability. The sectionaliser will isolate the faulted section of the network after the full number of counts has elapsed of the relay, leaving that part of the feeder upstream still in service. In figure 3.2 shows a 115kV radial distribution system in which substation resistance value is 14.27 ohm. There is a step-down transformer right after the substation, and the substation is feeding 3MVA load. The voltage rating of the transformer is 115kV/13.2kV. The winding configuration of the transformer on the primary and secondary sides is Y-Y. 25MVA is the power rating of the transformer, and positive sequence leakage reactance is 0.019 pu. There are five bus bars between substations and loads (Bus 1, Bus 2, Bus 3, Bus 4, Bus 5). The line impedance values between Bus 2 and Bus 3, Bus 3 and Bus 4, and Bus 4 and Bus 5 are 0.84041, 2.3491, 0.206507 ohm consecutively.

3.2.2.5   Load Flow Analysis

Due to the source impedance, the voltage magnitude at Bus 1 is 0.9973 pu instead of 1. Only the transformer in the circuit consumes reactive power; for that reason, there is a small amount of MVAR flowing from the substation at Bus 1, and there is no other reactive power flow downstream. The voltage magnitude of Bus 2 is less than 1 because of the transformer reactance. Between Bus 2 and Bus 3, there is a line impedance, which causes the voltage magnitude smaller at Bus 3 than Bus 2. Always power flows higher bus voltage angle to the lower bus voltage angle since it is a radial distribution system; thus, the voltage angle at Bus 1 should be higher than Bus 2. Similarly, the voltage angle should be higher at Bus 2 compare to Bus 3; Bus
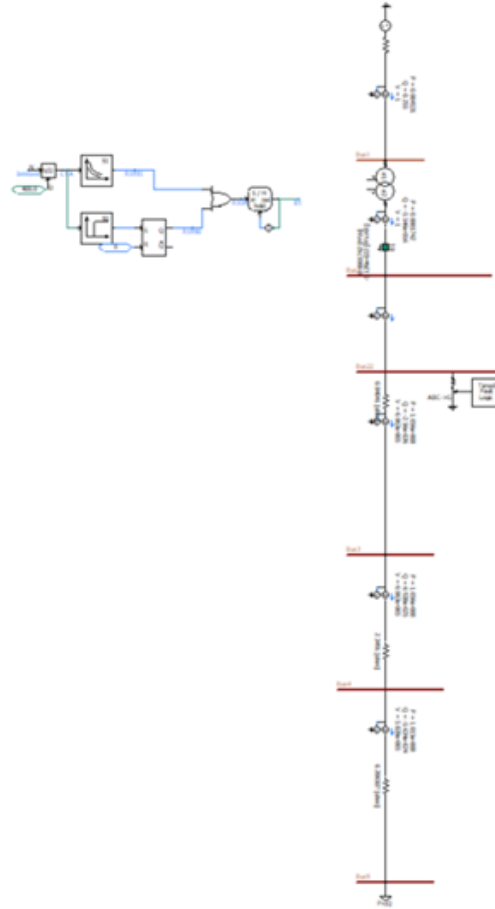
Figure 3.2: Single line diagram of model 2.

3 compare to Bus 4, and Bus 4 compare to Bus 5.

Table 3.3: Load flow of model 2

Bus Number	Voltage Magnitude (PU)	Voltage Angle (radian)	Active Power (MW)	Reactive Power (MVAR)
Bus 1	0.9973	0.000275487	2.817	0.2545
Bus 2	0.9972	-0.001878514	2.816	0
Bus 3	0.9835	-0.001878525	2.778	0
Bus 4	0.9454	-0.001878553	2.67	0
Bus 5	0.9421	-0.016902818	2.661	0

Table 3.4: Short Circuit Analysis of model 1

Bus Number	Fault Type	Short Circuit Current (A)		
		PSCAD® Model Value	Hand Calculation Value	Error Percentage
Bus 1	LLLG	31990.6	31993	-0.0075
	LLG	21.2464	NA	NA
	LL	21.3679	NA	NA
	LG	0.267832	NA	NA
Bus 2	LLLG	31990.6	31993	-0.0075
	LLG	21.2464	NA	NA
	LL	21.3679	NA	NA
	LG	0.267832	NA	NA
Bus 3	LLLG	7279.6	7066	3.0229
	LLG	4.8337	NA	NA
	LL	4.8522	NA	NA
	LG	0.2625	NA	NA
Bus 4	LLLG	2247.8	2224	1.0701
	LLG	1.5026	NA	NA
	LL	1.4993	NA	NA
	LG	0.2478	NA	NA
Bus 5	LLLG	2118.8	2097	1.0395
	LLG	1.3748	NA	NA
	LL	1.4157	NA	NA
	LG	0.2425	NA	NA

3.2.2.6   Short Circuit Analysis

3.3   Protection Device Modeling in PSCAD®

In the distribution system, the main protection components are relay, fuse, circuit breaker, sectionaliser, and recloser. There is no specific standard for the overall protection in the distribution network, some general indication of how this system work can be assumed

3.3.1   Relay Modeling

A relay is an electromagnetic switch operated by a relatively small electric current that can turn on or off a much larger electric current. The heart of a relay is an electromagnet (a coil of wire that becomes a temporary magnet when electricity flows through it).Relays are using for the protection of the power system. Some of them are primary relays meaning that they are the first line of defense. Such relays sense the fault and send a signal to the proper circuit breaker to trip and clear the fault. In the following sections different type of relay modeling discussed.

3.3.1.1   Inverse Time Over-current Relay Modeling

Inverse time overcurrent relay set up parameter:

- Time Dial

- Pick Up

- Characteristics curve

For modeling an Inverse time overcurrent relay above parameters set up correctly by using the characteristics curve of the relay.

3.3.1.2   Over-current Relay 50 and 51 Modeling

The first step is to check the short circuit at the node where the relay is planning to set. Relay 50 and relay 51 carefully integrated into the system. As soon as the relay 50 sees that the current is about to exceed its limit, it will comment on a trip signal into the circuit breaker to ensure the protection of the system. Time-delayed overcurrent relay operates according to their characteristic curve. It waits a specified period according to its time-current characteristics curve.

3.3.1.3   Block Diagram of Relay in PSCAD®

Figure 3.3 shows the PSCAD® implementation of overcurrent protection. Current transformers are modeled as simple turns ratio. Transformer saturation is not con-
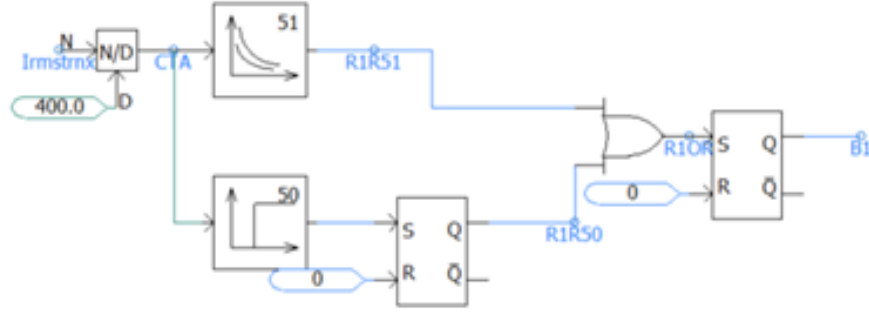
Figure 3.3: Inverse time overcurrent and overcurrent relay combination.

sidered for this study. PSCAD$^{\circledR}$ library models are used for time overcurrent (51) element and instantaneous overcurrent (50) element. A circuit breaker is operated if either 50 or 51 elements is high. SR latch is used to hold the output high. No reset button is a model for this study but will be added in future work.

3.3.1.4   Response of Relay in PSCAD$^{\circledR}$

The discussion of this section is to analyze the performance of the relay (R50 & R51). In the base model of model 2, a breaker (B1) added. For the instantaneous response of relay 50, an LLLG fault applied at Bus 2. Since the fault is closer to the substation, and there is no line impedance, From the table we can see that fault current is higher compared to Bus 3. We are expecting to relay 50 elements to operate. From figure 3.4, we can observe that relay 50 picks up for that short circuit current and functions seamlessly.

An LLLG fault applied in the different buses and checked how the relays are responding for faults. In conclusion, instantaneous and time-delayed relays were able to detect and operate successfully.

3.3.2   Fuse Modeling

A fuse is an overcurrent protection device; it possesses an element that is directly heated by the passage of current, and that is destroyed when the current exceeds a predetermined value. A suitably selected fuse should open the circuit by the destruc-

Figure 3.4: Single line diagram of relay response.

tion of the fuse element, eliminate the arc established during the destruction of the element and then maintain circuit conditions open with the nominal voltage applied
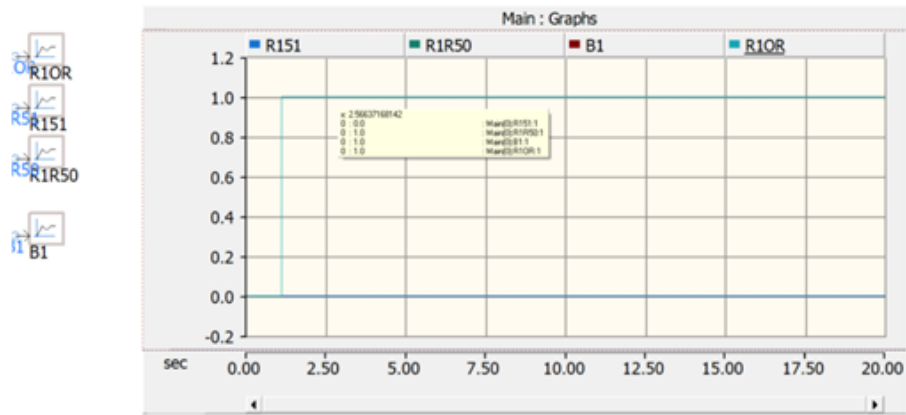
Figure 3.5: instantaneous relay(R50) response graph in PSCAD®
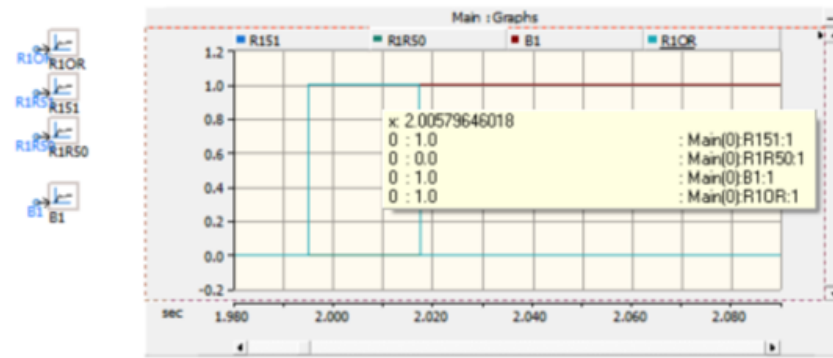
Figure 3.6: time delay relay(R51) response graph in PSCAD®.

Table 3.5: Relay response table of model 2

Fault Location	Relay 50	Relay 51	Comment
Bus 1	Operate		Instant response by R50
Bus 2	Operate		Instant response by R50
Bus 3		Operate	R51 work successfully (it waited a certain period before the operation)

to its terminals (i.e., no arcing across the fuse element).

In the distribution system type of fuses are:

- K type (this type of operation is fast)

- T type (this type of operation is slow)

Fuse first and slow operation depending on the speed ratio. The SR is the ratio of minimum melt current that causes fuse operation at 0.1 s to the minimum melt current for 300-s operation. For the K link, an SR of 6to8 is defined and, for a T link, 10to13.
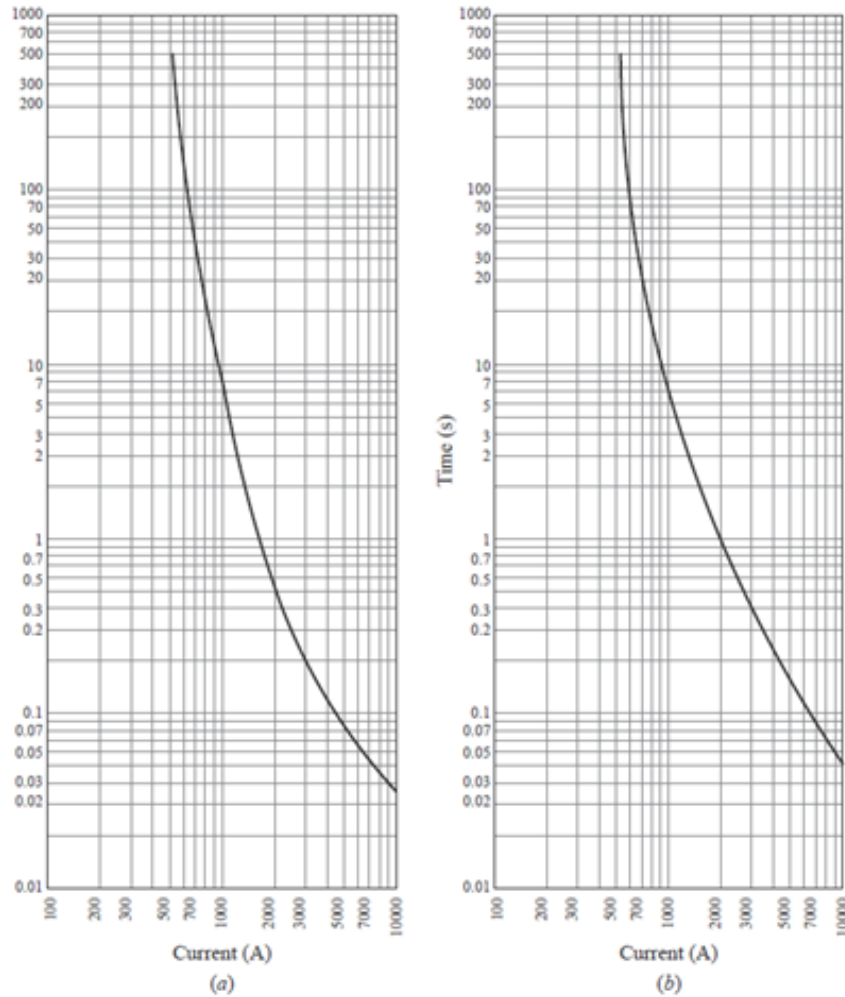
Figure 3.7: Time/currents characteristics of typical fuse-links.

Figure 3.7 shows the comparative operating characteristics of type 200K and 200T fuse links. For the 200K fuse, a 4400 A current is required for 0.1 s clearance time and 560 A for 300 s, giving an SR of 7.86. For the 200T fuse, 6500 A is necessary for 0.1 s clearance, and 520 A for 300 s; for this case, the SR is 12.5.

3.3.2.1   Representation of Fuse in PSCAD®

The time/current characteristics curve is essential for fuse modeling. There is a software which can generate time/current characteristics curve for any type and any rating of the fuse. The name of the software is S&C. For modeling the proposed model 2, characteristics curve of 40T and 6T fuse generated in S&C, then those curves implemented in two X-Y function blocks of PCAD. The following discussion is divided into two-part. In the first part, fuse modeling was done for only 10 data points (data depends on the short circuit current) Then fuse modeled for all data points. All the data point is available in S&C software. Figure 3.8 shows the detailed model of Fuse.
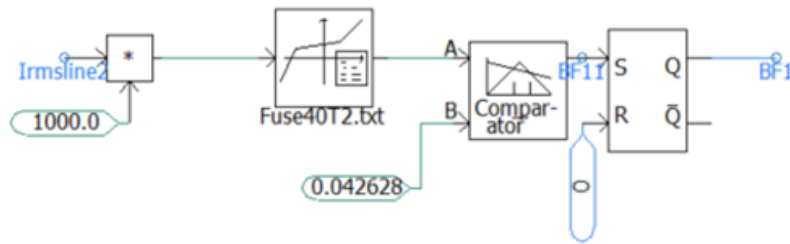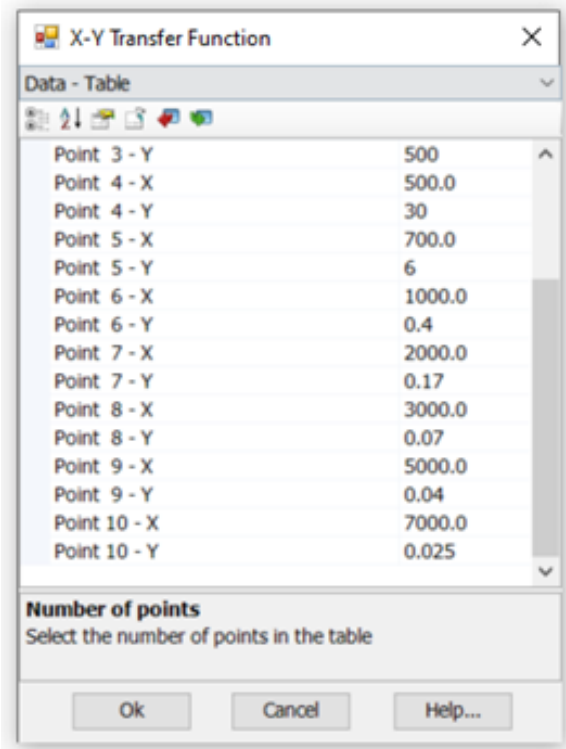
Figure 3.8: Initial Fuse model in PSCAD®.

The following Lookup table developed for 200K fuse (using the figure 3.9). Initially, this table used for fuse modeling then this table updated for all the available data point of characteristics curve from S & C software.

S & C software used for characteristic curve and coordination of 6T and 40T for model 2 as well.

3.3.3   Recloser Modeling

A recloser is a device that can detect phase and phase-to-earth overcurrent conditions, automatically reclose to reenergize the line if the overcurrent persists for a predetermined amount of time, and then interrupt the circuit. After a predetermined number of operations, the recloser will remain open to isolate the faulted section from

Figure 3.9: Lookup table for 200k fuse link.
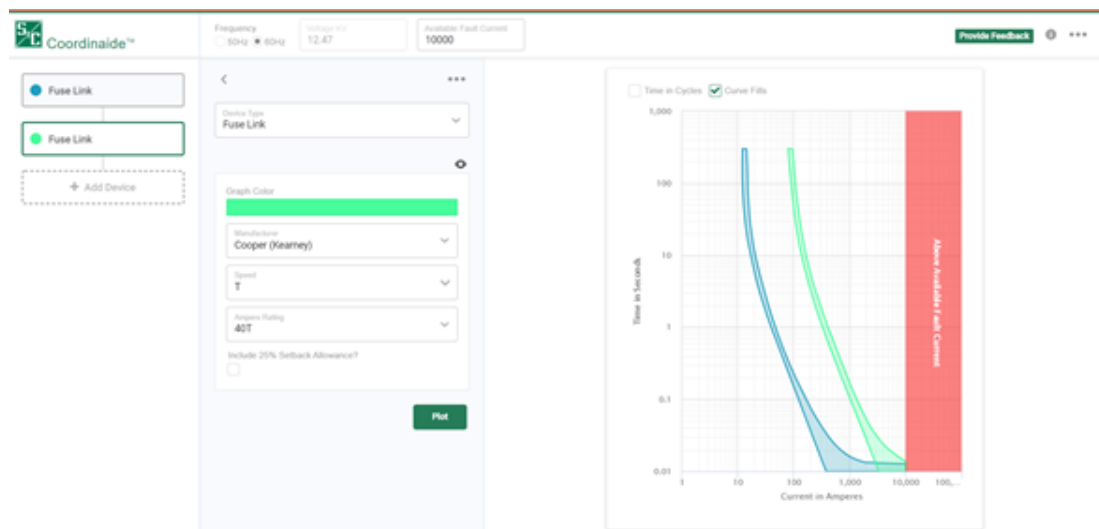
Figure 3.10: Characteristics curves for fuse 40T and 6T.

the rest of the system if the operation's fault still exists.

Figure 3.11 shows the design philosophy of recloser in PSCAD. Time overcurrent element is used to detect the fault, and the SR latch is used to hold the output high.
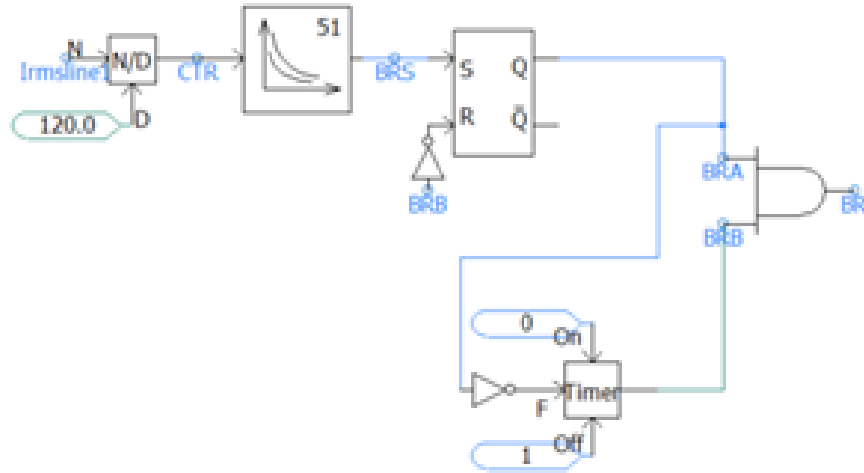
Figure 3.11: Recloser model in PSCAD®.

A timer is used to provide multiple reclose attempt. However, a counter has not been included in this model and will be added in a future enhancement.

3.3.4   Sectionaliser Modeling

A sectionaliser, which is typically installed downstream of a recloser, is a device that automatically isolates faulted sections of a distribution circuit after an upstream breaker or recloser has interrupted the fault current. Sectionalizers cannot break fault current, so they must be used in conjunction with a backup device that can break fault current.During fault conditions, sectionalizers count the number of operations performed by the recloser. The sectionaliser opens and isolates the defective section of line after a predetermined number of recloser openings while the recloser is open.The recloser can thus close and re-establish supplies to fault-free areas. The sectionalizer's operating mechanism is reset if the issue is temporary.

Figure 3.12 shows the sectionaliser model in PSCAD®. It is modeled with a controlled switch as the purpose is to open a portion of a circuit following a permanent fault.
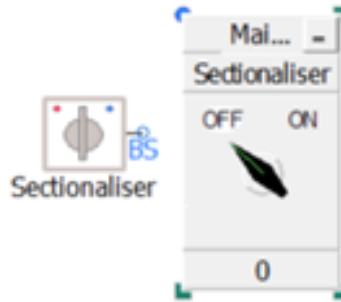
Figure 3.12: Sectionaliser model in PSCAD®.

3.4 Distribution Circuit Models With Protection Devices

In this section distribution system modeling with protection devices discussed also several test case perform to validate the performance of the modeling if distribution system protection.

3.4.1 Model 1 with Protection Devices

In figure 3.13, a substation is feeding 9MVA load. A step-down transformer is right after the substation. There are four relays between substation and load for protecting the distribution system. Coordination between relays appropriately designed.

3.4.1.1 Protection Device Settings for model 1 in PSCAD®

To design any protection set up in the system, the very first step to perform load flow and the short circuit. Nominal current and short circuit used to calculate the transformer ratio. To acquire the TAP setting, the nominal current is multiplied by 1.5 then divided by the current transformer ratio.

3.4.1.2 Case Studies

The critical idea of protection coordination is that protection devices near the fault location should respond and take the necessary step to keep the normal part isolated.

Figure 3.13: Proposed model 1 with protection devices.

Table 3.6: summary of protection device setting for proposed model 1

Breaker Number	Short Circuit Current (A)	(5/100) * Short Circuit Current(A)	CT Ratio	Pickup	Time Dial
BA	4395.9	219.795	300/5	2.5	NA
BB	18170.739	908.53695	800/5	4	2
BC	18170.739	908.53695	1100/5	8	2
BL	5171.4	258.57	300/5	4	5

Coordination between protective devices for model 1 appropriately acquired. An LLLG fault applied at each of the buses. From the table below, it is visible that

coordination is working between protection devices.

Table 3.7: summary of a case study for proposed model 1

Cases	Fault Type	Relay Operation	Operation Time	Comment
Fault at bus A	LLLG fault	BA Operated	1s	BA is supposed to operate if any fault occurs at Bus A as it is closest to the fault location, which is achieved successfully
Fault at bus B	LLLG fault	BB Operated	0.6s	BB is supposed to operate if any fault occurs at Bus B as it is closest to the fault location, which is achieved successfully
Fault at bus C	LLLG fault	BC Operated	0.1s	BC is supposed to operate if any fault occurs at Bus C as it is closest to the fault location, which is achieved successfully

3.4.2 Model 2 with Protection Devices

In figure 3.13, a substation is feeding 9MVA load. A step-down transformer is right after the substation. There are four relays between substation and load for protecting the distribution system. Coordination between relays appropriately designed

3.4.2.1 Protection Device Settings for Model 2 in PSCAD®

In the following system figure 3.14, a substation is feeding a 3MVA load. Between substation and load protection components are two relays, one recloser, and two fuses. Coordination between those devices is adequately acquired.

3.4.2.2 Case Studies

The main idea of protection coordination is that protection devices near the fault location should respond and take the necessary step to keep the healthy isolated. Coordination achieved between all the protection devices. Finally, an LLLG fault applied in each of the buses to observe the functionality of the protection components.
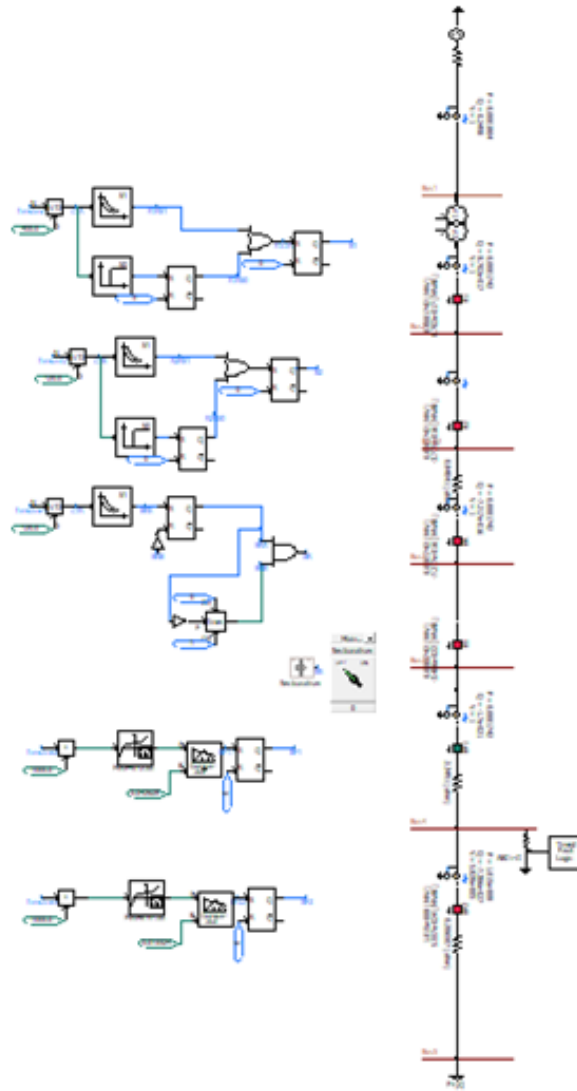
Figure 3.14: Proposed model 2 with protection devices.

3.5   Microgrid Short Circuit Study with Synchronous Machine Based Resources

3.5.1   Without Effective Grounding

Figure 3.15a shows the sequence network for a single line to ground fault for a synchronous machine sourced distribution system. Equations (3.3) shows the equivalent impedance between node F1 and N1. Equations (3.4) and (3.5) shows the equivalent

Table 3.8: summary of a case study for proposed model 1

Cases	Description	Relay Operation	Operation Time	Comment
Fault at bus 2	LLLG fault	B1(Relay 1) Operated	1s	B1 is supposed to operate if any fault occurs at Bus2 as it closed to the fault location, Which is achieved successfully.
Fault at bus 3	LLLG fault	BR(Recloser) Operated	0.6s	BR is supposed to operate if any fault occurs at Bus3 as it closed to the fault location, Which is achieved successfully.
Fault at bus 4	LLLG fault	BF1(Fuse1) Operated	1.6s	BF1 is supposed to operate if any fault occurs at Bus4 as it closed to the fault location, Which is achieved successfully.
Fault at bus 5	LLLG fault	BF2(Fuse2) Operated	0.11s	BF2 is supposed to operate if any fault occurs at Bus5 as it closed to the fault location, Which is achieved successfully.

impedance between for positive and negative seq between node F1, N1 and F2, N2 respectively. After solving the network, (3.6) presents the sequence voltage expressions and phase voltages are derived from sequence voltages.

$$Z_{th1} = [(Z_{xfmr} + Z_2 \parallel Z_{load2}) + Z_{load0} \parallel Z_{load1} \qquad (3.3)$$

$$= \frac{(Z_{xfmr} + Z_2) \times Z_{load2}}{(Z_{xfmr} + Z_2 + Z_{load2})} + Z_{load0} \parallel Z_{load1}$$

$$= \frac{(Z_{xfmr} + Z_2) \times Z_{load2} + (Z_{xfmr} + Z_2 + Z_{load2}) \times Z_{load0}}{(Z_{xfmr} + Z_2 + Z_{load2})} \parallel Z_{load1}$$

$$= \frac{(Z_{xfmr} + Z_2) \times Z_{load2} Z_{load1} + (Z_{xfmr} + Z_2 + Z_{load2}) \times Z_{load0} Z_{load1}}{(Z_{xfmr} + Z_2) \times Z_{load2} + (Z_{xfmr} + Z_2 + Z_{load2}) \times Z_{load0}}$$

$$+ Z_{xfmr} + Z_2 + Z_{load2} \times Z_{load1}$$

$$Z_{th2} = \frac{(Z_{xfmr} + Z_2) \times Z_{load2} + (Z_{xfmr} + Z_2 + Z_{load2}) \times Z_{load0}}{(Z_{xfmr} + Z_2 + Z_{load2})} \tag{3.4}$$

$$Z_{th3} = \frac{(Z_{xfmr} + Z_2) \times Z_{load2}}{(Z_{xfmr} + Z_2 + Z_{load2})} \tag{3.5}$$

$$V_1 = Z_{th1} \times I \tag{3.6}$$

$$V_2 = Z_{th3} \times I_1 \tag{3.7}$$

$$V_0 = Z_{load0} \times I_1 \tag{3.8}$$

$$I = \frac{V}{(Z_{xfmr} + Z_{th1} + Z_1)} \tag{3.9}$$

$$I_1 = (\frac{Z_{L1}}{Z_{th2} + Z_{L1}}) \times I \tag{3.10}$$

3.5.2   With Effective Grounding

This section describes the voltage expression for synchronous machine if the source is grounded through a grounding transformer. Figure 3.15b illustrates the sequence network in the presence of a grounding transformer Z_{GT}. After solving the network similar expressions for voltages are obtained like previous sections. Notably the zero sequence equivalent impedance $Z_T = Z_{GT}||Z_{load0}$ is different than the without grounding transformer case in section 3.5.1.

$$Z_{th1} = [(Z_{xfmr} + Z_2 \parallel Z_{load2}) + Z_{loadT} \parallel Z_{load1} \tag{3.11}$$

$$= \frac{(Z_{xfmr} + Z_2) \times Z_{load2}}{(Z_{xfmr} + Z_2 + Z_{load2})} + Z_{loadT} \parallel Z_{load1}$$

$$= \frac{(Z_{xfmr} + Z_2) \times Z_{load2} + (Z_{xfmr} + Z_2 + Z_{load2}) \times Z_{loadT}}{(Z_{xfmr} + Z_2 + Z_{load2})} \parallel Z_{load1}$$

$$= \frac{(Z_{xfmr} + Z_2) \times Z_{load2} Z_{load1} + (Z_{xfmr} + Z_2 + Z_{load2}) \times Z_{loadT} Z_{load1}}{(Z_{xfmr} + Z_2) \times Z_{load2} + (Z_{xfmr} + Z_2 + Z_{load2}) \times Z_{loadT}}$$

$$+ Z_{xfmr} + Z_2 + Z_{load2} \times Z_{load1}$$

$$Z_{th2} = \frac{(Z_{xfmr} + Z_2) \times Z_{load2} + (Z_{xfmr} + Z_2 + Z_{load2}) \times Z_{loadT}}{(Z_{xfmr} + Z_2 + Z_{load2})} \qquad (3.12)$$

$$Z_{th3} = \frac{(Z_{xfmr} + Z_2) \times Z_{load2}}{(Z_{xfmr} + Z_2 + Z_{load2})} \qquad (3.13)$$

$$V_1 = Z_{th1} \times I \qquad (3.14)$$

$$V_2 = Z_{th3} \times I_1 \qquad (3.15)$$

$$V_0 = Z_T \times I_1 \qquad (3.16)$$

$$I = \frac{V}{(Z_{xfmr} + Z_{th1} + Z_{inv1})} \qquad (3.17)$$

$$I_1 = (\frac{Z_{L1}}{Z_{th2} + Z_{L1}}) \times I \qquad (3.18)$$
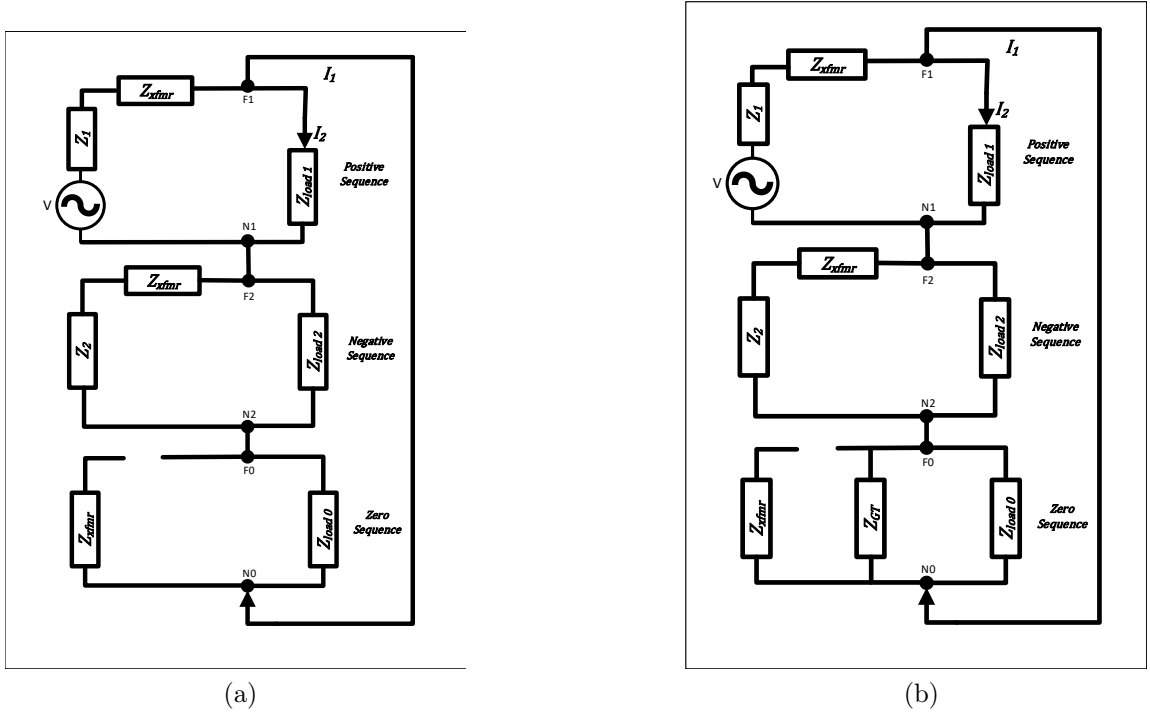
Figure 3.15: Sequence network for Synchronous Machine-Based Microgrid for a single line to ground fault (a) without grounding transformer, (b) with grounding transformer.

Comparison of section 3.5.1 and section 3.5.2 shows that the zero sequence voltage

expression value decreases for with grounding case as including a grounding transformer decreases the equivalent zero sequence impedance and hence the phase voltage for the healthy phases decreases as well.

3.6 Microgrid Short Circuit Study with Inverter-Based Resources

This section derives the voltage expressions for an inverter-based resource. The inverter source is represented by a current source in positive sequence and the negative sequence impedance. The negative sequence impedance varies a lot depending upon the inverter control objectives [70].

3.6.1 Without Effective Grounding

As shown in the case of synchronous machine, voltage expression are derived solving the network shown in Figure 3.16a. Note that as inverter is a current regulated source the current is considered constant here.

$$
\begin{aligned}
Z_{th1} &= [(Z_{xfmr} + Z_{inv2} \parallel Z_{load2}) + Z_{load0} \parallel Z_{load1} \\
&= \frac{(Z_{xfmr} + Z_{inv2}) \times Z_{load2}}{(Z_{xfmr} + Z_{inv2} + Z_{load2})} + Z_{load0} \parallel Z_{load1} \\
&= \frac{(Z_{xfmr} + Z_{inv2}) \times Z_{load2} + (Z_{xfmr} + Z_{inv2} + Z_{load2}) \times Z_{load0}}{(Z_{xfmr} + Z_{inv2} + Z_{load2})} \parallel Z_{load1} \\
&= \frac{(Z_{xfmr} + Z_{inv2}) \times Z_{load2} Z_{load1} + (Z_{xfmr} + Z_{inv2} + Z_{load2}) \times Z_{load0} Z_{load1}}{(Z_{xfmr} + Z_{inv2}) \times Z_{load2} + (Z_{xfmr} + Z_{inv2} + Z_{load2}) \times Z_{load0}} \\
&\qquad + Z_{xfmr} + Z_{inv2} + Z_{load2} \times Z_{load1}
\end{aligned}
$$

$$Z_{th2} = \frac{(Z_{xfmr} + Z_{inv2}) \times Z_{load2} + (Z_{xfmr} + Z_{inv2} + Z_{load2}) \times Z_{load0}}{(Z_{xfmr} + Z_{inv2} + Z_{load2})} \qquad (3.19)$$

$$Z_{th3} = \frac{(Z_{xfmr} + Z_{inv2}) \times Z_{load2}}{(Z_{xfmr} + Z_{inv2} + Z_{load2})} \qquad (3.20)$$

$$V_1 = Z_{th1} \times I \qquad (3.21)$$

$$V_2 = Z_{th3} \times I_1 \qquad (3.22)$$

$$V_0 = Z_{load0} \times I_1 \qquad (3.23)$$

$$I_1 = \left(\frac{Z_{L1}}{Z_{th2} + Z_{L1}}\right) \times I \qquad (3.24)$$

3.6.2   With Effective Grounding

Figure 3.16b shows the sequence network for an ungrounded inverter source grounded with a grounding transformer. Equation (3.25) shows the expression for voltages. One of the important things to notice is that the the voltage expression depends on the negative sequence impedance of the and it is a parameter which can be controlled through inverter controls. So, how much the overvoltage will be during a ground fault and how much it can be mitigated by conventional ground transformer depends on the inverter behaviour. As pointed out in [70], it is difficult to provide conclusive decision without confirming the inverter response. The next section provides an overview of inverter control topology and how the negative sequence impedance can be controlled to mitigate overvoltage observed in an inverter based system.

$$Z_{th1} = [(Z_{xfmr} + Z_{inv2} \parallel Z_{load2}) + Z_{loadT} \parallel Z_{load1}$$

$$= \frac{(Z_{xfmr} + Z_{inv2}) \times Z_{load2}}{(Z_{xfmr} + Z_{inv2} + Z_{load2})} + Z_{loadT} \parallel Z_{load1}$$

$$= \frac{(Z_{xfmr} + Z_{inv2}) \times Z_{load2} + (Z_{xfmr} + Z_{inv2} + Z_{load2}) \times Z_{loadT}}{(Z_{xfmr} + Z_{inv2} + Z_{load2})} \parallel Z_{load1}$$

$$= \frac{(Z_{xfmr} + Z_{inv2}) \times Z_{load2} Z_{load1} + (Z_{xfmr} + Z_{inv2} + Z_{load2}) \times Z_{loadT} Z_{load1}}{(Z_{xfmr} + Z_{inv2}) \times Z_{load2} + (Z_{xfmr} + Z_{inv2} + Z_{load2}) \times Z_{loadT}} + \quad (3.25)$$

$$Z_{xfmr} + Z_{inv2} + Z_{load2} \times Z_{load1}$$

$$Z_{th2} = \frac{(Z_{xfmr} + Z_{inv2}) \times Z_{load2} + (Z_{xfmr} + Z_{inv2} + Z_{load2}) \times Z_{loadT}}{(Z_{xfmr} + Z_{inv2} + Z_{load2})} \quad (3.26)$$

$$Z_{th3} = \frac{(Z_{xfmr} + Z_{inv2}) \times Z_{load2}}{(Z_{xfmr} + Z_{inv2} + Z_{load2})} \quad (3.27)$$

$$V_1 = Z_{th1} \times I \quad (3.28)$$

$$V_2 = Z_{th3} \times I_1 \quad (3.29)$$

$$V_0 = Z_T \times I_1 \quad (3.30)$$

$$I_1 = (\frac{Z_{L1}}{Z_{th2} + Z_{L1}}) \times I \quad (3.31)$$

Table 3.9 summarizes the findings of the section above. It shows that the phase overvoltage observed for the without grounding case is not as high for Inverter based resources compared to the synchronous machine based resources. And adding grounding reduces the phase overvoltage for both the synchronous machine and inverter case.

3.7   Issues With Existing Electric Distribution system Protection

In this section issues with existing electric distribution system protection is illustrated through a test system.
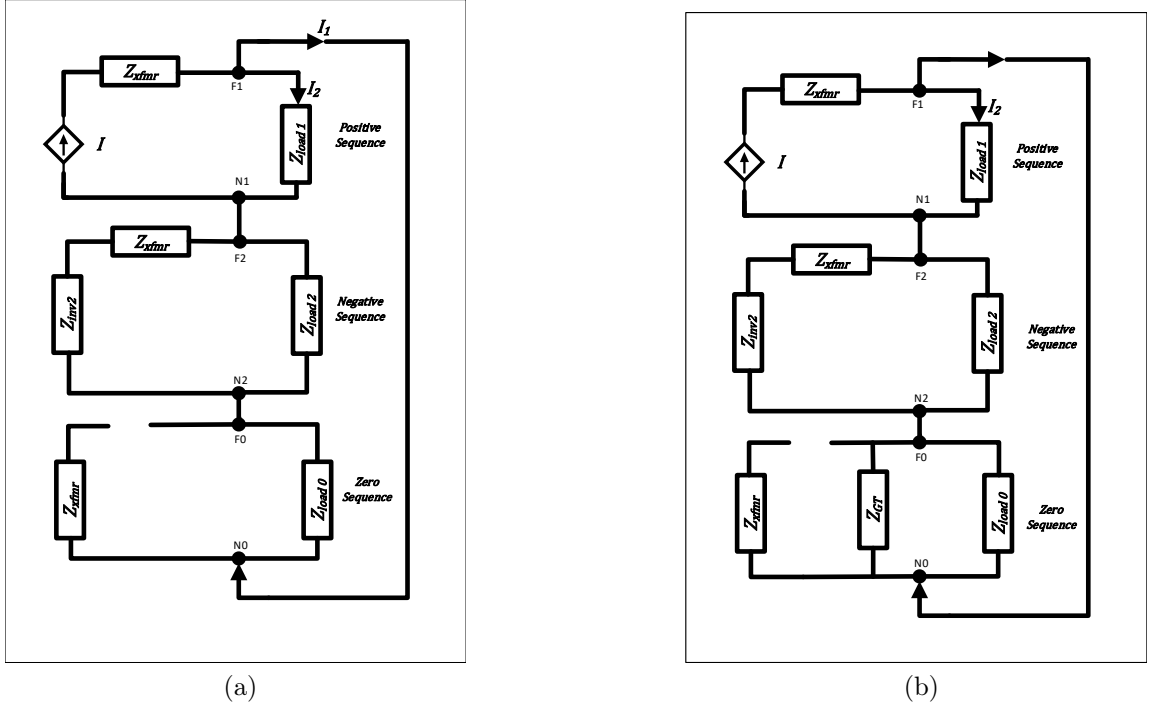
Figure 3.16: Sequence network of Inverter-Based Microgrid for a single line to ground fault (a) without grounding transformer, (b) with grounding transformer.

Table 3.9: DER without effective grounding and with effective grounding

DER type	Grounding Status	Sequence Voltage (PU)	Phase Voltage (PU)
Synchronous	Without Grounding	V0=0.7422	Va=0
	Without Grounding	V1=0.8295	Vb=1.0663
	Without Grounding	V2=0.2139	Vc=1.6483
Synchronous	With Grounding	V0=0.3653	Va=0
	With Grounding	V1=0.6613	Vb=0.9737
	With Grounding	V2=0.2964	Vc=1.0138
Inverter	Without Grounding	V0=0.3389	Va=0
	Without Grounding	V1=0.6621	Vb=0.9383
	Without Grounding	V2=0.3263	Vc=1.2481
Inverter	With Grounding	V0=0.1675	Va=0
	With Grounding	V1=0.5448	Vb=1.0721
	With Grounding	V2=0.4520	Vc=0.6617
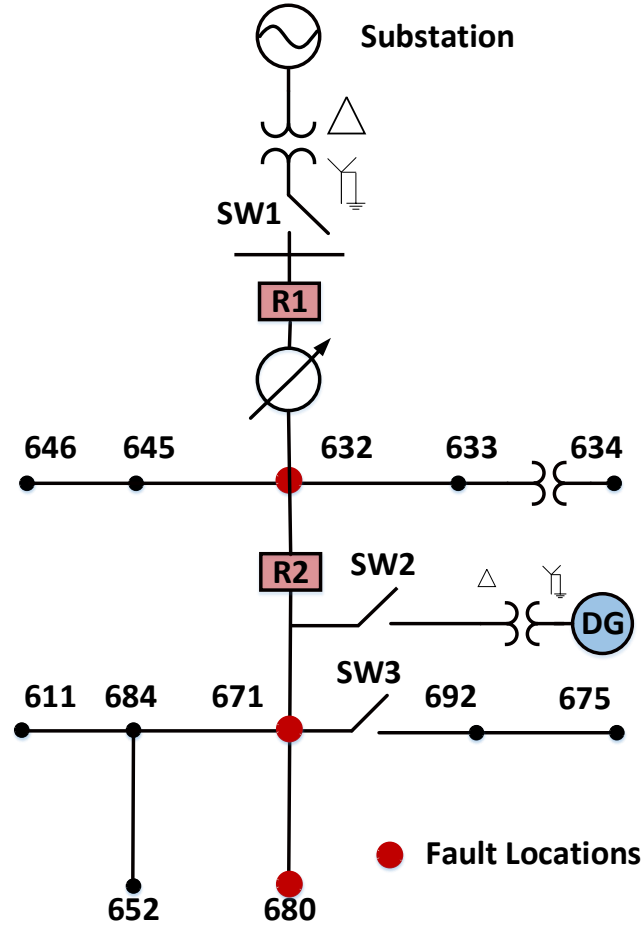
Figure 3.17: Modified IEEE 13 Node Test System [5].

3.7.1   Test System Description

The test system used for performing the studies is a IEEE 13 node unbalanced test system [6].13 node test feeder, which is a radial distribution feeder with one voltage regulator, both underground and overhead lines with different phases, in line step down transformers and spot and distributed loads. There is a substation transformer of rating $5MVA$ and $115kV/4.16kV$ and the positive and zero sequence impedance of the substation is given in [6]. First the test system is developed a real time simulator called RT-Lab from Opal-Rt and power flow and short circuit analysis are performed. ARTEMiS-SSN is the solver specifically designed to provide fast and accurate real-time simulation without introducing artificial delays The results are validated with

the benchmark [6]. Then the test system is modified to connect a DG rated $4750kW$ at node 671. Depending upon the scenario under study, the connected DG can be either conventional synchronous generator or inverter based energy resources. Two relays $R1$ and $R2$ have been connected at the feeder with the goal that $R2$ protects the far end of the feeder and $R1$ provides backup.

3.7.2   grid following Mode of Operation

In this mode of operation, the DG is connected to the feeder. Both the substation and the DG serves the load in the feeder. Three scenarios have been studied,

- **Scenario 1:** Switch $SW2$ is open and no DG is connected to the feeder

- **Scenario 2:** Switch $SW2$ is closed and an inverter based DG actively generating $3000kW$, is connected to the feeder

- **Scenario 3:** Switch $SW2$ is closed and a conventional synchronous generator based DG producing $3000kW$, is connected to the feeder

Table 3.10: grid following Mode: Fault Current Comparison for Fault at Node 680.

Case Scenario	Phase	Fault Currents (A)		
		From Substation	Total Fault	From DG
Scenario 1	A	2878.0	2878.0	0
	B	2834.5	2834.5	0
	C	2587.7	2587.7	0
Scenario 2	A	2704.4	2928.1	844.9
	B	2789.5	2883.8	844.9
	C	2458.4	2632.8	844.9
Scenario 3	A	2092.0	3295.8	1212.2
	B	2045.8	3242.1	1199.4
	C	1816.9	2927.7	1117.2

Conventional DG is modeled as a synchronous generator rated at 5000 kVA/ 4.16 kV. The positive sequence impedance of the generator is 0.86528Ω and zero sequence

impedance is 1.2979Ω. Inverter based DG is modelled with current limiters to limit maximum fault current to 150% of the rated value which is 844.9A. Faults are applied at three different locations node 632,671 and 680. Only The summary of total fault currents for fault at node 680 is presented at Table 3.10. It shows that in grid following mode the fault current contribution from IDG is less compared to SDG. Similar conclusions can be made about other fault locations. Standard inverse curve is selected for both relay settings and the pick up and time dial are set to maintain coordination between both the relays. Figure 3.18a shows the current through R1 and 3.18a shows the current flowing through R2 for scenario 1. The results show that for a fault at node 680, R2 operates first as expected to clear the fault and the current flowing through R1 decreases as some loads are disconnected from the circuit. For scenario 2, R2 operates faster than scenario 1 and for scenario 3, the operating time is even faster for increased fault current. Table 3.11 and Table 3.12 shows the fault currents for two different inverter interconnection transformer configurations. If the transformer is $Yg - D$ connected then the IDG contributes zero sequence currents and if it is $Yg - Y$ connected then it does not contribute any zero sequence current. In grid following mode, the zero sequence current contribution from the inverter can increase the sensitivity of existing utility protection devices.

3.7.3 Islanded Mode of Operation

In the islanded mode of operation, only IDG is serving to the load in the feeder. The IDG is connected to node 671. Faults are applied on bus 671, 632, and 680. The total fault current is a lot less compared to the fault current in grid-connected mode. This makes it difficult for fault detection by a relay, and it takes a significant time for both relays R1 and R2 to operate. The effect of transformer configuration is summarized in Table 3.15 and 3.16. For YG-Y configuration there is no path of zero sequence current and it does not contribute any fault current during L-G fault which makes it difficult to detect such faults. A grounding transformer bank is needed for

such configuration.
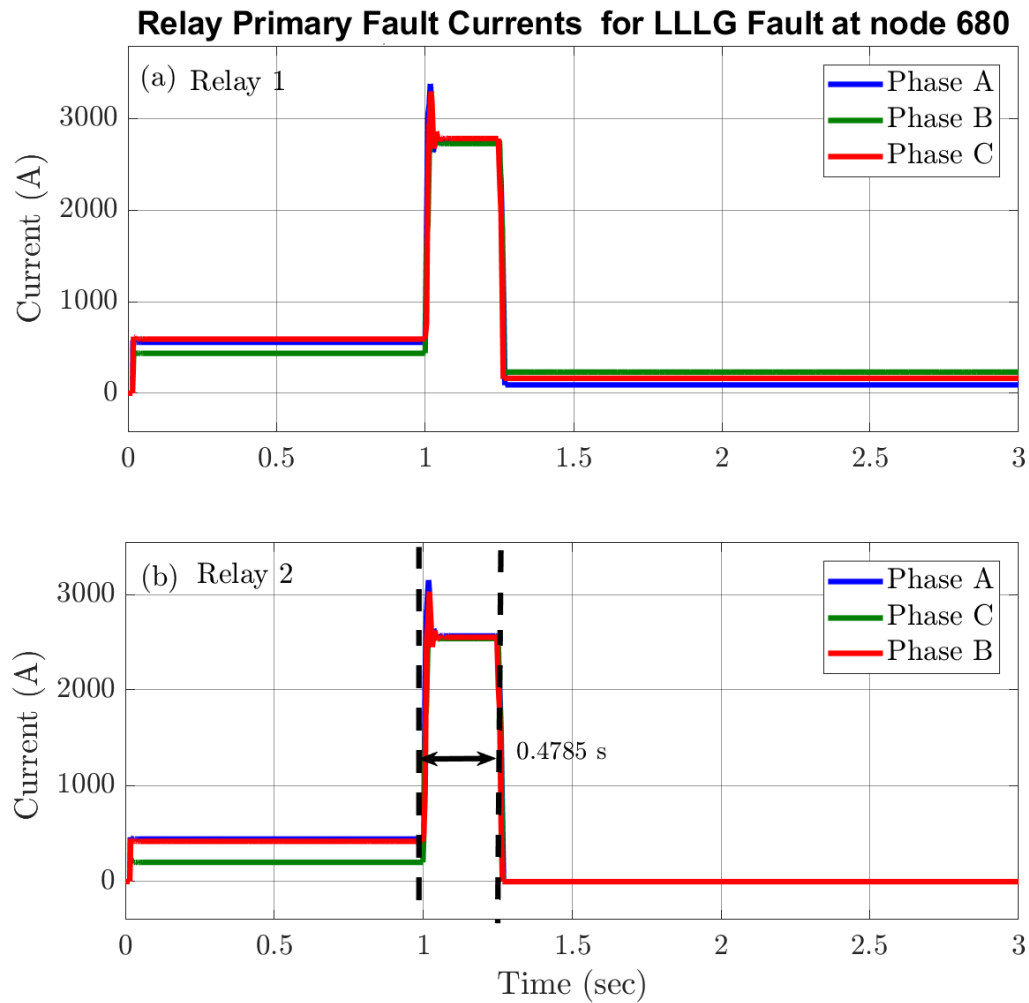
Figure 3.18: Relay operation in grid forming mode.

3.8   Chapter Summary

This chapter presents the basic fundamental of microgrid short circuit studies and an overview of distribution system protection. It provides details about how the protection devices can be modeled in the EMT application PSCAD®. It also explains the protection method used in power distribution system. Based on the results presented in the chapter it is noticed that it is challenging to model protection devices in

Table 3.11: Fault Current Comparison for Fault at Node 671

Case Scenario	Phase	Fault Currents (A)		
		From Substation	Total Fault	From DG
Scenario 1	A	3314.8	3314.8	0
	B	3265.6	3265.6	0
	C	3007.6	3007.6	0
Scenario 2	A	3144.5	3372.5	844.9
	B	3215	3322.5	844.9
	C	2875.2	3060	844.9
Scenario 3	A	2462.8	3882.0	1429.0
	B	2408.7	3818.8	1413.8
	C	2159.5	3476.7	1324.6

Table 3.12: Fault Current Comparison for Fault at Node 632

Case Scenario	Phase	Fault Currents (A)		
		From Substation	Total Fault	From DG
Scenario 1	A	4756.7	4756.7	0
	B	4695.9	4695.9	0
	C	4447.4	4447.4	0
Scenario 2	A	4619	4839.5	844.9
	B	4647.7	4777.7	844.9
	C	4332.1	4524.8	844.9
Scenario 3	A	3812.7	6021.9	2223.3
	B	3735.9	5930.4	2201.2
	C	3459.9	5552.5	2104.2

EMTP software but is it an essential step for microgrid designs. The presented work enhances the understanding of state-of-the-art and provide more accurate information about microgrid protection and design. The protection of microgrid depends heavily on the invert characteristics. And, inverter response to abnormal grid conditions is primarily governed by inverter control functionalities. For that reason it is important to understand the inverter control mechanism. The next chapter presents the details of inverter control modes and on-board protection functionalities.

Table 3.13: Single Line to Ground Fault at Node 680 for Yg-Δ Inverter Transformer Connection

Case Scenario	Phase /Sequence	Fault Currents (A)		
		From Substation	Total Fault	From DG
Phase	A	1562.1∠52.75	1938.8	957.1∠135.00
	B	1037.7∠-139.30	0	1037.7∠40.70
	C	593.2∠95.32	0	593.2∠-84.68
Sequence	I1	849.65∠-165.16	646.28	844.91∠150
	I2	646.27∠-97.97	646.27	0∠-118.37
	I0	387.31∠-95.13	646.27	260.15∠77.80

Table 3.14: Single Line to Ground Fault at Node 680 for Yg-Y Inverter Transformer Connection

Case Scenario	Phase /Sequence	Fault Currents (A)		
		From Substation	Total Fault	From DG
Phase	A	1753.2∠55.32	1883.1	844.9∠150
	B	844.9∠-150.00	0	844.9∠30
	C	844.9∠90	0	844.9∠-90
Sequence	I1	844.11∠13.63	627.70	844.91∠150.00
	I2	627.70∠81.88	627.70	0∠-125.62
	I0	627.70∠81.88	627.70	0∠119.72

Table 3.15: Islanded Mode: Single Line to Ground Fault at Node 680 for Yg-Y Inverter Transformer Connection

Phase Voltage(kV)	Phase Current(A)	Sequence Voltage(V)	Sequence Current(A)
Va = 0	Ia = 0	V0 = 2401.76	I0 = 0.01
Vb = 4.1600	Ib = 0	V1 = 2401.77	I1 = 0.01
Vc = 4.1600	Ic = 0	V2 = 0.01	I2 = 0.01

Table 3.16: Islanded Mode: Single Line to Ground Fault at Node 680 for Yg-Δ Inverter Transformer Connection

Phase Voltage(kV)	Phase Current(A)	Sequence Voltage(V)	Sequence Current(A)
Va = 1.8810	Ia = 1846.0	V0 = 171.65	I0 = 615.32
Vb = 2.3975	Ib = 0	V1 = 2225.40	I1 = 615.32
Vc = 2.3990	Ic = 0	V2 = 178.78	I2 = 615.32

CHAPTER 4: INVERTER MODELING FOR GRID FOLLOWING AND GRID
FORMING MODE FOR BOTH BALANCED AND UNBALANCED SYSTEM

Grid-tied inverters are typically modeled as a voltage source converter(VSC), where
the DC link voltage is maintained by a DC voltage source. Now the inverter oper-
ational characteristics and control objectives varies based on the mode of operation.
When the inverter is connected to the grid, it performs different grid applications
and operates in grid-connected mode. In grid following mode, the inverter tries
to regulate it's current output and provides a balance current output. When the
inverter is isolated from the power grid, it can serve local loads in a microgrid is-
landing application and operates in grid-forming mode. In grid-forming mode, the
inverter tries to regulate the voltage and magnitude at it's terminal. Also, the in-
verter has onboard-protection functionalities that supplements the control objective
and protects the inverter from abnormal conditions. This chapter discusses the de-
tails modeling and control architecture of inverter along with it's typical onboard
functionalities. This chapter shows the implementation of proposed inverter control
architecture in PSCAD® and the results show the functionalities of different mode
of operation. This Chapter also discusses how inverter based resource like Battery
Energy Storage (BESS) is modeled and studied for an Utility microgrid. The method
of finding the optimal placement of a BESS in Commonwealth Edison's Bronzeville
Microgrid(BCM) is presented.

4.1   Chapter Introduction

Voltage source converters (VSCs) are utilized in a variety of settings, from small
VSC-HVDC power converters for offshore wind generation [76, 77] to low-voltage

microgrid applications [78]. The majority of renewable energy sources, including photovoltaic panels, doubly fed induction generator (DFIG), and permanent magnet synchronous generator (PMSG) wind turbines, have successfully utilized a VSC as a grid connection interface. The most widely used method for controlling the VSC, synchronous reference frame vector control (SRFVC), has been shown to deliver satisfactory performance for balanced operation [79]. There has been an increase in interest in the creation of novel approaches to device control as a result of the grid's increased use of renewable energy. The so-called ride-through capability, which enables the device to remain connected to the grid without having to disconnect during various grid disturbances, is one important feature. The most common type of grid disturbance is voltage sags. They are voltage amplitude reductions that are typically categorized as balanced or unbalanced when the voltage reduction is the same for each phase. The starting transients of large machines and three-phase short circuits typically cause balanced voltage sags. The most prevalent types of imbalanced voltage sags are single-phase or two-phase short circuits [79]. The introduction of power reduction mechanisms into the SRFVC has demonstrated the ride-through capability for balanced voltage sags, as lowering the grid voltage causes the converter to reach its maximum allowed current. This, in turn, raises the voltage of the dc bus as a result of the excess power input to the bus [80, 81]. Ride-through capabilities for unbalanced voltage sags, on the other hand, face a number of difficulties. A ripple in the power supplied to the AC grid results from the presence of negative-sequence components in the voltage. This results in a ripple in the dc bus voltage, which may be critical in some situations [82]. Additionally, in order to lessen the dc bus's ripple, negative-sequence current must be controlled when negative-sequence voltage is present. The conventional SRFVC is made to control currents in the positive sequence, but it performs poorly when controlling currents in the negative sequence [83]. In the past, various options for alternative controller designs have been suggested. A

current reference calculation method for suppressing active power oscillations during unbalanced voltage sags was proposed in [84]. This method uses enhanced current controllers that are able to track reference current signals that contain both the positive and negative sequence. A new current control design with a double SRFVC and independent controllers for positive and negative components was introduced in [83]. This current control is used to coordinate the control of a DFIG turbine's back-to-back converter in [82] and [85] to reduce machine torque and the ripple of the dc bus voltage caused by network imbalances. A double SRFVC with linear quadratic regulator (LQR) current controllers is proposed in [86] for the operation of a PMSG wind turbine in the presence of unbalanced voltage sags. The coordinated control of the DFIG's back-to-back converter with proportional-resonant controllers and stationary frame current control is suggested in [87] and [88]. In addition, it has been demonstrated that the stationary frame control simplifies the structure of the current controller while still delivering satisfactory performance under VSC's unbalance operation [89]. In this Chapter, a negative sequence based inverter control architecture is presented that can serve both balanced and unbalanced load in grid following and grid forming mode of operation. Also, the method is used in a utility microgrid to evaluate the optimal placement of a BESS in the utility microgrid.

The main contributions of this chapter are:

- Presents a combined control architecture for grid-connected and grid-forming mode of control that works for both balanced and unbalanced system.

- The proposed inverter model also includes inverter onboard protection functionalities.

- Method for finding the optimal placement of a BESS in and utility microgrid system

The rest of the Chapter is structured as follows. Section 4.2 provides a description

of the inverter controls in grid following mode of operation. Section 4.3 describes the grid forming mode of control and the presents the controls architecture. Description of inverter on-board protection functionalities are listed in section 4.4. Section 4.5 presents the methodology of finding the optimal placement of a Battery Energy Storage Systems (BESS) in Commonwealth Edison's, an utility headquartered in Chicago, microgrid. Section 4.6 illustrates the simulation results to show the performance of proposed inverter models. Section 4.7 concludes the chapter and outlines the future work.

4.2   Inverter Controls for Grid Following Mode of Operation

A synchronization unit that is capable of precisely extracting the positive and negative sequences of the grid voltage is required in order to develop a control structure that can successfully operate during unbalanced faults. A Dual Second-Order Generalized Integrator PLL (DSOGI-PLL) [90] or a Decoupled Double Synchronous-Reference Frame PLL (DDSRF-PLL) are two examples of this. The current controller must be able to regulate both the positive and negative sequence currents in addition to accurately tracking the components of the positive and negative sequence. In most cases, PR controllers in the stationary reference frame or a dual-sequence SRF current controller in the synchronous reference frame with four proportional-integral (PI) controllers, two for each sequence component, are used to accomplish this. In addition, the manner in which the current reference is generated, the subject of this chapter, has a significant impact on the converter's behavior. Since this chapter aims to provide grid-supporting functionalities in accordance with contemporary grid codes, it is desired to employ a method that allows for the flexible injection and control of both positive and negative sequence currents. This includes injecting active power that is in sync with the voltage of the positive sequence, injecting capacitive reactive power that is in sync with the voltage of the positive sequence (positive-sequence support), and injecting inductive reactive power that is in sync with the voltage of the negative

Figure 4.1: Inverter control loop for a) positive sequence control in grid following mode, b)positive sequence control in grid forming mode, c)negative sequence control in grid following mode, and d)negative sequence control in grid forming mode .

sequence (negative-sequence attenuation). This work makes use of the flexible positive and negative sequence control (FPNSC) framework [90] to generate the current references, which will be calculated using the proposed strategy, in order to address this issue. In order to accomplish this, PR controllers are utilized to regulate the positive and negative sequence currents, and a DSOGI-PLL is utilized to extract the individual voltage sequences in this chapter.Figure 4.1a and Figure 4.1c shows the control loop during grid following mode of operation. Figure 4.1a shows that in grid following mode inverter follows active and reactive power set points and the i_d^+ and i_q^+ current references are generated accordingly to output the specified active and reactive power. Figure 4.1c shows that in grid following mode the inverter tries to reduce the negative sequence current to minimize output current unbalance.

4.3   Inverter Controls for Grid Forming Mode of Operation

The control methodology for grid forming mode of operation is presented here. In grid forming mode, inverter provides it's own voltage and frequency reference set points. And instead of following an active and reactive power set point the inverter tries to maintain the reference voltage and frequency . Figure 4.1b shows that in the positive sequence control loop inverter tries to maintain a V_d reference of 1 pu which indicates that inverter is trying to maintain 1 pu voltage. The frequency reference is kept at 60 Hz. Figure 4.1d shows that the unlike grid following mode in grid forming mode the inverter tries to supply negative sequence current so that it can serve unbalanced load. Figure 4.2 shows an enhancement of the already discussed control architecture .A new approach is proposed where the inverter negative sequence impedance is controlled by looking at the phase overvoltage and phase unbalanced at the grid point of interconnection (POI). Instead of controlling only voltage or current, the proposed approach can adjust both through controlling impedance.
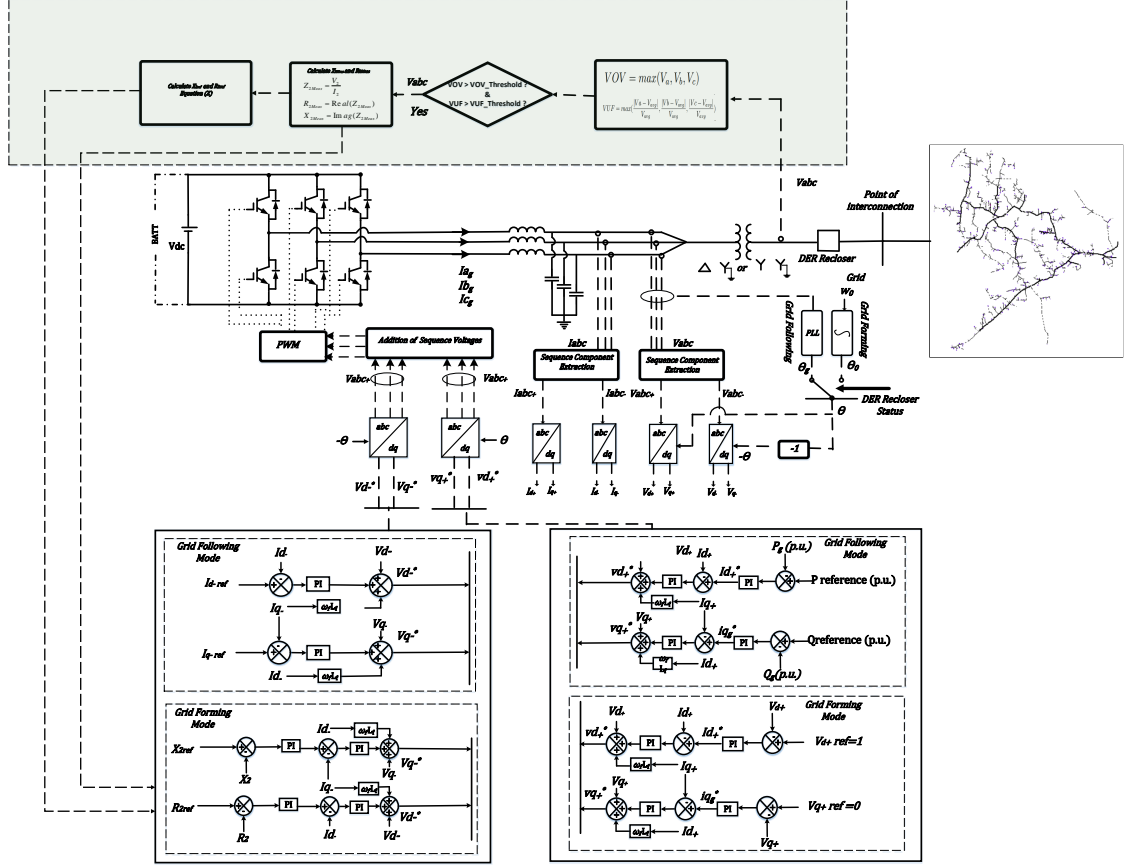
Figure 4.2: Inverter Control Topology with advanced negative sequence impedance control.

4.4   Inverter On-board Protection Design

Traditionally, power flow from substations to loads has been the goal of distribution systems. There are a number of security issues associated with DER integration with these distribution systems [91, 92, 93, 94]. Utility radial systems, for instance, may need to be upgraded or redesigned because they were typically intended for short-circuit sensing and unidirectional current flow. It may be necessary to replace relays without directional power flow sensing. Relays may not be able to detect some reverse-direction short-circuits, have insufficient sensitivity to detect them, and DER protection must work with the utility auto-reclosing scheme, among other things. Microgrids pose additional challenges due to the nature of their operation and the in-

corporation of DERs within them [71]. These challenges are in addition to those that independently connected DERs pose to their respective utility or grid systems. When operated in an island or grid-tied mode, for instance, microgrids are likely to have significantly different and varying short-circuit levels. They might only contribute a small amount of short-circuit current, especially from DERs that mostly use inverters (e.g., photovoltaics, battery-based energy storage, full-converter-based wind turbine generators, etc.). Microgrid feeders may have a power flow in both directions depending on how the generation, load, and circuit topology are different. During and after the microgrid's transition from grid-tied to island operation, a normally grounded distribution system may lose a relatively low-impedance zero-sequence path. It might be hard to find a utility source that has gone missing. Adapting microgrid protection systems to a new generation, circuit topology, or load should be carefully planned. When a microgrid moves from an island to a normal grid-tied mode, the process of resynchronizing it with its utility grid can cause issues like excessive inrush current, voltage and frequency disturbances, transient stability, and other issues. A commercial inverter is equipped with several onboard protection functionalities. Figure 4.3 provides an overview of the inverter functionalities. Inverter has several trip mechanisms in the form of islanding detection, DC overvoltage protection, Inverter AC overvoltage and Over-current protection, transient overvoltage protection, insulation monitoring and voltage & frequency ride through.

4.5   Optimal Placement of Battery Energy Storage (BESS) in an Utility Microgrid

Common Wealth Edison (Comed's) Bronzeville Community Microgrid (BCM) is an advanced microgrid testbed that is used to test various emerging microgrid technology.

The BCM microgrid is served by two feeders. The details of the microgrid one line diagram can not be provided because of confidentiality reasons. There are several operating modes for the microgrid. When both the feeders that are feeding the microgrid experience an outage the microgrid is operated in "Full Islanding" mode. In
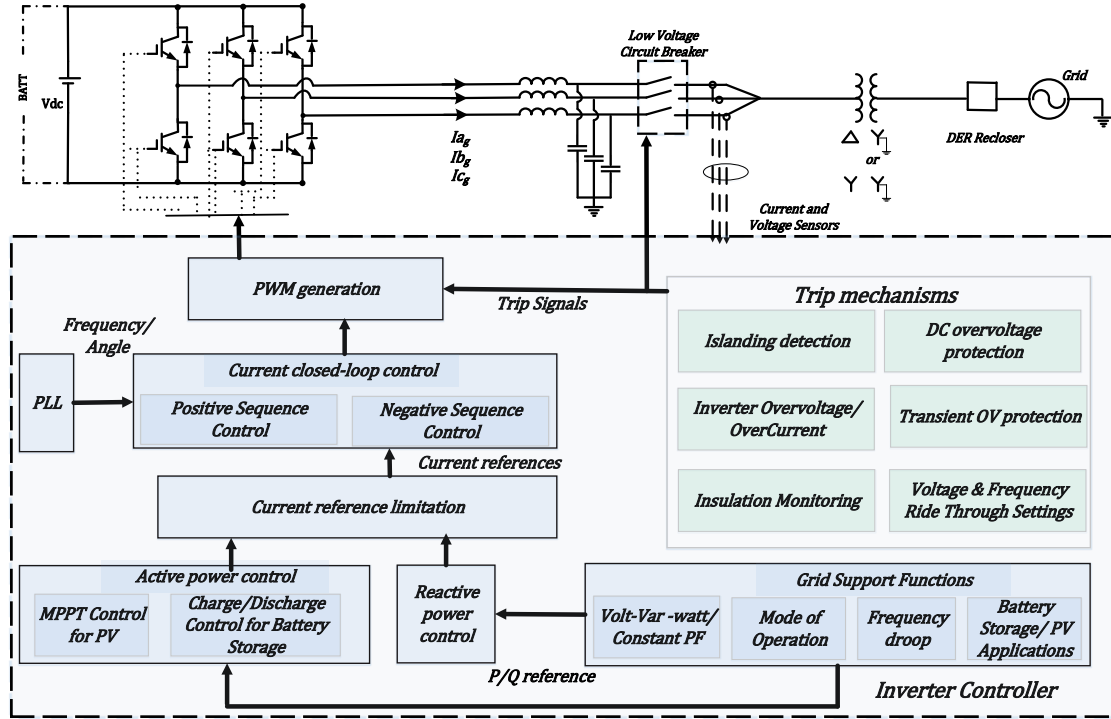
Figure 4.3: Inverter On-board functionalities.

this mode, the microgrid is completely isolated from the bulk power grid and microgrid loads are served from the microgrid generation only. Currently, the microgrid has a 4.8 MW Gas generator, 750 kW solar, and a 500kW/2000 kWh battery energy storage system (BESS). Solar operates at a unity power factor. The microgrid has a maximum generation capacity of 6 MW. Figure 4.4 below shows the microgrid annual load profile (MW) for the year 2021. It is noticeable from the figure that during peak season there are times when the microgrid load exceeds the max generation capacity of 6 MW. This prompted the addition of a new BESS in the BCM microgrid. In this chapter a method for finding the optimal location of the new BESS for BCM thoroughly discussed. There are several factors that need to be accounted for to determine the optimal location of the new BESS.
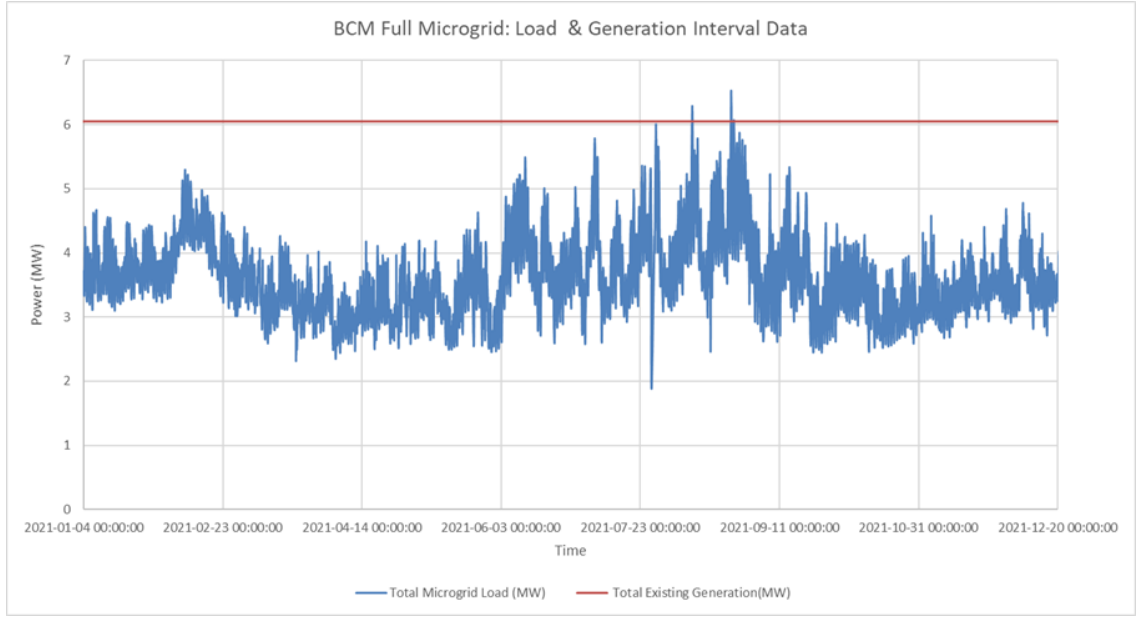
Figure 4.4: Annual microgrid load (MW) profile for 2021 and max generation capacity
.

4.5.1   Problem Formulation

To find the optimal location of the BESS it is important to define the objective function. The main objective is to reduce the runtime and power generation of the gas generator and serve the critical loads during a full islanding scenario. This will help to use the renewable resources more during microgrid operation and hence will lead to a more sustainable operation of the microgrid during a grid outage. The optimal location also needs to ensure that the microgrid voltages at all nodes are within the ANSI voltage class A range and that the thermal limits of the conductors and the equipment are not exceeded. Moreover, each generating source also needs to abide by its local operating constraints. The BESS needs to run within the maximum and minimum state of charge (SoC) range. The max SoC was set at 95% and the min SoC was set at 5%. The gas generator has a maximum and minimum power output limit of 250 kW and 4800 kW respectively. The solar generation is controlled by the solar irradiance data. . A mathematical model is formed to express the logic as shown in eqns 4.1- 4.10 .

$$Minimize, \sum_{i=1}^{N} P_{gas}^{i} * [t(i) - t(i-1)] \tag{4.1}$$

$$Subject\,to, \tag{4.2}$$

$$P_{gas}^{i} + P_{pv}^{i} + P_{BESS1}^{i} + P_{BESS2}^{i} = P_{Load}^{i}$$

$$Q_{gas}^{i} + Q_{pv}^{i} + Q_{BESS1}^{i} + Q_{BESS2}^{i} = Q_{Load}^{i} \tag{4.3}$$

$$V_{min} \leq V_{x}^{i} \leq V_{max} \tag{4.4}$$

$$P_{gas,min}^{i} \leq P_{gas}^{i} \leq P_{gas,max}^{i} \tag{4.5}$$

$$P_{Equipment}^{i} \leq P_{Equipment,max}^{i} \tag{4.6}$$

$$SoC_{BESS1,min}^{i} \leq SoC_{BESS1}^{i} \leq SoC_{BESS1,max}^{i} \tag{4.7}$$

$$SoC_{BESS2,min}^{i} \leq SoC_{BESS2}^{i} \leq SoC_{BESS2,max}^{i} \tag{4.8}$$

$$SoC_{BESS1}^{i} = SoC_{BESS1}^{i-1} - \frac{P_{BESS1}^{i} * [t(i) - t(i-1)]}{ERated_{BESS1}} \tag{4.9}$$

$$SoC_{BESS2}^{i} = SoC_{BESS2}^{i-1} - \frac{P_{BESS2}^{i} * [t(i) - t(i-1)]}{ERated_{BESS2}} \tag{4.10}$$

$$Where,$$

$$(4.11)$$

$$P_{gas}^i = Active \quad power \quad output \quad of \quad gas \quad generator \quad at \quad time \quad step \quad i$$

$$P_{pv}^i = Active \quad power \quad output \quad of \quad photovoltaic \quad at \quad time \quad step \quad i$$

$$P_{BESS1}^i = Active \quad power \quad output \quad of \quad BESS \quad 1 \quad at \quad time \quad step \quad i$$

$$P_{BESS2}^i = Active \quad power \quad output \quad of \quad BESS \quad 2 \quad at \quad time \quad step \quad i$$

$$Q_{gas}^i = Reactive \quad power \quad output \quad of \quad gas \quad generator \quad at \quad time \quad step \quad i$$

$$Q_{BESS1}^i = Reactive \quad power \quad output \quad of \quad BESS \quad 1 \quad at \quad time \quad step \quad i$$

$$Q_{BESS2}^i = Reactive \quad power \quad output \quad of \quad BESS \quad 2 \quad at \quad time \quad step \quad i$$

$$P_{Equipment,max}^i = Equipment \quad rating$$

$$V_{max} = Voltage \quad Max \quad Limit \quad = \quad 1.05pu$$

$$V_{min} = Voltage \quad Min \quad Limit \quad = \quad 0.95pu$$

$$P_{gas}^{min} = Minimum \quad gas \quad generator \quad output \quad power \quad = \quad 250 \quad kW$$

$$P_{gas}^{max} = Maximum \quad gas \quad generator \quad output \quad power \quad = \quad 4800 \quad kW$$

An optimization problem is solved to determine the optimal dispatch profile for the two BESS systems and the gas generator. Solar profile generation data is also fed into the model. Load data for the microgrid is also an input to the model. The profile determined by the optimization routines is introduced in the CYME model to run a time series analysis and it is checked that if the resources are run as per the optimization routine whether it will be able to meet the voltage and thermal limit of the microgrid. Then the results of the CYME time series are fed back to the optimization routine and then the optimization is run for a new location of the new BESS. Figure 4.5 below shows the overall implementation flow chart. And Figure 4.6
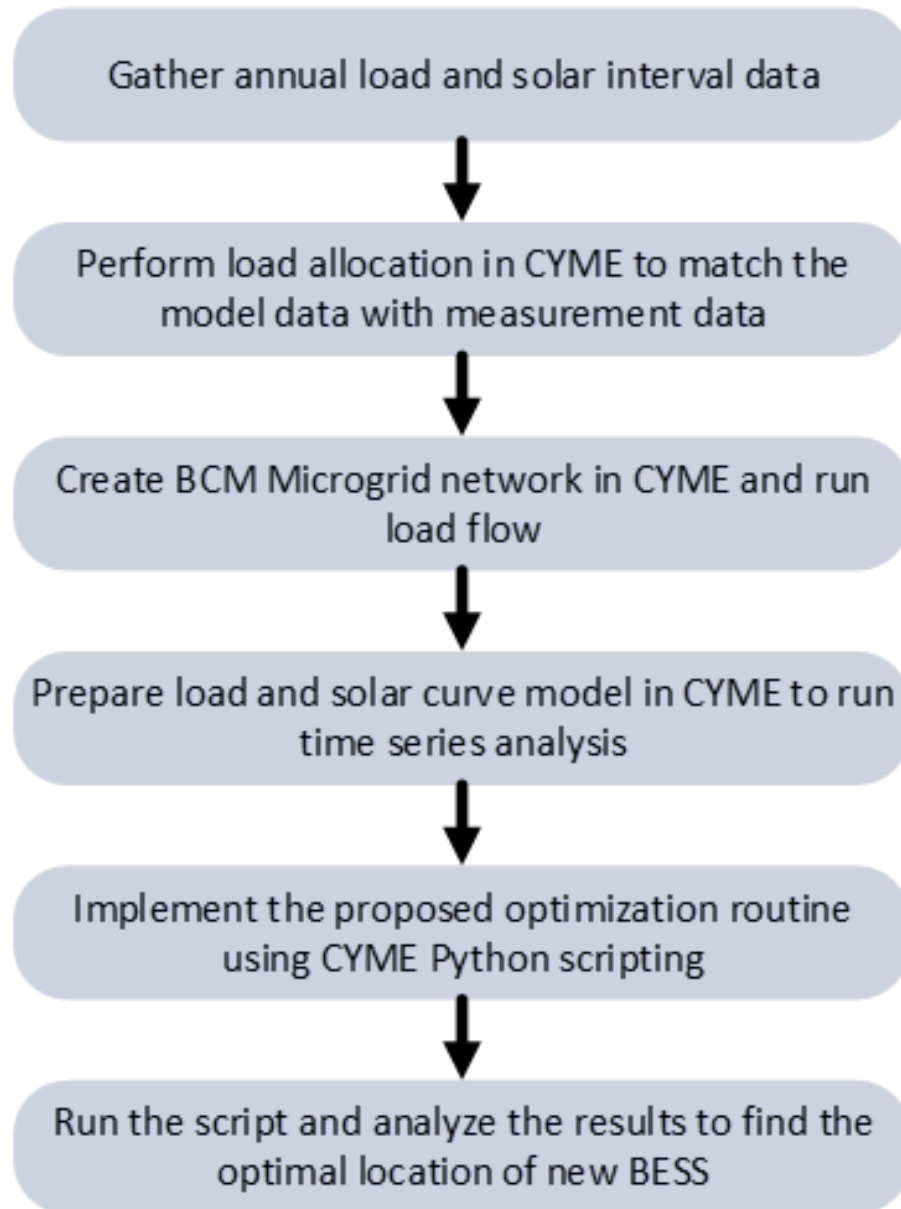
Figure 4.5: Flow chart of the implementation of proposed method .

shows how the data flows between different tools and how the studies have been performed.

4.5.2   Protection Screening

Once the optimal location for the new BESS is selected based on the optimization routine mentioned above, the next step is to perform protection adequacy screening with the addition of new BESS. First step in protection screening is to perform short
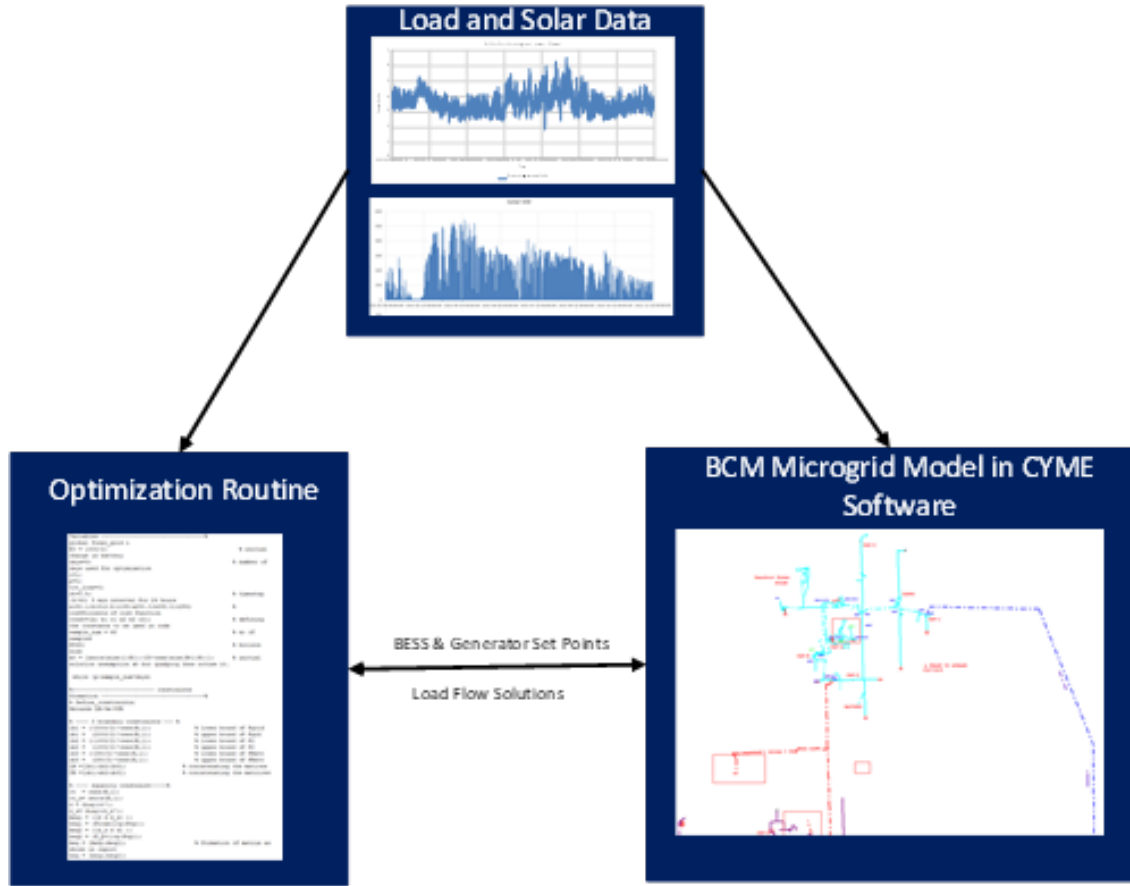
Figure 4.6: Data flow between different tools for the implementation of proposed method.

circuit studies. Addition of the new BESS increased the faults currents for both symmetrical faults and unsymmetrical faults in microgrid mode of operation. The microgrid in full islanding mode also has the gas generator connected which provides a significant amount of fault current. Even though the addition of new BESS increased the fault current but it is not significant compared to the fault current without the new BESS. As a result the sensitivity and the selectivity of the existing protection is not affected a lot. The addition of new BESS creates scenarios where only the inverter based resources (BESS and PV) can carry the microgrid load at certain times of the year. In case of only inverter generation based microgrid operation the available fault currents from the sources will not be enough for the existing overcurrent protection scheme. And, this will need development of new custom protection scheme for the

microgrid.

4.6   Simulation Results

The efficacy of the proposed inverter models are validated in this section through simulation. An IEEE test system and an utility microgrid system is used show the performance of proposed inverter models. Firstly, different control mode of operation is shown in IEEE test systems case. secondly, limited simulation results are shown for the utility microgrid system.

4.6.1   Case: IEEE Test Systems

The procedure for setting protective device settings for a distribution system, such as an IEEE 34 node unbalanced test system [6], is discussed in this section. The 34-node test feeder is a radial distribution feeder that has spot and distributed loads, in-line step-down transformers, two voltage regulators, overhead and underground lines with different phasing, and a radial distribution feeder. Between nodes 832 and 888, there is a transformer with a rating of $0.5MVA$ and a voltage rating of $24.9kV/4.16kV$. The substation's positive and zero sequences impedances are listed in [6]. An EMT program known as PSCAD® is used to create the test system (Figure 4.7). Relays, reclosers, fuses, and circuit breakers are added to the test system as a protective measure. Feeder protection is provided by the addition of a numerical relay substation circuit breaker. To divide the circuit into smaller zones and offer better isolate faults, three line reclosers (R0, R1, and R2) are added (Figure 4.7). In order to safeguard both single-phase and double-phase loads, two additional fuses, F1 and F2, are installed in the laterals. The inverter is operated in grid forming mode and is the only generating resource in the microgrid. The islanding recloser (IR) is open and disconnects the microgrid from the main grid. Figure 4.8a shows the active power of the microgrid supplied from the inverter. The microgrid loads are unbalanced which is evident from the figure. Figure 4.8b shows the reactive power of

all the phases in the microgrid. Figure 4.8c shows that the all three phase voltages are pretty stable during the microgrid operation. Figure 4.8d shows that the all three phase current wave forms are also stable during the microgrid operation.
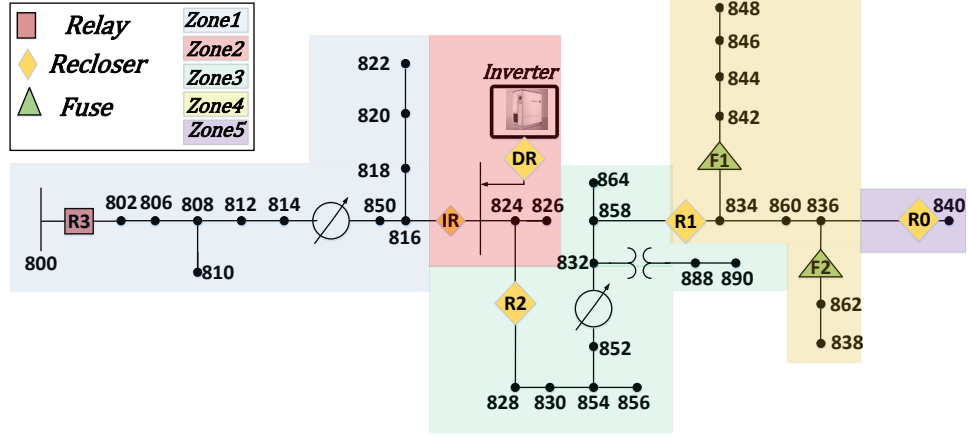
Figure 4.7: Modified IEEE 34 bus test system with protection devices and utility scale inverter connected [6].

4.6.2   Case: Utility Test Scenario

In this case the results of the method presented in section 4.5 are discussed. The Bronzeville Community Microgrid (BCM) model is developed in CYME® software. The microgrid already have an existing BESS Of 500 kW/2000 kWh. A new BESS is designed in CYME with inverter and other components. A microgrid study is performed using the CYME® microgrid module.Where multiple sectionalizers are opened to create a full islanding scenario. The optimization routine outlined in section ?? is implemented as described in Figure 4.6. Four locations have been studied as possible location of new BESS 2 based on availability of real-estate. Then the optimisation routine is run to determine the optimal dispatch of different generating resources with an objective to minimize the run time of gas generators. Figures 4.9a, 4.9b, and 4.9c show active power, reactive power and Point of Common Coupling voltage of BESS 2 , respectively, for one example day results in case of possible location 1. Similarly, Figures 4.10a, 4.10b, and 4.10c show active power, reactive power and
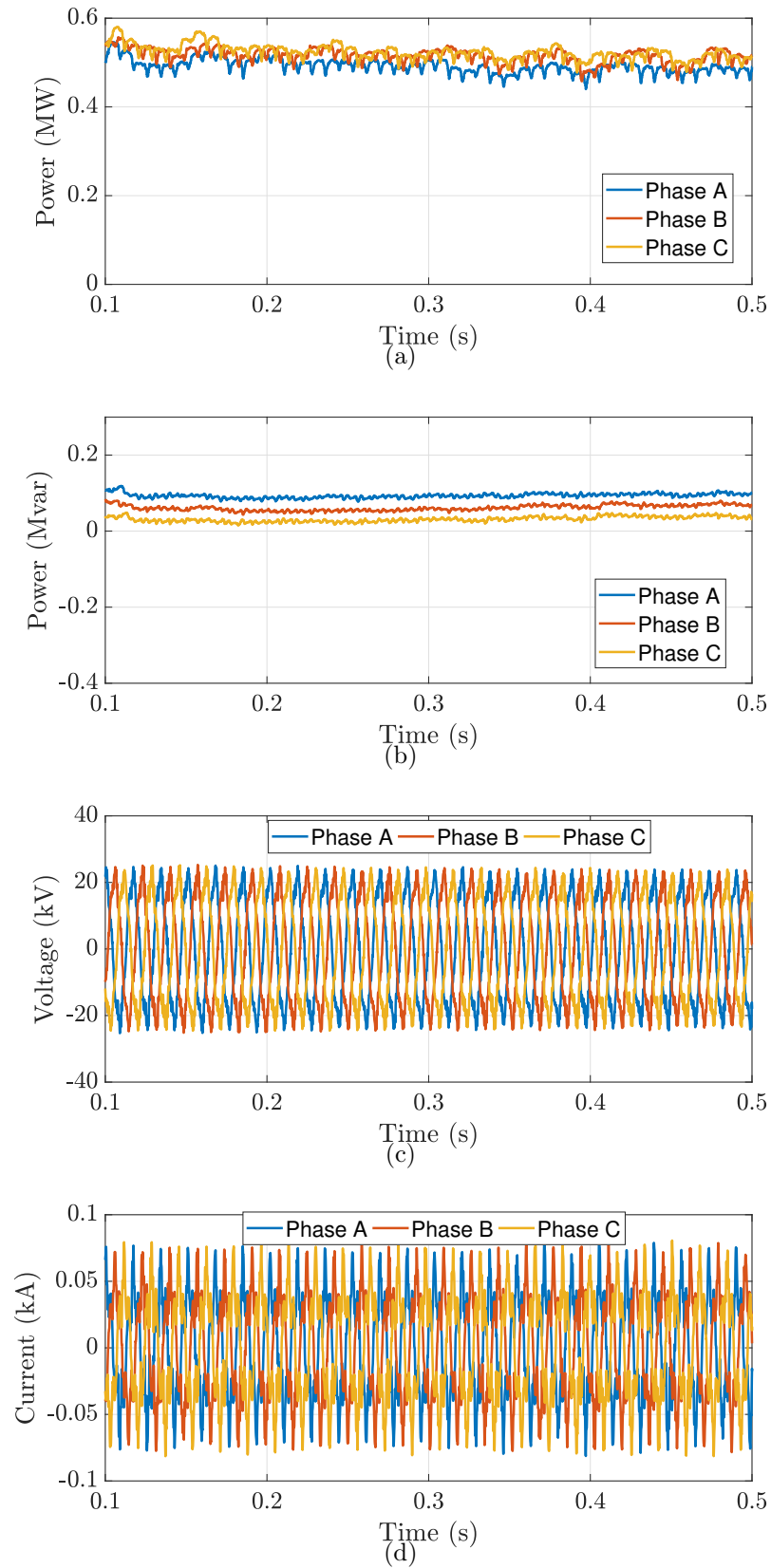
Figure 4.8: Microgrid power for all phases in grid forming mode (a) active Power, (b) reactive Power, c) Phase voltages, and d) Phase currents.

Figure 4.9: BESS2 Possible Location 1 (a) Active Power of different resources , (b) Reactive Power of different resources, (c) voltage profiles at BESS POI .

Point of Common Coupling voltage of BESS 2 , respectively, for one example day results in case of possible location 2. Similar, example results are shown for other locations as well. Figures 4.11a, 4.11b, and 4.11c show active power, reactive power and Point of Common Coupling voltage of BESS 2 for possible location 3. And, Finally, Figures **??**, **??**, and **??** show active power, reactive power and Point of Common Coupling voltage of BESS 2 for possible location 4. It is observable from the different figures that the active and reactive power dispatch of the generating resources varies with possible locations of BESS 2. Also, the voltages at the microgrid is maintained within the normal operating range for all the cases. With the proposed method location 2 was selected as the optimal location with the least run-time for the gas generator. One thing to note is that the microgrid has a significant amount of load and need support from the gas generator most often.

4.7   Chapter Summary

This chapter presents a comprehensive overview of inverter controls and functionalities. Grid following inverter controls are more well known as these are used for solar inverters. However, grid forming inverter controls which are required for IBMG operations is significantly different from typical grid following inverter controls. This chapter highlights the differences in control modes. Depending on how the inverter controls are modeled the fault response of the inverter can vary a lot. Grid forming control strategies are presented and simulation results are shown for a test system. Results show that the grid forming inverter controls can maintain the voltage and frequency of a microgrid very stable and well withing standard limit. It has also been shown how these inverter modeling approach can be applied in an utility microgrid to find the optimal location of BESS within the microgrid. The next chapter presents how the inverter control can be leveraged to enhance the microgrid design and help mitigate grid integration challenges of inverter based resources.
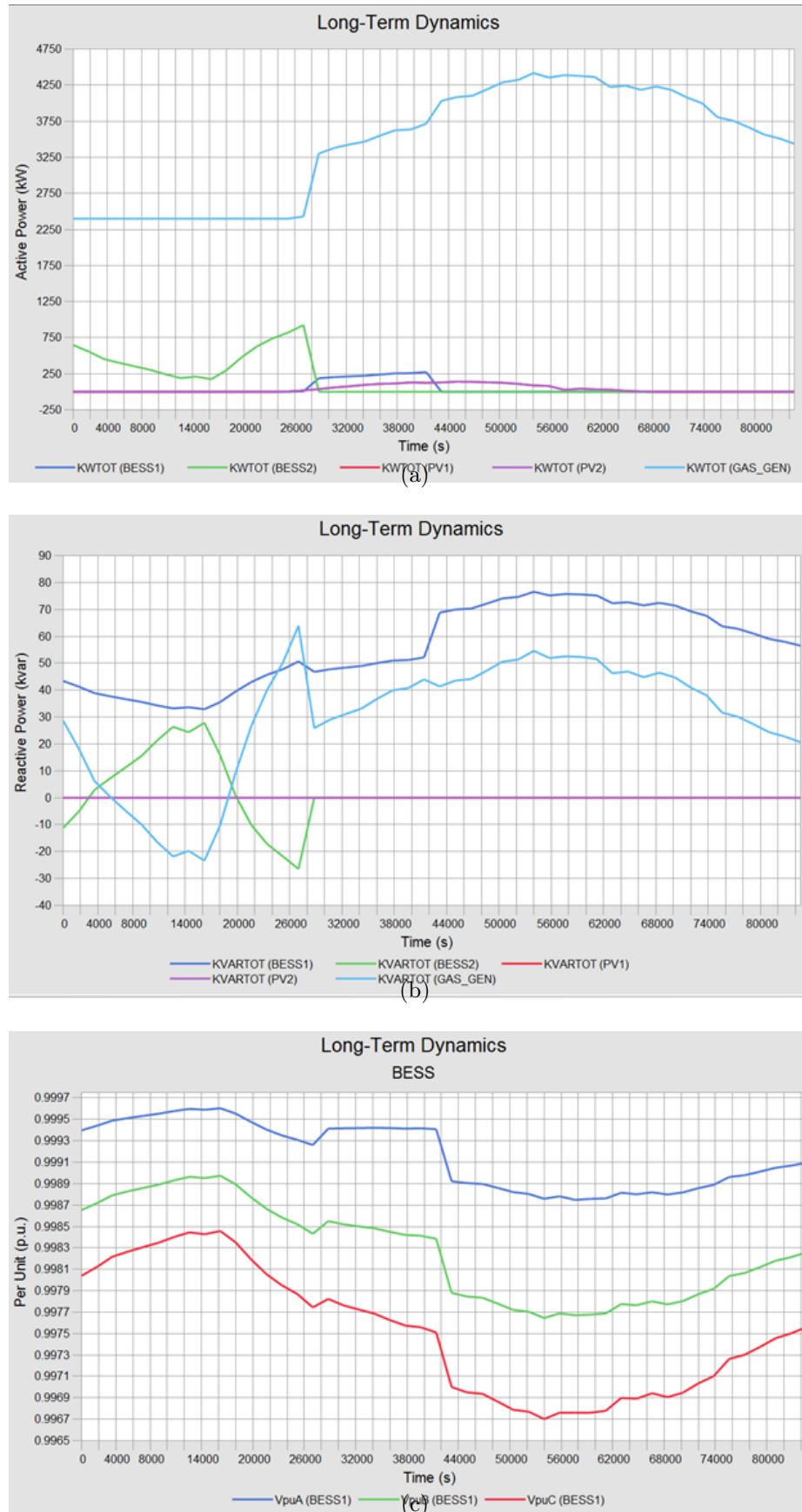
Figure 4.10: BESS2 Possible Location 2 (a) Active Power of different resources , (b) Reactive Power of different resources, (c) voltage profiles at BESS POI .
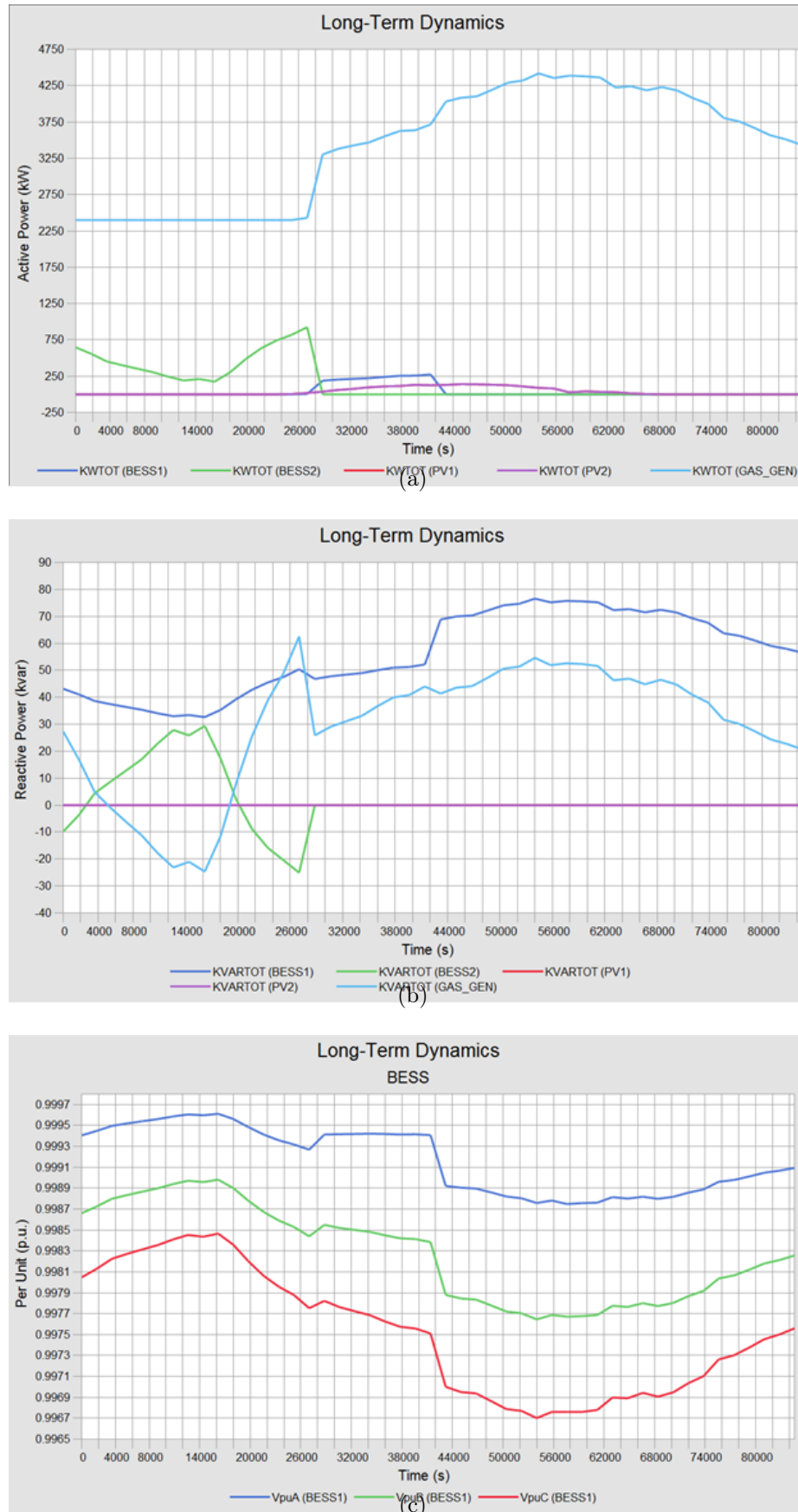
Figure 4.11: BESS2 Possible Location 3 (a) Active Power of different resources , (b) Reactive Power of different resources, (c) voltage profiles at BESS POI .
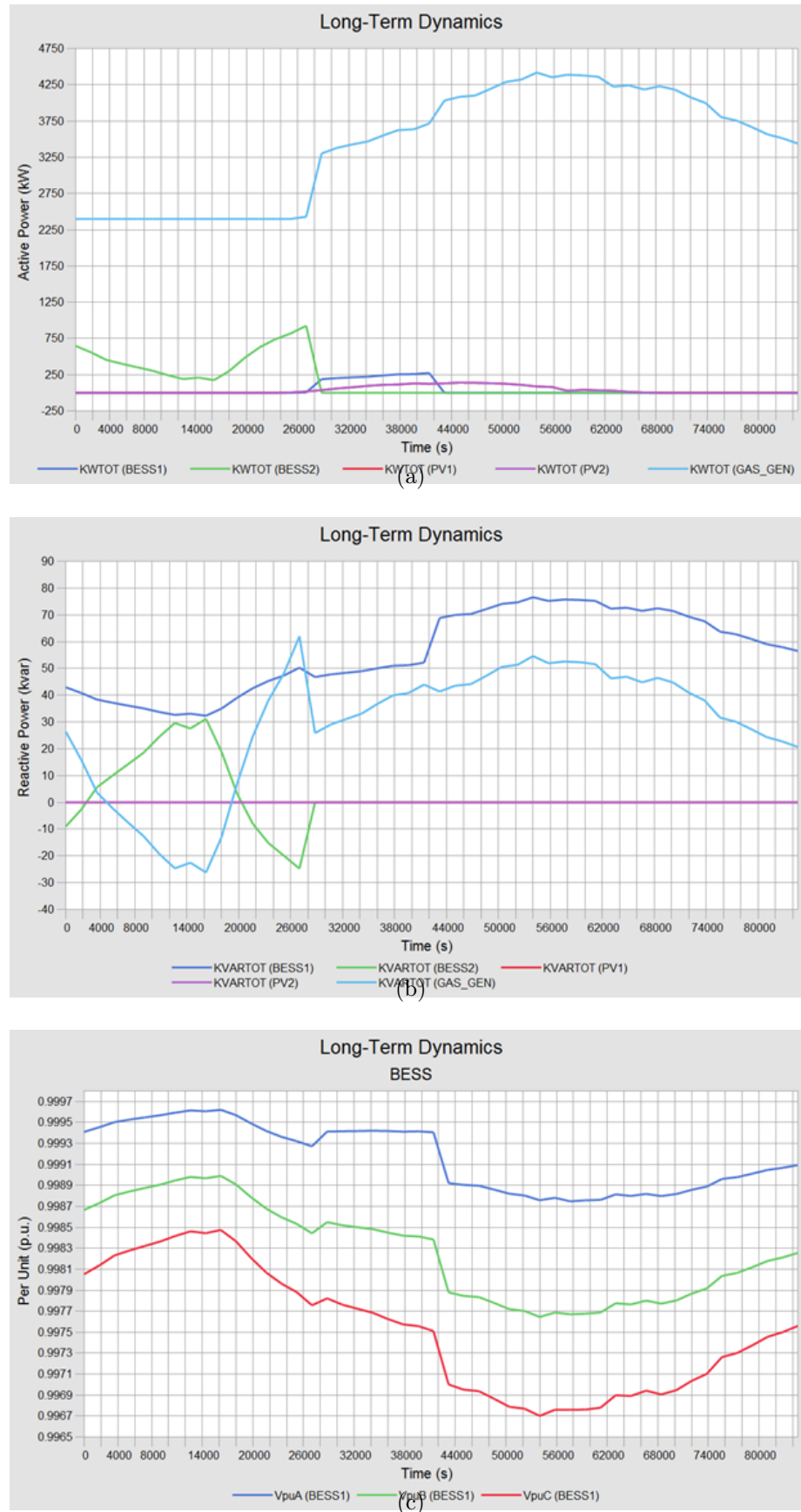
Figure 4.12: BESS2 Possible Location 4 (a) Active Power of different resources , (b) Reactive Power of different resources, (c) voltage profiles at BESS POI .

CHAPTER 5: CONTROL OF TRANSIENT OVERVOLTAGE FOR INVERTER
ONLY BASED MICROGRID IN POWER DISTRIBUTION SYSTEM

When connecting inverter-based generation resources to a four-wire distribution
system, TOV is an important design consideration.Photovoltaic (PV) inverters oper-
ating in a grid-following mode of operation were the subject of previous research into
temporary overvoltage caused by GFOV and load rejection overvoltage (LROV).Due
to its contribution to improving the resilience of the power system, the grid-forming
mode of operation of inverters has received increased attention.The overvoltage ob-
served in the system during an unbalanced ground fault can be affected by the control
methodology of an inverter, which determines how it responds to faults.To help re-
duce the risk of transient overvoltage, a method for controlling the negative sequence
impedance during a ground fault is proposed. On a small system and an IEEE 34 bus
test system, PSCAD® is used to perform an electromagnetic transient simulation to
verify the characteristics of the inverter and the method's efficacy.

5.1   Chapter Introduction

Microgrid implementation has garnered interest in recent grid advancements and
the incorporation of renewable energy generation [64, 95]. Not only can a microgrid
serve a remote community or a critical load [65], but it can also boost the system's
resilience and dependability [96]. The work in both [19] and [66] point to the potential
for utility energy efficiency and cost savings offered by microgrids as one essential
component of resilient distribution systems.

A power electronic interfaced converter connects numerous renewable resources to
the grid. Coordination among protective devices, transformer configuration for inter-

connection, and load rejection overvoltage are just a few of the difficulties associated with an IBR microgrid. The design of a system for distribution integration presents a significant obstacle in the form of TOV. TOV is caused by a number of factors, including ferroresonance, generation to load ratio, and a single line to ground fault. A single line to ground fault can cause significant overvoltage in an electric power system supplied by an ungrounded source [97, 98]. TOV poses a serious threat to the power system's safe and dependable operation [67] and the catastrophic failure of surge arresters. The system must be designed to ensure effective grounding in all operating scenarios in accordance with IEEE standard C62. 92. 1 [68]. Depending on the configuration and requirements of the utility system, effective grounding restricts the overvoltage to 125-138 percent of the nominal voltage. By introducing a low impedance return path, effectively grounded systems quickly respond to ground faults [99, 100].

Systems are designed to meet the following criteria for zero sequence reactance, resistance, and positive sequence reactance: $0<\frac{X_0}{X_1}<3$ and $0<\frac{R_0}{X_1}<1$. Effective grounding criteria for synchronous machine-based generations are well defined [69, 101]. According to IEEE standard C62. 92. 6 [70], the GFOV mechanism differs for current regulated resources, such as an inverter, and varies depending on the inverter control topology. However, a system's effective grounded depends on a number of things, like the design of the utility system and the configuration of the inverter and distribution interconnection transformer. As discussed in [102, 103], some utilities require effective grounding for their system.

Effective grounding can be significantly affected by the winding configuration of an IBR step-up transformer [104, 100]. For PV inverters, transient overvoltage has been thoroughly investigated [105, 106]. In [107], only the inverter's grid-following mode's ground fault overvoltage was investigated. As a result, grid formation requires a comprehensive discussion of ground fault overvoltage. Both synchronous machines

and an inverter's TOV mechanisms, ground fault and load rejection overvoltage, are examined in this chapter. To reduce phase overvoltage and phase unbalance in microgrids, a method for controlling the negative sequence impedance of an inverter is proposed.

The initial findings of this work has been published into [5] and then the work is further expanded in this chapter. The main contributions of this chapter are:

- For inverter machine-based microgrids, expressions for phase overvoltage and investigation of TOV, when the inverters operate in grid forming mode.

- Proposed method to control inverter negative-sequence impedance to mitigate the phase overvoltage and voltage unbalance observed in the microgrid.

- Comparison of the overvoltage results for different inverter control modes and transformer configurations.

- Dynamically adjust the inverter negative-sequence impedance to mitigate the phase overvoltage and voltage unbalance for varying system conditions, fault locations and DER sizes.

- Novel algorithm for calculating the required inverter negative-sequence impedance for secure and safe operation of microgrid.

The rest of the chapter is organized as follows: Section 5.2 presents the theoretical background related to ground fault overvoltage,and inverter modeling. Section 5.3 describes the proposed negative sequence impedance control methodology. Simulation results are discussed on Section 5.4 and Section 6.5 concludes the chapter and outlines the future work.

5.2   Modeling of Ground Fault Overvoltage for Inverter based DERs

For the modeling, Voltage expressions for an IBR are presented. The IBR is represented by a current source in the positive sequence and negative sequence impedance,

with the negative sequence impedance varying per on the inverter control objectives [70, 108].

5.2.1 Without Effective Grounding

Per the network shown in Figure 5.1a, voltage expressions are derived in this section for an IBR without effective grounding.

After solving the network, (5.1) and (5.9) present expressions for the sequence voltage and phase voltages.

$$Z_{th1} = \frac{Z_b \times Z_{load2} Z_{load1} + Z_a \times Z_{load0} Z_{load1}}{Z_b \times Z_{load2} + Z_a \times Z_{load0}}$$

$$+ Z_b + Z_{load2} \times Z_{load1} \tag{5.1}$$

$$Z_{th2} = \frac{Z_b \times Z_{load2} + Z_a \times Z_{load0}}{Z_a} \tag{5.2}$$

$$Z_{th3} = \frac{Z_b \times Z_{load2}}{Z_a} \tag{5.3}$$

$$Z_a = (Z_{xfmr} + Z_{inv2} + Z_{load2}) \tag{5.4}$$

$$Z_b = Z_{xfmr} + Z_{inv2} \tag{5.5}$$

$$V_1 = Z_{th1} \times I \tag{5.6}$$

$$V_0 = Z_{load0} \times I_1 \tag{5.8}$$

$$V_2 = Z_{th3} \times I_1 \tag{5.7}$$

$$I_1 = (\frac{Z_{L1}}{Z_{th2} + Z_{L1}}) \times I \tag{5.9}$$

5.2.2 With Effective Grounding

The sequence network for an unground inverter source is displayed in Figure 5.1b, which also includes a grounding transformer. The negative sequence impedance, which can be controlled by the inverter, is the determinant of the voltage expression in (5.10). To effectively mitigate overvoltage, an inverter's response must be understood,

as stated in Per [70].

$$Z_{th1} = \frac{Z_b \times Z_{load2} Z_{load1} + Z_a \times Z_{loadT} Z_{load1}}{Z_b \times Z_{load2} + Z_a \times Z_{loadT}}$$

$$+Z_{xfmr} + Z_{inv2} + (Z_{load2} \times Z_{load1}) \qquad (5.10)$$

$$Z_{th2} = \frac{Z_b \times Z_{load2} + Z_a \times Z_{loadT}}{Z_a} \qquad (5.11)$$

$$Z_{th3} = \frac{Z_b \times Z_{load2}}{Z_a} \qquad (5.12)$$

$$Z_a = (Z_b + Z_{load2}); Z_b = Z_{xfmr} + Z_{inv2} \qquad (5.13)$$

$$V_1 = Z_{th1} \times I \qquad (5.14) \qquad\qquad V_0 = Z_T \times I_1 \qquad (5.16)$$

$$V_2 = Z_{th3} \times I_1 \qquad (5.15) \qquad\qquad I_1 = (\frac{Z_{L1}}{Z_{th2} + Z_{L1}}) \times I \qquad (5.17)$$

(a)   (b)
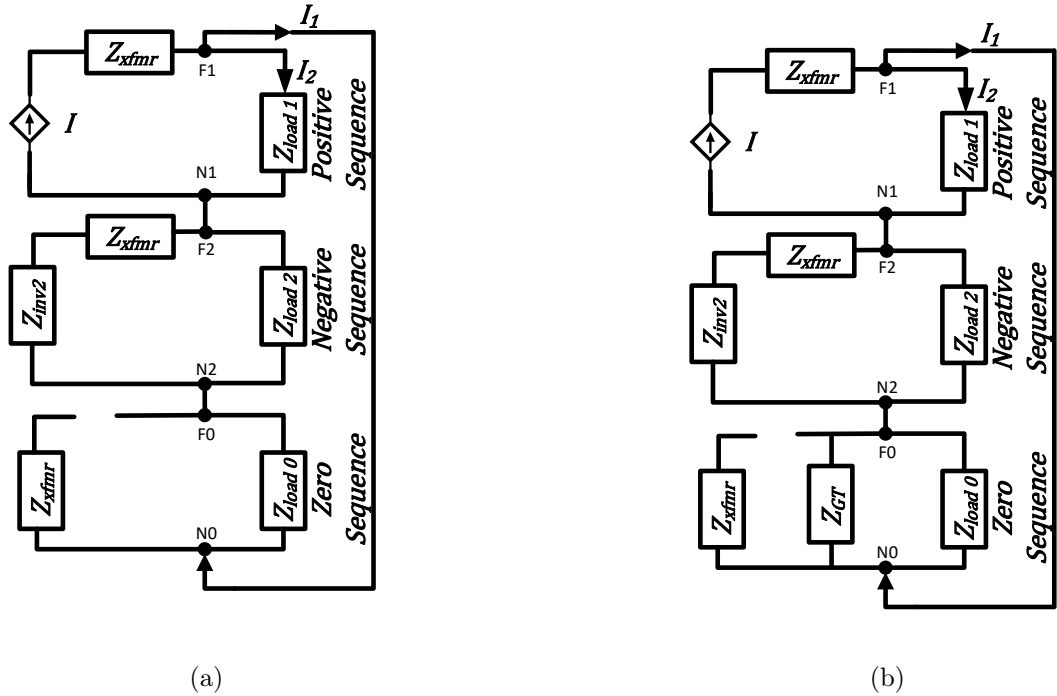
Figure 5.1: Sequence network of inverter for a single line to ground fault (a) without grounding transformer, (b) with grounding transformer [5].

The system's overvoltage varies as well due to the inverter's wide range of negative

sequence impedance variations based on control mode. The maximum overvoltage that can be observed in an unground system with a one-to-one generation to load ratio during a single line-to-ground fault is shown in Figure 5.2. When the inverter is used as a current-regulated source in the grid-connected mode, the overvoltage in the healthy phases is not as severe as it would be in a synchronous machine. The X_2/R_2 ratio and the negative sequence resistance both have a significant impact on the magnitude of the voltage. For a negative sequence reactance of 0.5 to 2.5 pu, the voltage has a greater magnitude at a lower resistance $(< 1pu)$. The overvoltage decreases if the resistance rises $(> 1pu)$.
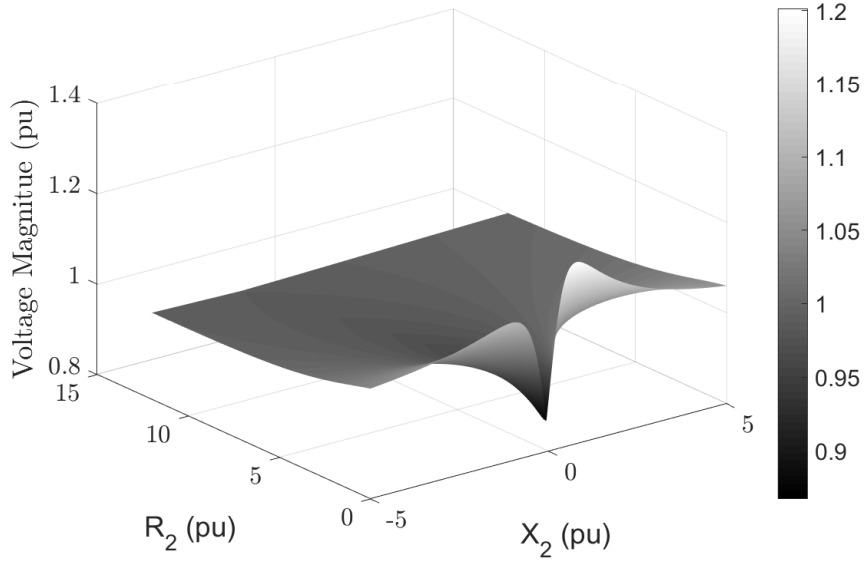
Figure 5.2: Maximum overvoltage observed versus inverter negative sequence impedance (R_2 and X_2) [5].

5.2.3   Effect of Inverter Control Topology on Inverter Negative Sequence Impedance

Unintentional islanding with an ungrounded source is the result of the IBR's $Yg-Y$ step-up transformer connection to the grid, where the voltages in other healthy phases at the load bus jump up to 1.27pu, as shown by Figure 5.3a, and the DER recloser opens to clear the fault at 1.3s. The DER recloser is opened for the purpose of
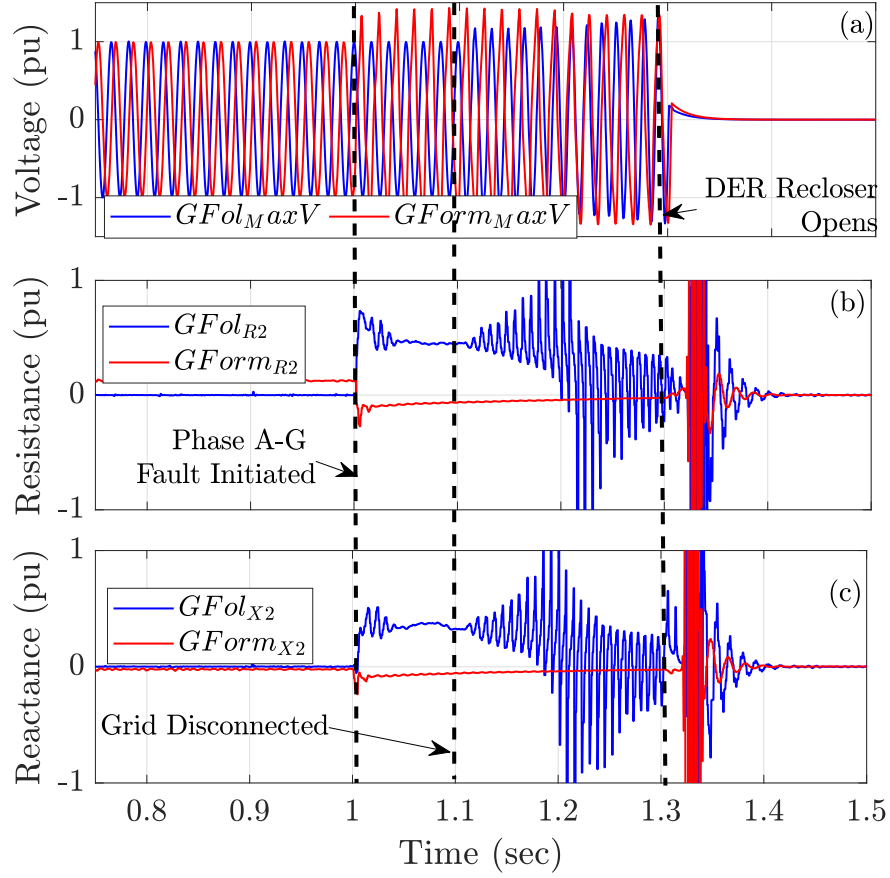
Figure 5.3: grid following mode 1:1 generation to load ratio a) Phase voltage, b) Negative sequence resistance c) Negative sequence reactance [5].

studying the temporary overvoltage 0.2 seconds after the grid disconnects.

The effective negative sequence impedance at the inverter terminal is depicted in Figure 5.3b and Figure 5.3c. The impedance is $0.5 + 0.4j$pu during a ground fault when the grid serves as a ground reference between 1s and 1.1s.

When the inverter is in grid-forming mode and a line to ground fault is applied, the Figure 5.3a display indicates a 1.38pu overvoltage. The negative sequence impedance for grid forming mode is $0.002 - 0.04j$pu, as shown by Figure 5.3b and Figure 5.3c. In this test, the grid-forming mode does not have a negative sequence current control and exhibits more overvoltage than the grid-following mode.
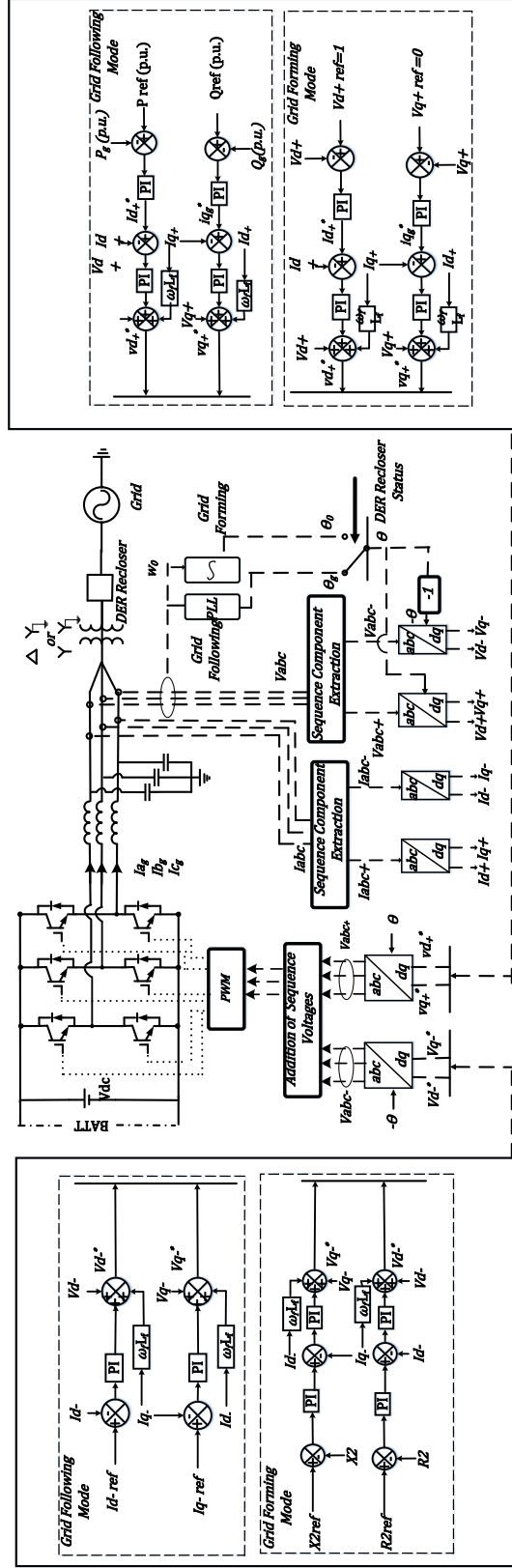
Figure 5.4: Inverter design architecture with proposed method [5].
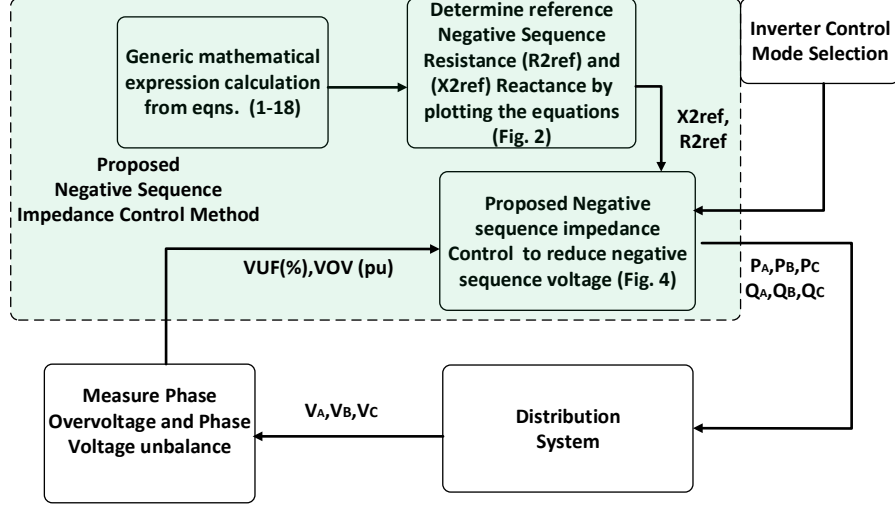
Figure 5.5: Implementation flowchart of proposed negative sequence impedance control [5].

5.3   Proposed Methodology

The grid-tied inverter's general configuration, which can operate in grid following or grid forming mode, is depicted below for the inverter (Figure 5.4). The outer control loop in Figure 5.4 demonstrates how the control objective varies for various inverter operation modes, where the inverter adjusts accordingly. The inverter operates in the grid following mode to conform to the application-specific active and reactive power setpoints (e. g., PV smoothing, energy time-shift, etc.). Figure 5.4 shows the control loop for positive sequence control, in grid following mode, where the active and reactive power setpoints are used to generate the reference for the inner current control loop, which is then used to generate the references for the positive sequence voltage. In grid forming mode, the inverter tries to keep the islanded section's voltage and frequency as close to their nominal values as possible. The phase-locked loop (PLL) is given a constant frequency of 60 Hz, and a $d - q$ reference frame is used to set the unity voltage reference point. The outer control loop for grid forming mode is shown by the inverter in Figure 5.4, which makes use of V_d and V_q to generate the reference signals. The inverter's capacity to regulate negative sequence current is yet

another feature.

This chapter introduces an outer control loop that is applied on top of the inner negative sequence current control loops. During unbalanced operating conditions, this loop controls the effective negative sequence impedance seen at the inverter terminal by using the negative sequence resistance and reactance as an input reference. Figure 5.2 demonstrates that the overvoltage decreases at specific values of R_2 and X_2. The reference points for R_2 and X_2 have been chosen to be $1pu$ and $-0.1pu$, respectively. The flowchart for putting this proposed control architecture into action is shown in Figure 5.5.

5.3.0.1   Automated measurement of R_2^{Ref} and X_2^{Ref} using system voltage and current

This section discussed the automated measurement of the negative-sequence impedance, R_2 and X_2, using the system voltage and current. Recall the impedance, $Z_{inv} = \frac{V_{inv}}{I_{inv}}$, as a function of the voltage and current. Therefore, the negative-sequence impedance, Z_2^{inv} , can be expressed as,

$$
\begin{aligned}
Z_2^{inv} &= \frac{V_2^{inv} \angle \delta}{I_2^{inv} \angle \delta} = R_{2Meas}^{inv} + jX_{2Meas}^{inv} \\
&= \frac{V_{x2}^{inv} + jV_{y2}^{inv}}{I_{x2}^{inv} + jI_{y2}^{inv}} \\
&= \frac{(V_{x2}^{inv} + jV_{y2}^{inv})(I_{x2}^{inv} - jI_{y2}^{inv})}{(I_{x2}^{inv} + jI_{y2}^{inv})(I_{x2}^{inv} - jI_{y2}^{inv})} \\
&= \frac{V_{x2}^{inv} I_{x2}^{inv} + V_{y2}^{inv} I_{y2}^{inv}}{(I_{x2}^{inv})^2 + (I_{y2}^{inv})^2} + j\frac{V_{y2}^{inv} I_{x2}^{inv} - I_{x2}^{inv} I_{y2}^{inv}}{(I_{x2}^{inv})^2 + (I_{y2}^{inv})^2}.
\end{aligned}
\tag{5.18}
$$

Thus, per (5.18), R_{2Meas}^{inv} and X_{2Meas}^{inv} can be expressed as a function of the system voltage and current,

$$
R_{2Meas}^{inv} = \frac{V_{x2}^{inv} I_{x2}^{inv} + V_{y2}^{inv} I_{y2}^{inv}}{(I_{x2}^{inv})^2 + (I_{y2}^{inv})^2}
\tag{5.19}
$$

$$
X_{2Meas}^{inv} = \frac{V_{y2}^{inv} I_{x2}^{inv} - I_{x2}^{inv} I_{y2}^{inv}}{(I_{x2}^{inv})^2 + (I_{y2}^{inv})^2}
\tag{5.20}
$$

where R_{2Meas}^{inv} and X_{2Meas}^{inv} are the measurement-based negative-sequence impedance components, V_{y2}^{inv} is the measured voltage, and I_{x2}^{inv} is the measured current.

The overvoltage, VOV, can be shown as a function of the phase voltages.

$$VOV = max(V_a, V_b, V_c) \tag{5.21}$$

Recall that the phase voltages can be expressed as a function of the sequence voltages as follows,

$$
\begin{aligned}
V_A &= V_0 + V_1 + V_2 \\
V_B &= V_0 + \alpha^2 V_1 + \alpha V_2 \\
V_C &= V_0 + \alpha V_1 + \alpha^2 V_2
\end{aligned}
\tag{5.22}
$$

Considering the phase voltage, V_A, as a function of the impedance and current,

$$
\begin{aligned}
V_A &= Z_{load0}I + Z_{th1}I + Z_{th3}I \\
&= \left[\frac{Z_{load0}Z_{L1}}{Z_{th2} + Z_{L1}} + Z_{th1} + \frac{Z_{th3}Z_{L1}}{Z_{th2} + Z_{L1}} \right] I \\
&= \left[\frac{Z_{load0}Z_{L1} + Z_{th1}Z_{th2} + Z_{th1}Z_{L1} + Z_{th3}Z_{L1}}{Z_{th2} + Z_{L1}} \right] I \\
&= \frac{n_1 + n_2 + n_3}{d_1}
\end{aligned}
\tag{5.23}
$$

where n_1, n_2, n_3, and d_1 are as follows,

$$n_1 = (Z_{xfmr} + Z_{inv2}) Z_{load2} \tag{5.24}$$

$$n_2 = (Z_{xfmr} + Z_{inv2} + Z_{load2}) Z_{load0} \tag{5.25}$$

$$n_3 = Z_{L1}Z_a \tag{5.26}$$

$$d_1 = Z_{xfmr} + Z_{inv2} + Z_{load2}. \tag{5.27}$$

Then, in a similar fashion, VUF_A is found as follows,

$$
\begin{aligned}
VUF_A &= \frac{|V_A - V_{avg}|}{V_{avg}} \\
&= \frac{3V_A - V_A - V_B - V_C}{V_A + V_B + V_C} \\
&= \frac{Z_{th1}I + Z_{th3}I_1}{Z_{load0}I_1} \\
&= \frac{n_a + n_b + n_c + n_d + n_e}{d_a}
\end{aligned}
\tag{5.28}
$$

where $n_a, ..., n_e$, and d_a are as follows,

$$
n_a = [(Z_{xfmr} + R_2 + jX_2 + Z_{load2})(Z_{xfmr} + R_2 + jX_2)(Z_{load2}Z_{load1})]I \tag{5.29}
$$

$$
n_b = [(Z_{xfmr} + R_2 + jX_2 + Z_{load2})^2(Z_{load0}Z_{load1})]I \tag{5.30}
$$

$$
n_c = (Z_{xfmr} + R_2 + jX_2 + Z_{load2})(Z_{xfmr} + R_2 + jX_2)I \tag{5.31}
$$

$$
n_d = (Z_{xfmr} + R_2 + jX_2 + Z_{load2})(Z_{load2}Z_{load1})I_1 \tag{5.32}
$$

$$
n_e = (Z_{xfmr} + R_2 + jX_2)(Z_{load2})I \tag{5.33}
$$

$$
d_a = \frac{Z_{xfmr} + R_2 + JX_2 + Z_{load2}}{Z_{load0}I_1}. \tag{5.34}
$$

5.4   Simulation Results and Discussion

In this section, simulation results are presented for two systems. First one is a small system modeled to match the simulation results with hand calculation and provide proof of concept. Then second system is an IEEE 34 bus system as shown in Figure 5.10 to show the scalability and practical implementation of the proposed method.

5.4.1   Transient Overvoltage for Different DERs

The test system that was utilized to demonstrate the transient overvoltage using a synchronous machine and a grid-forming inverter is depicted in Figure 5.6, both with and without grounding. A 115kV radial distribution system is depicted in Figure 5.6,

---

Algorithm 1 Proposed Method to Calculate R_2^{Ref} and X_2^{Ref} Reference

---

Step: 1 Calculate phase voltages (V_{abc}^{PCC}),(V_{abc}^{Inv}) and currents (I_{abc}^{PCC}),(I_{abc}^{Inv}) at the point of common coupling and inverter terminal, respectively.

Step: 2 Measure Inverter Negative-sequence Impedance using equations (5.19)-(5.20).

Step: 3 Compute VOV and VUF using equations (5.21)-(5.28)

Step: 4 Compare measured VOV and VUF with thresholds $VOV_{Threshold}$ and $VUF_{Threshold}$

Step: 5   **if** $(VOV \geq VOV_{Threshold})$ or $(VUF \geq VUF_{Threshold})$ **then**
    Determine VOV_{Phase} and/or VUF_{Phase}
  end if

Step: 5   **if** $VOV_{Phase} == $ 'Phase A' **then**
    $VOV_{eqn} = V_0 + V_1 + V_2$
  else if $VOV_{Phase} == $ 'Phase B' **then**
    $VOV_{eqn} = V_0 + a^2 V_1 + a V_2$
  else if $VOV_{Phase} == $ 'Phase C' **then**
    $VOV_{eqn} = V_0 + a V_1 + a^2 V_2$
  end if

Step: 6   **if** $VUF_{Phase} == $ 'Phase A' **then**
    $VUF_{eqn} = \frac{V_1 + V_2}{3V_0}$
  else if $VUF_{Phase} == $ 'Phase B' **then**
    $VUF_{eqn} = \frac{a^2 V_1 + a V_2}{3V_0}$
  else if $VUF_{Phase} == $ 'Phase C' **then**
    $VUF_{eqn} = \frac{a V_1 + a^2 V_2}{3V_0}$
  end if

Step: 7 Solve for R_2^{Ref} and X_2^{Ref},

$$VOV_{eqn} = VOV_{ref.}, \ VUF_{eqn} = VUF_{ref.} \tag{5.35}$$

---

with a substation resistance of 14.27Ω and a 3MW load fed by a step-down transformer immediately after the substation. The transformer has a rating of 115 kV/12.47 kV. Its winding configuration on the primary and secondary sides is Delta-Y. Its power rating is 25 MVA, and its positive sequence leakage reactance is 0.019 pu. The respective line impedance values between Bus 2 and Bus 3, Bus 3 and Bus 4, Bus 4 and Bus 5 are 0.84041Ω, 2.3491Ω, 0.206507Ω.
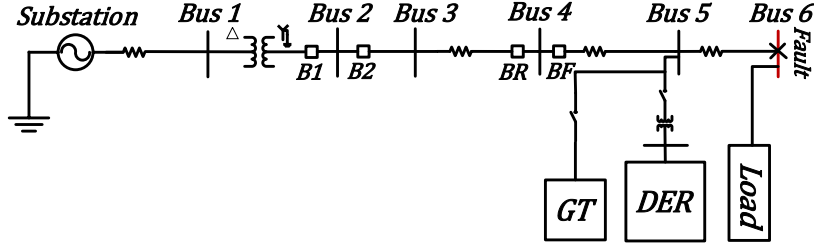
Figure 5.6: Test system single line diagram [5].

5.4.1.1 TOV for Synchronous Machine Based DER Sourced Microgrid

The distribution circuit is connected to a synchronous machine-based DER (SMDER) in Figure 5.6. The recloser BR is opened to create a microgrid with the circuit downstream, which is only fed by the SMDER. In the first scenario the SMDER is connected to the test System through a step-up transformer with the vector configuration $YN0yn$. In order to observe the TOV [109, 110], two scenarios use a single line to ground (A-G) fault. The islanded microgrid is not effectively grounded in the first scenario.

In the second scenario, an efficient grounding bank (Yn0d1) is constructed in accordance with [111]. The comparison between the two scenarios is displayed in Figure 5.7. At 2s, an A-G (line to ground) fault is applied. Figure 5.7a shows that the voltage (for an incapably grounded framework) comes to 1.69pu for phase C, which exceeds the 1.38pu limit.

After the fault, the maximum voltage for the effectively grounded system with the

grounding bank was approximately 1.08 pu, which is within the limit. The zero-sequence voltage for the effectively grounded case is higher than that for the ineffectively grounded case, as shown by Figure 5.7b. For the case with a grounding bank, Figure 5.7c demonstrates that an effectively grounded case can generate zero-sequence current, whereas for the ineffectively grounded case, there is no zero-sequence current. Figure 5.7 depicts the sequence voltages and currents. The DER step-up transformer's medium voltage (MV) side is where these parameters are measured.

5.4.1.2   TOV for Inverter Based DER Sourced Microgrid

In this test case, the inverter is connected to the system via a Yg-Y transformer without a grounding transformer and operates in grid-connected mode. The system is subjected to a phase A to ground fault at 2s. For the effectively grounded and ineffectively grounded conditions, two scenarios are run.

A comparison of the test scenarios is shown in Figure 5.8. The voltage for the system that is not effectively grounded reaches 1.51pu for phase C, which is higher than the 1.38pu threshold, as shown by Figure 5.8a. After the fault, the maximum voltage for the effectively grounded system with the grounding bank is approximately 1.23 pu. Per Figure 5.7b and Figure 5.7c, the sequence voltage and currents at the MV side of grid-forming inverters exhibit similar trends to those of synchronous machines.

The negative sequence components of the IBR are higher than those of a synchronous machine, while the zero sequence components are lower, as shown in Figure 5.7 and 5.8. There is a significant negative sequence voltage component in the IBR overvoltage. The IBR overvoltage remains at 1.23pu even after the grounding transformer bank is added.

5.4.2   Transformer configuration Impact on Microgrid Operation

The microgrid's operation is significantly influenced by the configuration of the step-up transformer, which is connected to the distribution circuit by a DER [112,
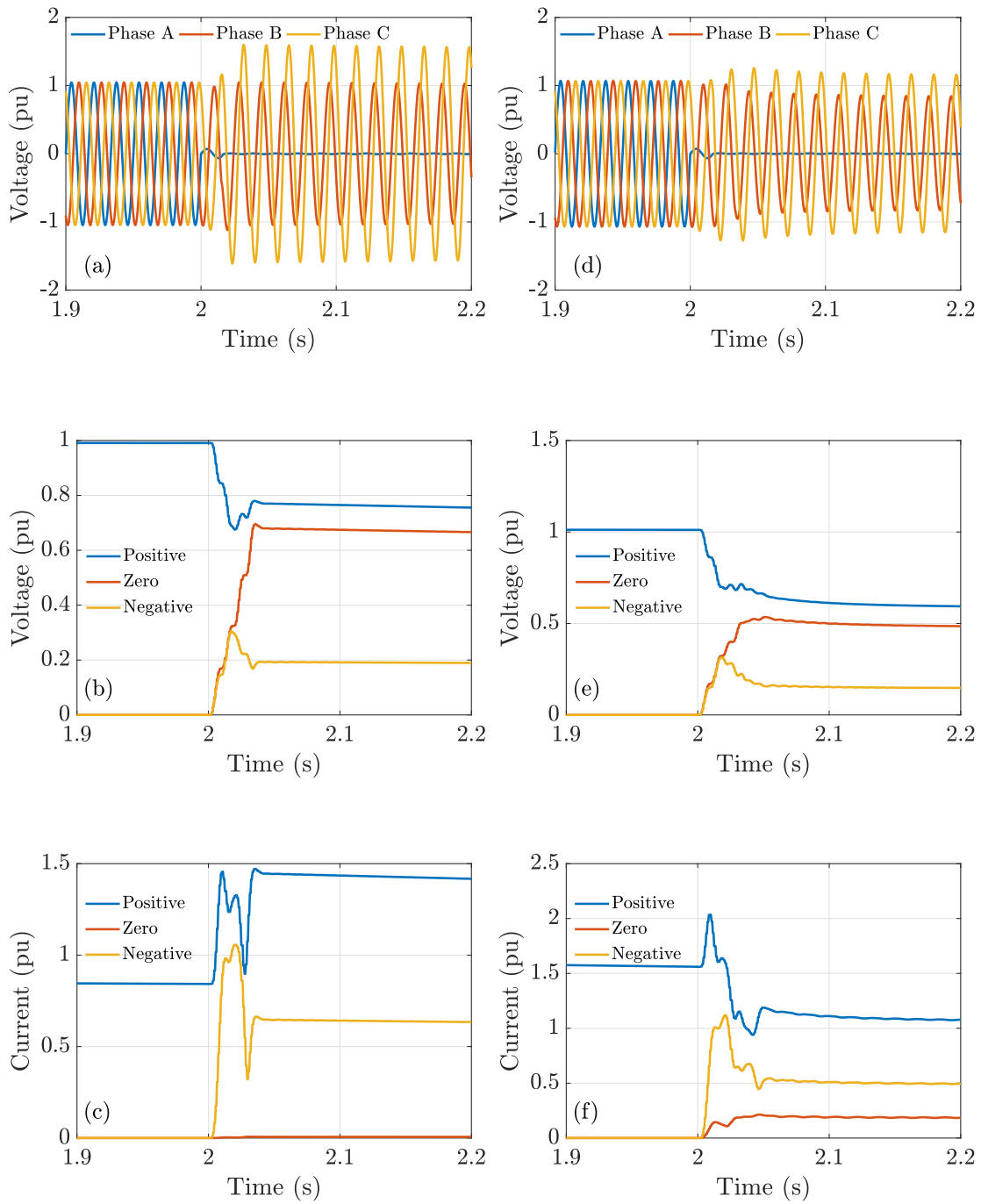
Figure 5.7: Synchronous machine without effective grounding (L) and with effective grounding (R) TOV comparison for PCC voltage for generation to load ratio 1:1 (a) Phase Voltage, (b) Sequence Voltage, (c) Sequence Currents [5].
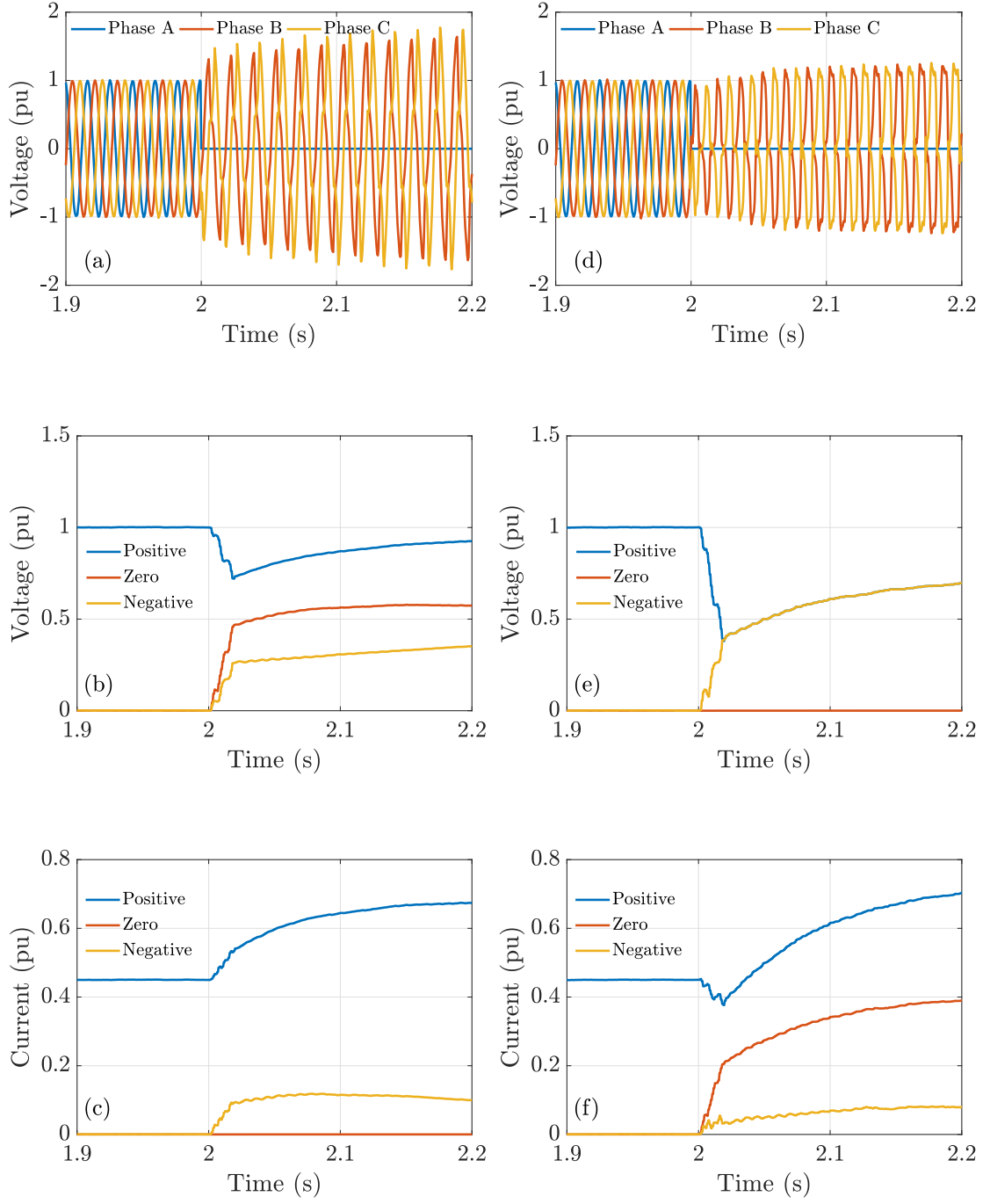
Figure 5.8: Inverter without effective grounding (L) and with effective grounding (R) TOV comparison for PCC voltage for generation to load ratio 1:1 (a) Phase Voltage, (b) Sequence Voltage, (c) Sequence Currents [5].
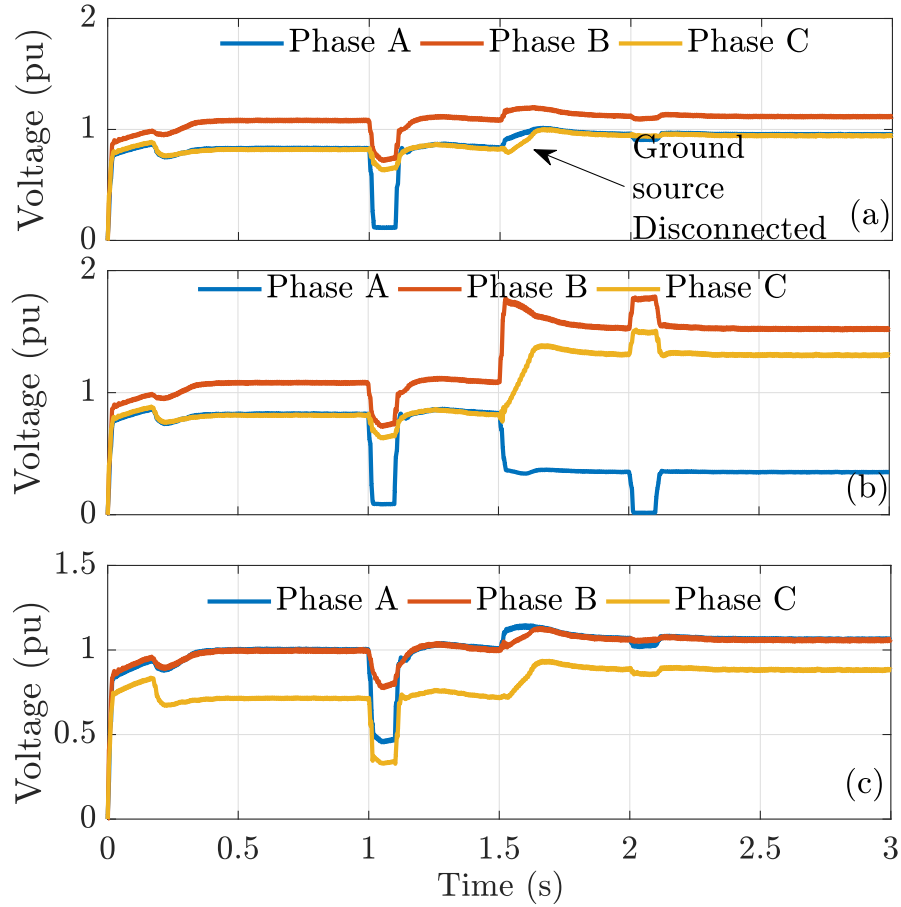
Figure 5.9: Voltage and Power profile for different transformer winding configuration (a) Inverter LV side L-N (RMS), (b) PCC MV side L-N (RMS), and (c) PCC MV side L-L (RMS) [5].

113, 114]. As shown in Figure 5.6, a small test system is used. An islanding recloser, BR, is used to create a microgrid by isolating a portion of the distribution circuit following a grid outage in the Test System. The inverter provides balanced currents and is modeled as a grid-forming inverter.

The microgrid loses its effective grounding when the transformer winding configuration is changed to YN0yn at 1. 5 seconds. Figure 5.9 demonstrates that there is no significant overvoltage at the inverter terminal's phase to ground voltage [115].

As can be seen in Figure 5.9b, the transformer configuration has a significant impact on the phase to ground voltage on the MV side of the transformer. A phase A to ground fault at 1s causes no overvoltage when the IBR is effectively grounded. How-

ever, when the transformer winding configuration is changed at 1. 5s to an ineffectively grounded source, the load's unbalance causes a phase overvoltage. Figure 5.9c demonstrates that unlike phase voltages, line-to-line voltages do not experience an overvoltage.

5.4.3 Proposed Inverter based distributed generation with negative sequence impedance control

The voltage unbalance factor (VUF) is calculated via (5.36).

$$VOV = max(V_a, V_b, V_c) \tag{5.36}$$

$$V_{avg} = \frac{V_a + V_b + V_c}{3} \tag{5.37}$$

$$VUF = max(\frac{|Va - V_{avg}|}{V_{avg}}, \frac{|Vb - V_{avg}|}{V_{avg}}, \frac{|Vc - V_{avg}|}{V_{avg}}) \tag{5.38}$$

Figure **??** shows that with the proposed method, the phase unbalanced decreases to 0.4% and the phase overvoltage on phase C decreases to 1.01. Figure **??** and Figure **??** show that proposed method tracks the R_2 and X_2 set points and has a higher value than grid forming inverter without negative sequence control. Figure **??** shows that negative sequence voltage for the proposed method is lower.

5.4.4 Simulation Results for Proposed methodology for larger IEEE 34 Bus system

The proposed method is evaluated for three distinct scenarios in this section. The proposed method's efficacy under a variety of system conditions is tested in Case 1. Case 2 demonstrates that the proposed method works for various fault locations. The proposed method's performance with various DER locations is evaluated in Case 3. The procedure for setting protective device settings for a distribution system, such as an IEEE 34 node unbalanced test system [6], is discussed in this section. The 34 node test feeder is a radial distribution feeder that has spot and distributed loads,

in-line step-down transformers, two voltage regulators, overhead and underground lines with different phasing, and a radial distribution feeder. Between nodes 832 and 888, there is a transformer with a rating of $0.5MVA$ and a voltage rating of $24.9kV/4.16kV$. The substation's positive-sequence and zero-sequence impedances are listed in [6]. An EMT program, PSCAD$^{®}$, is used to create the test system, as shown in Figure 5.10). Relays, reclosers, fuses, and circuit breakers are added to the test system as a protective measure. Feeder protection is provided by the addition of a numerical relay substation circuit breaker. To divide the circuit into smaller zones, three line-reclosers (R0, R1, and R2) are added (see Figure 5.10) to more effectively isolate faults. In order to safeguard both single-phase and double-phase loads, two additional fuses, F1 and F2, are installed in the laterals. The IEEE standard for protective relays [116] is used for the design basis protection design. Analyses of power flow and short circuits are carried out. The work in [6] serves as a benchmark to confirm the findings.

5.4.4.1   Case 1: Proposed method performance for varying system condition

In this section, a Microgrid is created by opening the Islanding Recloser (IR), as shown in Figure 5.10. The inverter based DER is the only generating source in the microgrid. The inverter based DER is a large utility scale battery energy storage site and the inverters are equipped with grid forming capability. Inverter is connected to the Medium Voltage (MV) distribution grid through a step-up transformer. The transformer winding configuration is YN0yn. Two scenarios are run as part of this case. In first scenario the microgrid is run without proposed method and in second scenario the microgrid is run with the proposed negative-sequence impedance control method. Figure 5.11a shows the voltage at the PCC and Figure 5.11b and Figure 5.11c show the currents at PCC and at the inverter terminal respectively for scenario 1. A single line to ground fault is applied on Phase A at 0.5s which causes overvoltage upto 1.76 pu in the healthy phase C. This is a potential safety issue for

Table 5.1: Comparison between VOV and VUF at different node with and without proposed algorithm

Cases	Fault Location	DER Location	Over Voltage (VOV) (PU)		Voltage Unbalanced Factor (VUF) (%)	
			Without Proposed Method	With Proposed Method	Without Proposed Method	With Proposed Method
Case 2	Node 840	Node 824	1.76	1.20	20	0.15
	Node 854	Node 824	2.65	1.05	30	0.23
	Node 826	Node 824	1.60	1.0	25	0.19
Case 3	Node 840	Node 824	1.78	1.10	20	0.54
	Node 840	Node 854	1.70	1.02	21	0.49
	Node 840	Node 836	1.73	1.00	20	0.61
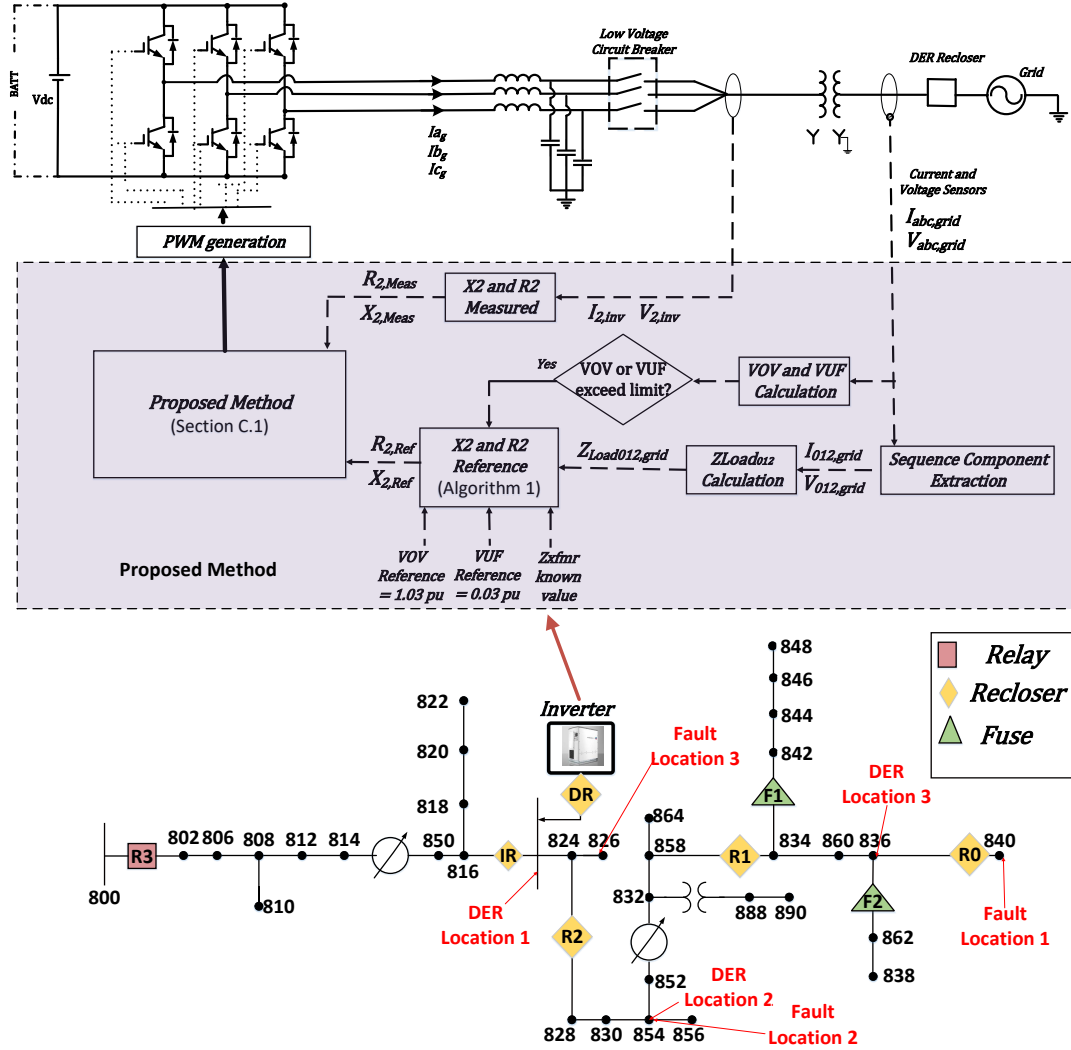
Figure 5.10: Implementation of proposed method with test system.

the distribution system as this can cause malfunction of the surge arresters which can typically withstand 1.4 pu voltage. This issues is created for the system not being effectively grounded and the inverter step up transformer configuration is YN0yn. Figure 5.12a shows the voltage at the PCC and Figure 5.12b and Figure 5.12c show the currents at PCC and at the inverter terminal respectively for scenario 2. Similar to scenario 1, a SLG fault is applied on phase A, but in the scenario with proposed method it does not cause any overvoltages on the healthy phases. Figure 5.13 provides a side by side comparison of overvoltage and unbalanced factor for with and without proposed method scenarios. Figure 5.13a shows that the maximum phase

Figure 5.11: Case 1: Without proposed method a) voltages at PCC, b)currents at PCC, and c) currents at inverter terminal.

voltage is around 1.2 pu for without proposed method scenario and it reached as high as 1.76 pu when a fault is applied. But with proposed method the maximum phase voltage always remains around 1 pu. So the proposed method protects the system from temporary overvoltage for different system conditions like with and without fault. Similar to phase overvoltage the proposed method also helps to improve phase unbalance. Figure 5.13b shows that the phase unbalance during normal condition was around 20% and during fault it increased to 80%. But with proposed method, during
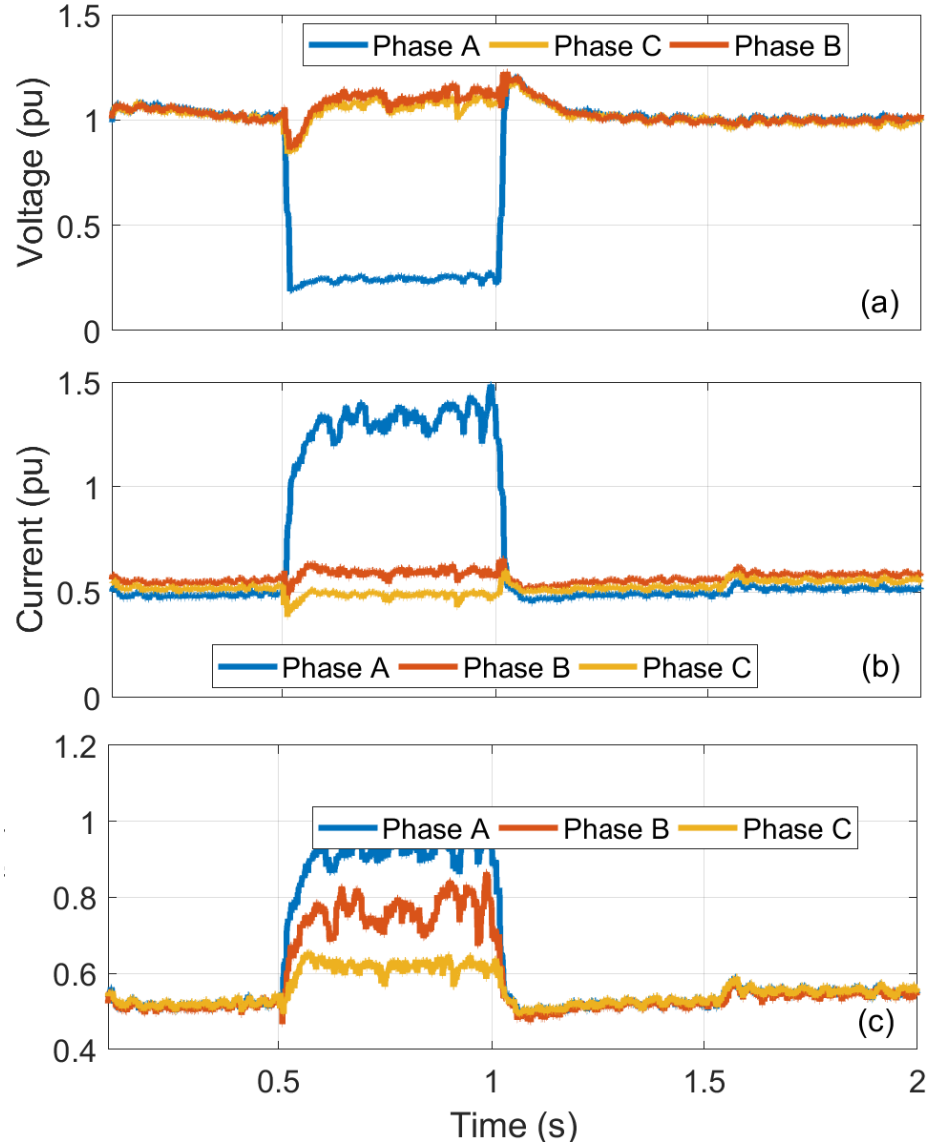
Figure 5.12: Case 1: With proposed method a) voltages at PCC, b)currents at PCC, and c) currents at inverter terminal.

normal condition the phase unbalance was below 1% and during fault it is around 60%. Phase unbalance during fault condition is fine but phase unbalance during normal condition is not good for system operation and power quality. Figure 5.14 shows the negative-sequence impedance calculated by the proposed method. It is noticeable that the negative-sequence resistance and reactance reference varies dynamically with system condition.
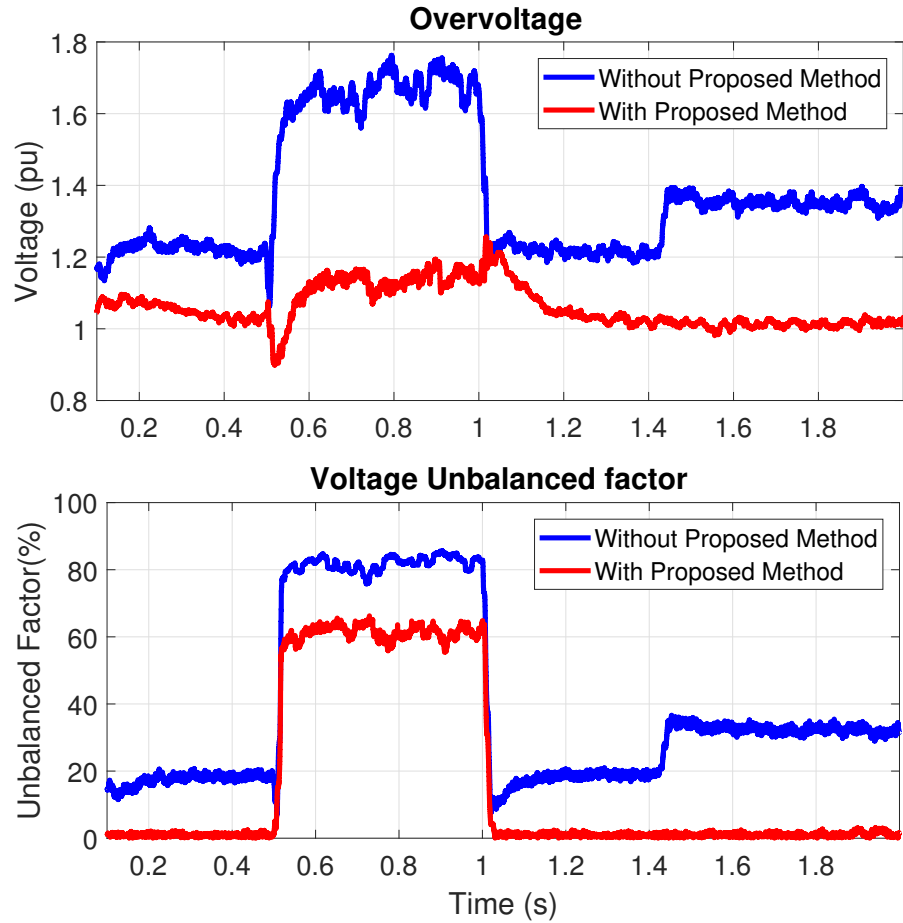
Figure 5.13: Over Voltage and Voltage unbalanced factor comparisons with and without proposed method.
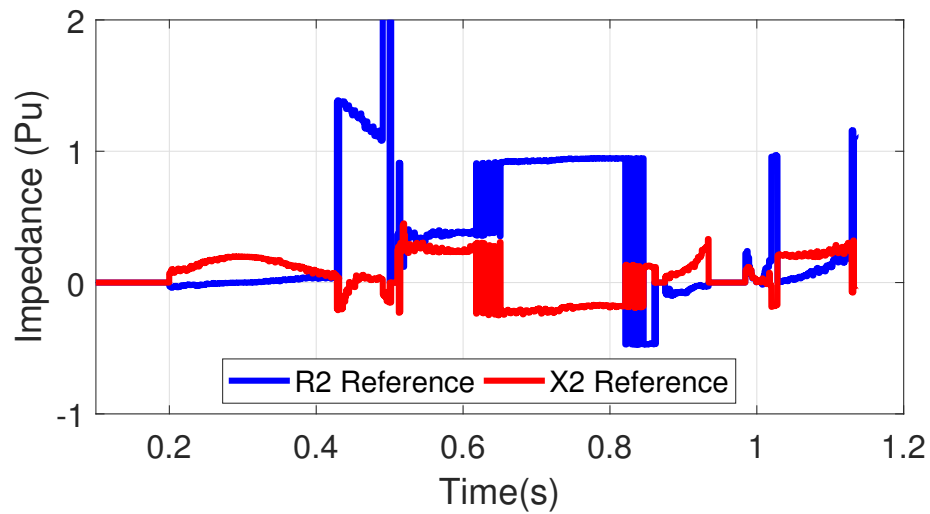
Figure 5.14: Impedance reference from the proposed method.

Economical Benefits

A 2.0 MVA grounding bank is needed to mitigate the overvoltage issues for the case without the proposed method. With the proposed method the size of grounding bank reduces significantly to 0.5 MVA from 2.0 MVA. Typical cost of a 2.0 MVA grounding transformer is around $170,000$. And, the typical cost of a 0.5 MVA transformer is around $60,000$. So the implementation of our method results in a savings of $110,000$.

5.4.4.2   Case 2: Proposed method performance for different fault location

A single line to ground fault is applied on Phase A at 0.5s, which causes overvoltage upto 1.76 pu in the healthy phase C. This is a potential safety issue for the distribution system as this can cause malfunction of the surge arresters which can typically withstand 1.4 pu voltage. This issues is created for the system not being effectively grounded and the inverter step up transformer configuration is YN0yn. Figure 5.12a shows the voltage at the PCC and Figure 5.12b and Figure 5.12c show the currents at PCC and at the inverter terminal respectively for scenario 2. Similar to scenario 1, a SLG fault is applied on phase A, but in the scenario with proposed method it does not cause any overvoltages on the healthy phases. Figure 5.15 provides a side by side comparison of overvoltage and unbalanced factor for with and without proposed method sce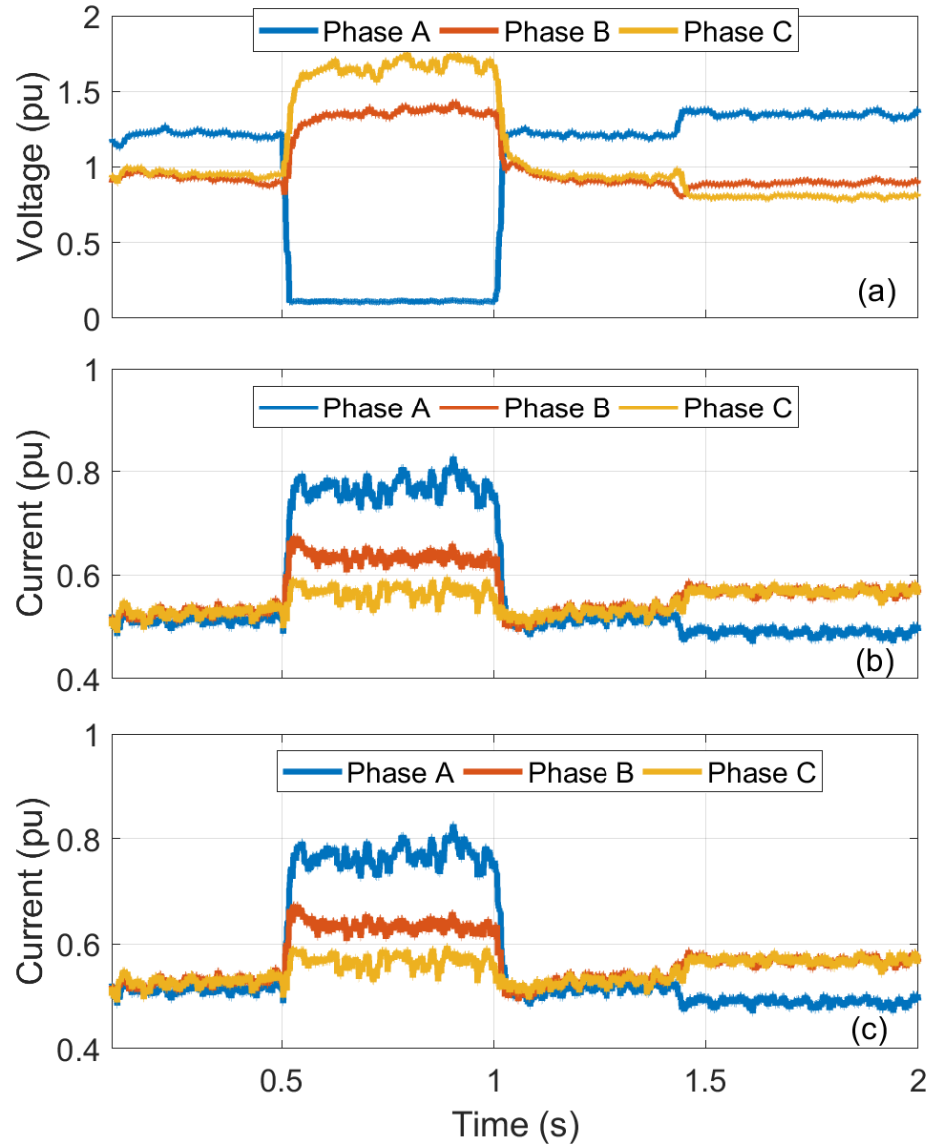narios. Figure 5.16a shows that the maximum phase voltage is around 1.2 pu for without proposed method scenario and it reached as high as 1.76 pu when a fault is applied. But with proposed method the maximum phase voltage always remains around 1 pu. So the proposed method protects the system from temporary overvoltage for different system conditions like with and without fault. Similar to phase overvoltage the proposed method also helps to improve phase unbalance.
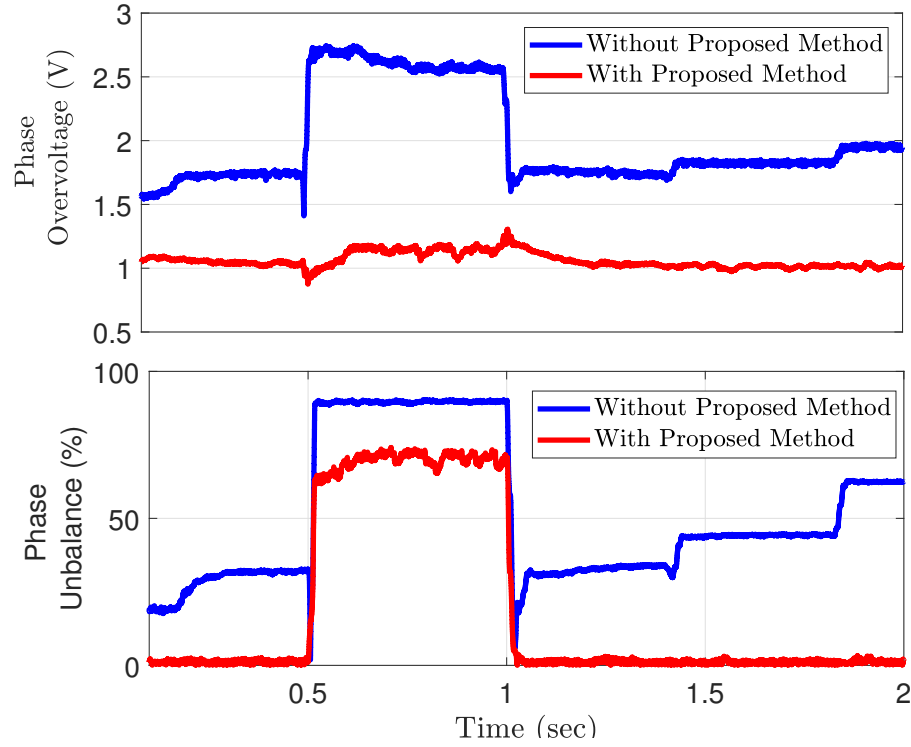
Figure 5.15: Over Voltage and Voltage unbalanced factor comparisons with and without proposed method for fault at Node 854.

5.4.4.3   Case 3: Proposed method performance for different DER location

In this case, the DER location is changed multiple time to evaluate the robustness of proposed method for different system configuration. Figure 5.17 shows the phase overvoltage and phase unbalance when the DER is connected towards the end of the microgrid at Node 836. A single line to ground fault is applied at Node 840 at 0.5s. Results show that without the proposed method the steady state voltage reaches almost upto 1.4 pu and voltage during fault reaches 1.8 pu. However, with proposed method voltage is kept around 1 pu during normal operating conditions and during fault maximum overvoltage observed is around 1.2 pu which is well within the withstand capability of the distribution surge arresters. Phase unbalance factor also shows similar improvements with proposed method. Without proposed method phase unbalanced is around 20% for normal operating condition and during a fault it reaches upto 90%. It is expected that during a fault the phase unbalance will be
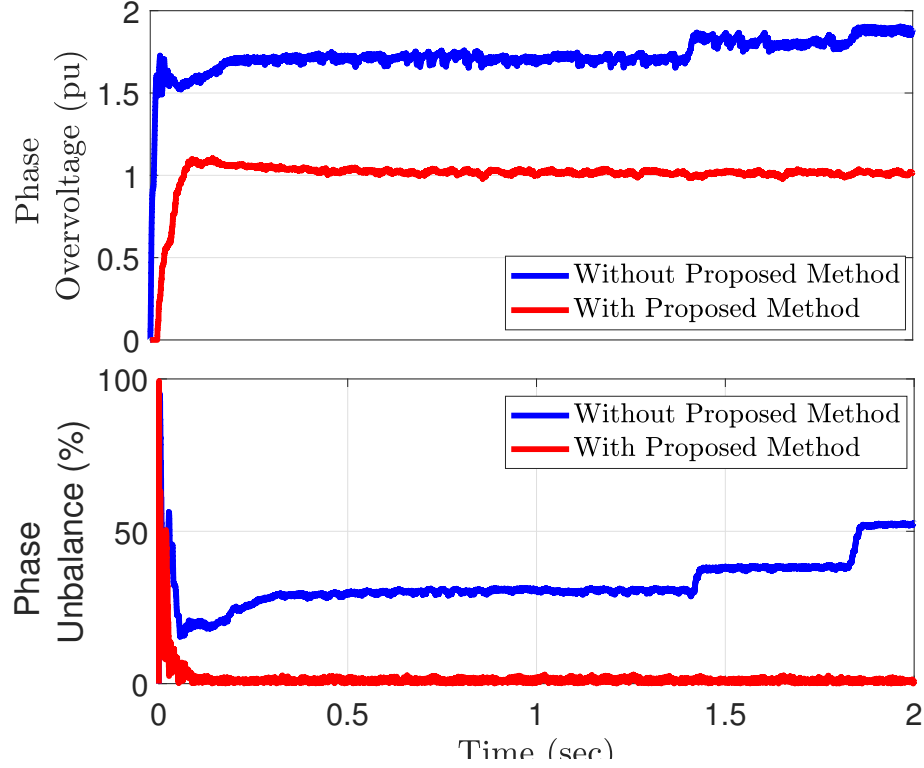
Figure 5.16: Over Voltage and Voltage unbalanced factor comparisons with and without proposed method for fault at Node 826.

more but 20% phase unbalance during normal operation is not acceptable. Proposed method helps to keep the phase unbalance during normal operating condition below 3%. Figure 5.18 shows the effectiveness of proposed method for a different location of the DER. This proofs that proposed method is not sensitive to a specific location or topology of the distribution system and can help improving system operation and safety parameters.

5.5   Chapter Summary

The TOV for a fully (100%) inverter-based microgrid distribution circuits is examined in this chapter. The findings indicate that IBRs' ground fault overvoltage mechanism differs from that of synchronous machine-based resources. Overvoltage mitigation is not always guaranteed by adding a grounding transformer. The work also demonstrates that microgrids with unbalanced loads must have a ground refer-
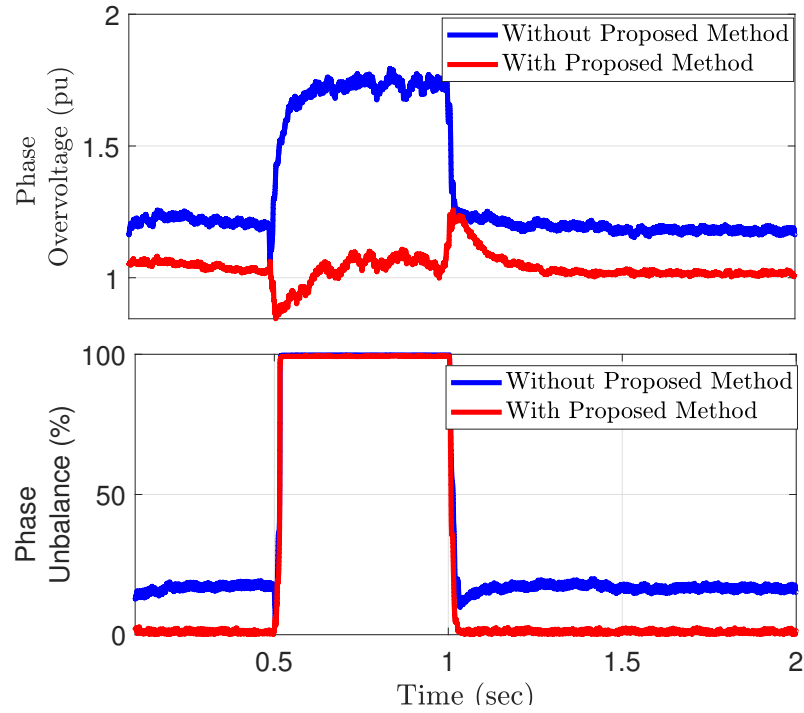
Figure 5.17: Over Voltage and Voltage unbalanced factor comparisons with and without proposed method for fault at Node 840 and DER at Node 836.
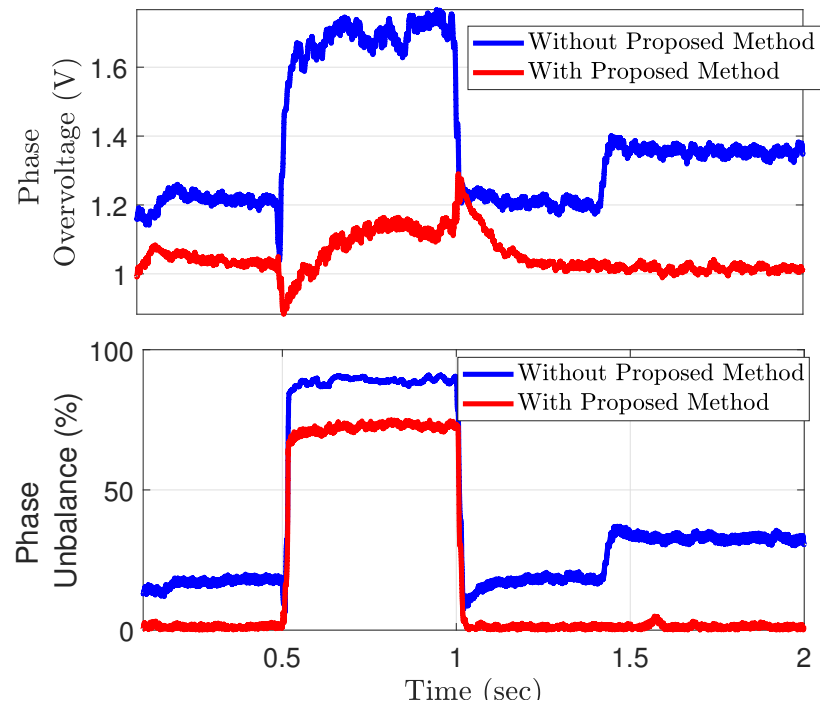
Figure 5.18: Over Voltage and Voltage unbalanced factor comparisons with and without proposed method for fault at Node 840 and DER at Node 854.

ence in order to maintain steady state operation. In order to lessen phase overvoltage and unbalance, the chapter suggests implementing a negative sequence impedance control. The study does not take into account inverter protection settings in the current work. In subsequent work, scenarios will be run with the settings for inverter protection, and the chapter's findings will be validated in hardware through the loop simulation.

CHAPTER 6: NOVEL PROTECTION METHOD FOR FULLY INVERTER-BASED DISTRIBUTION SYSTEM CONNECTED MICROGRID

The distribution system's use of distributed generation has grown rapidly in recent years. Reliability and resilience of the power system can both be enhanced by utilizing these resources. Inverter-based resources, such as solar and energy storage, which can provide distribution upgrade deferral, clean energy, backup power, short restoration times, and improved power quality, are becoming increasingly popular among distributed generation sources. However, inverter-based distributed generation presents a number of difficulties in fault detection and protection coordination among protective devices for distribution system protection. A novel approach to fault detection for distribution microgrids based on inverters is proposed in this chapter, which examines how inverter-based distributed generation affects the operation of distribution protection devices in various scenarios. PSCAD$^{\circledR}$ is used to perform simulations on an IEEE 34 bus unbalanced test system to demonstrate the method's efficacy.

6.1   Chapter Introduction

The increased use of renewable energy sources is altering the conventional structure of distribution networks [117, 118, 119, 120]. The utility sector has been forced to adopt new inverter-based resources like solar and energy storage at medium and low voltage networks as a result of rising renewable energy penetration [121]. Several studies in the literature demonstrate that the presence of DG influences the sensitivity and operating time of overcurrent relays (OCRs) [122, 123, 124]. Integration of IDG poses a number of challenges for distribution system protection [125, 126]. As a re-

sult, new security measures are needed that take these requirements into account and can adjust to the way the system works [127, 128]. In addition, IDGs may operate in either the grid-connected or islanded modes, necessitating a reevaluation of the necessary safety requirements [129, 130]. A microgrid is a self-sustaining island of load and generation that safely operates in either islanded mode or grid-connected mode when the small portion of the network is isolated from the grid [131, 128]. A practical microgrid is constructed from an existing distribution feeder during outages or extreme weather, despite the fact that some microgrids are designed specifically for prototype studies. This transforms such a feeder into a multi-source system while maintaining the radial network configuration, in which open switches prevent loops. During this transformation, the protection system is most likely to be impacted most. The work in [72] discusses some of the challenges associated with the design of microgrid protection based solely on inverter-interfaced generation. The issues with inverter-based microgrid protection have been addressed using a variety of approaches that have been suggested in the literature. However, there are some limitations to each proposed approach. The work in [132] suggest an adaptive overcurrent protection scheme for fault detection in microgrid and grid-connected operating modes. However, the current contribution from inverter-based resources decreases the sensitivity of fault detection significantly due to a limited source fault. For fault detection, differential protection has been proposed in [133], but the scheme is too expensive for large distribution microgrids due to the number of current transformers required. A current polarity and energy function-based fault detection method has been proposed in [134]; however, in order to comprehend the impact of switching events, additional research into its efficacy is required. on the proposed method, line losses and load modeling. A negative sequence resistance detection-based method is proposed in [135, 99], but its primary dependence is the inverter's control topology.

In the grid-connected mode of operation, the effects of inverter-based distributed
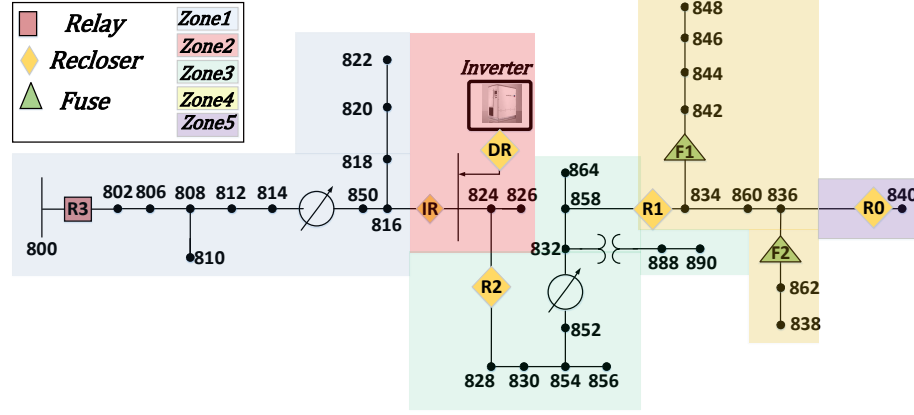
Figure 6.1: Modified IEEE 34 bus test system with protection devices and utility scale inverter connected [6].

generation (IDG) on overcurrent (OC) protection are examined first in this chapter, followed by the difficulties associated with microgrid protection when IDGs are the only generating source in the microgrid. Then, a new microgrid protection plan is proposed that effectively identifies faults within IBMGs by combining a number of algorithms and cutting-edge numerical relays. Using PSCAD®/EMTDC, research simulations are carried out on a modified IEEE 34 bus distribution network that features in-depth inverter models.

The initial findings of the proposed method has been published in the conference proceedings [7] and more validation work and enhancements have been performed in this chapter. The main contributions of this work include:

- A study regarding how the addition of IDG to a distribution system affects the sensitivity and selectivity of protection devices for both grids tied and grid forming mode of operation of IDGs.

- An outline of the challenges associated with overcurrent protection schemes for only inverter-based resource sourced microgrids is presented.

- A new microgrid protection scheme that overcomes the challenges of typical distribution system overcurrent protection for the only inverter sourced distri-

bution microgrids.

- The proposed protection method does not depend on the distribution feeder topology, DER size, or DER location.

- The proposed method can distinguish between faults and typical switching events, such as transformer energization, capacitor bank starts, and motor starts.

- The new proposed method does not require any communication with other devices to coordinate, since it works based on local measurements.

The rest of the chapter is organized as follows. Section 6.2 details the background related to existing distribution system protection, test system description with protection device settings, and inverter modeling. The proposed protection method is presented in Section 6.3. Simulation results are discussed in Section 6.4, before concluding the chapter and outlining possible future work in Section 5.5.

6.2   Protection Settings and Inverter Modeling

To identify various kinds of fault, the distribution system protection typically employs an overcurrent protection scheme. In distribution systems, there are three different kinds of overcurrent relay elements. Depending on the type of relay, system configuration, and protection requirements, these overcurrent relay elements can be directional or non-directional. [136].

6.2.1   Distribution System Protection Overview

A feeder breaker or recloser is typically where distribution feeder protection begins at the substation. Depending on the substation's design, this device is coordinated with either the upstream main bus breaker or transformer high voltage protection. Additionally, it is coordinated with downstream devices on the main feeder or tap sections (recloser, fuses) [137]. All of the protection devices in the distribution circuit

are time-current coordinated to reduce the impact of an outage on customers. Line currents are detected by the phase overcurrent relay element. The settings for the minimum response or pickup are set to be higher than the anticipated maximum feeder load current. The phase overcurrent relay pickup settings are typically set to 1.5 to 3.0 times the maximum expected feeder load current to prevent malfunctions. Due to feeder load unbalance, the ground overcurrent relay's pickup setting is set to greater than the expected maximum zero-sequence current. As a consequence of this, the majority of ground relays have a pickup range that is between 25% and 50% of the phase overcurrent relay pickup, resulting in a slight increase in sensitivity for phase-to-ground faults. The coordination of the downstream fuses and ground overcurrent relays is an additional significant factor to take into account. A negative sequence relay element is used for phase-to-phase fault detection, and it is more sensitive than phase overcurrent relays. Negative grouping transfers can likewise be applied to identify open stage conditions and low side stage to-ground shortcomings on delta-grounded wye transformers. Relay settings are determined by taking into account the anticipated maximum feeder loads, cold load pickup, and transformer magnetizing inrush. The IEEE standard C37.230 [138] provides additional information regarding distribution protection settings.

6.2.1.1   Test System and Protection Device Settings

The procedure for setting protective device settings for a distribution system, such as an IEEE 34 node unbalanced test system [6], is discussed in this section. The 34 node test feeder is a radial distribution feeder that has spot and distributed loads, in-line step-down transformers, two voltage regulators, overhead and underground lines with different phasing, and a radial distribution feeder. Between nodes 832 and 888, there is a transformer with a rating of $0.5MVA$ and a voltage rating of $24.9kV/4.16kV$. The substation's positive and zero sequences impedances are listed in [6]. An EMT software, PSCAD®, is used to create the test system, as shown in

Figure 6.1. Relays, reclosers, fuses, and circuit breakers are added to the test system as a protective measure. Feeder protection is provided by the addition of a numerical relay substation circuit breaker. To divide the circuit into smaller zones, three line-reclosers (R0, R1, and R2) are added (Figure 6.1) and better isolate faults. In order to safeguard both single-phase and double-phase loads, two additional fuses, F1 and F2, are installed in the laterals. The IEEE protection standard for protective relays is utilized for the design basis protection [138]. Analyses of power flow and short circuits are carried out. The work [6] serves as a benchmark to confirm the findings. The test system is then altered to connect a $2MVA$ IDG near node 824. Node 824, which is typically close but open during an upstream fault and has the potential to form a microgrid, is directly in front of the islanding recloser. Every safety device is properly coordinated. Table 6.1 displays the time dial and pickup settings for each relay and recloser's overcurrent elements.

Table 6.1: Protection Device Settings

Relay Number	Time Dial Setting	Pickup Current
R_0	$TD_0 = 0.01$	$I_0 = 0.1$ kA
R_1	$TD_1 = 0.03$	$I_1 = 0.15$ kA
R_2	$TD_2 = 0.05$	$I_2 = 0.21$ kA
R_3	$TD_3 = 0.25$	$I_3 = 0.3$ kA

6.2.2 Inverter Modeling

For IBMG protection studies, it is necessary to accurately model onboard protection elements and inverters for various control modes. The inverter's general configuration, which can be used in grid following or grid forming mode, is shown in Figure 6.2. The outer control loop in Figure 6.2 demonstrates how the control objective varies for various inverter operation modes. The inverter adjusts accordingly. The inverter operates in the grid following mode to conform to the application-specific active and reactive power setpoints (e.g., PV smoothing, energy time-shift, etc.). The control

loop depicted in Figure 6.2 shows how the active and reactive power set points are used to generate the reference for the inner current control loop, which is then used to generate the positive sequence voltage references. When serving a microgrid, the inverter operates in grid-forming mode. In grid-forming mode, the inverter tries to keep the islanded section's voltage and frequency as close to their nominal values as possible. The phase-locked loop (PLL) is given a constant frequency of 60 Hz, and a $d - q$ reference frame is used to set the unity voltage reference point.
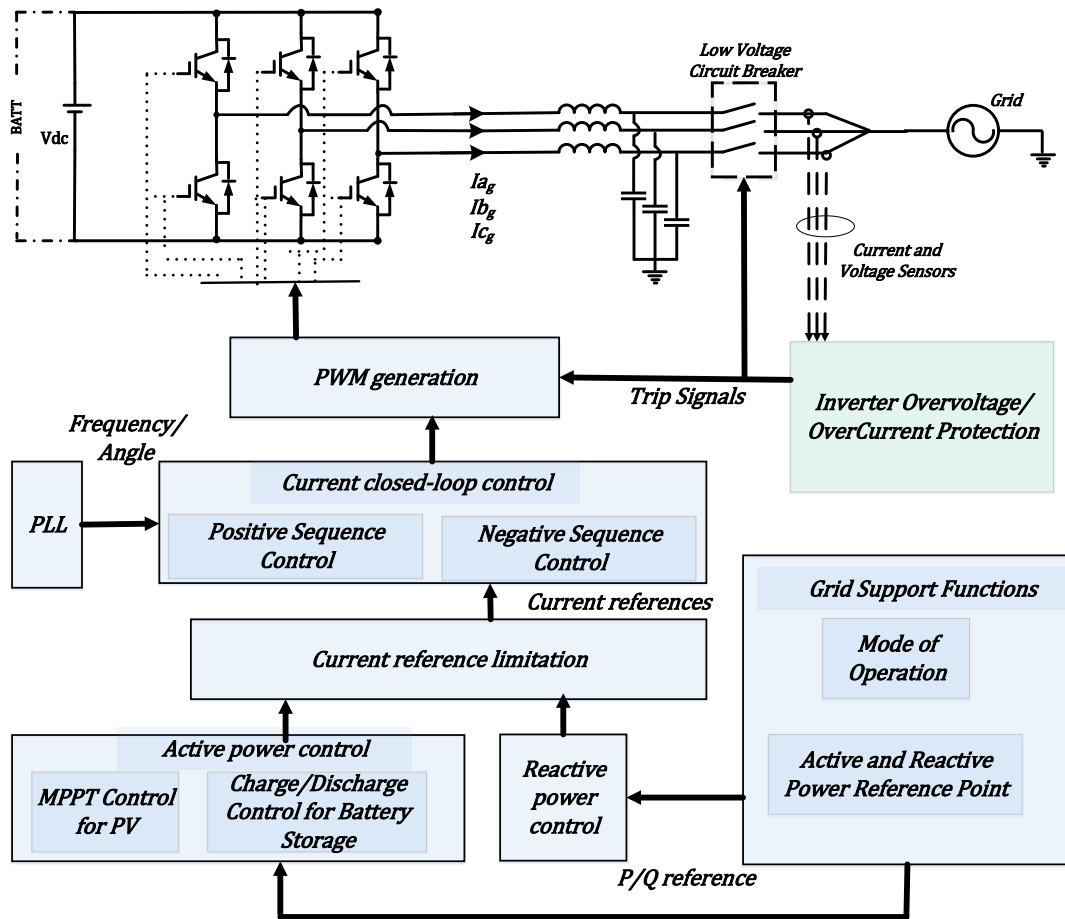
Figure 6.2: Inverter design architecture used in this chapter.

The outer control loop for grid forming mode is shown in Figure 6.2, which makes use of V_d and V_q to generate the reference signals. In microgrid operation, the inverter must serve an unbalanced load, so a negative sequence control loop that can generate

negative sequence currents in unbalanced conditions is added to the inverter control. In Figure 6.2, the current reference limitation block implements control strategies for limiting currents to the power electronic switches with a hardware limit of 1.6 pu. During faults, the inverter injects reactive power current through virtual impedance and blocks PWM when the fault current exceeds the device current limit. The model now includes trip set points for overvoltage and undervoltage as well as over-frequency and under-frequency inverter protection. On top of the inner negative sequence current control loops, a new outer control loop is added. During unbalanced operating conditions, this loop controls the effective negative sequence impedance seen at the inverter terminal by using the negative sequence resistance and reactance as an input reference. Zero-sequence current is not generated by the inverter, but a step-up transformer or additional grounding transformer can provide it during faults.

6.3   Proposed Protection Method

The theoretical background, an algorithm, and the protection philosophy of the proposed protection method for a fully inverter-based distribution system connected microgrid are presented in section 6.3.1 and then section 6.3.2 provides elaboration regarding the implementation approach.

6.3.1   Theoretical Background of the Proposed Method

Figure 6.3 depicts sequence networks for various operating conditions. Figure 6.3a displays the fault-free sequence network of an unbalanced system. The sequence networks for the LG and LLLG faults, respectively, are displayed in Figure 6.3b and Figure 6.3c. Because of the virtual impedance that is modeled in Section 6.2.2, grid forming inverters are modeled as a voltage source behind a variable impedance in a positive sequence network. Because it only generates negative sequence voltage when unbalanced loads necessitate negative sequence currents, it is modeled as a voltage source dependent on current. For each scenario, generic expressions of se-
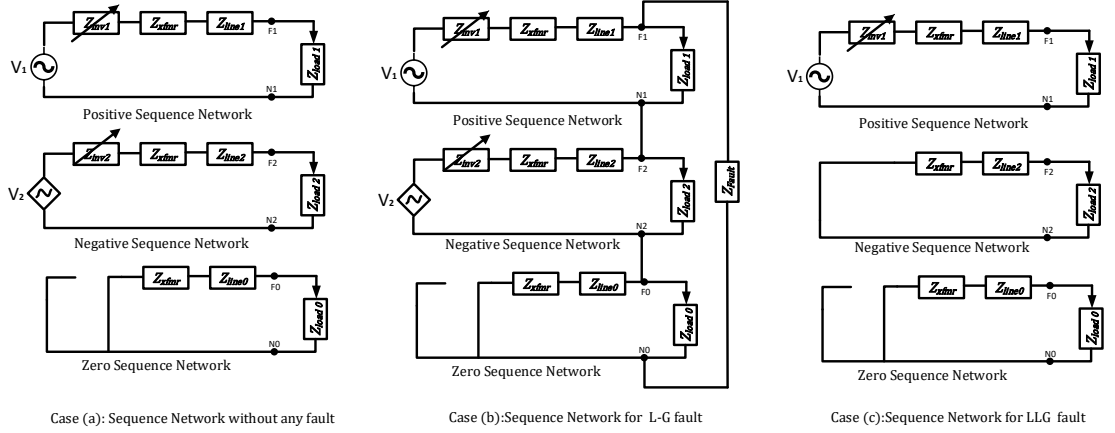
Figure 6.3: Sequence networks of grid forming inverter sourced system for different operating conditions.

quence voltages and currents are derived. Only a small number of equations are displayed in (6.1)-(6.10) due to page limitations. During an unbalanced fault, there is a significant amount of current flowing through zero sequences (I_0) and negative sequences (I_2). The proposed method uses the relative relationship between negative sequence currents and positive sequence currents ($\frac{3I_2}{I_1}, \frac{3I_0}{I_1}$) to detect unbalanced faults because the inverters in grid forming mode can generate zero sequences and negative sequences. The algorithm declares a fault condition when the ratio of $\frac{3I_2}{I_1}$ or $\frac{3I_0}{I_1}$ exceeds a predetermined percentage over a predetermined time period. For symmetrical faults, sequence-based protection schemes require additional protective functions and are difficult to coordinate. Two additional protection elements are added to the proposed method to make it effective for symmetrical faults. The Negative-Sequence Voltage-Based Detection looks for faults by comparing the magnitudes of the negative and positive voltages ($\frac{3V_2}{V_1}$). The negative sequence voltage that is observed at various protection devices varies and is used to detect symmetrical faults if the distribution system is unbalanced. However, the voltage difference is smaller and the voltage element is less sensitive if the faults occur close to the inverter terminal. The fault current waveform can become extremely distorted when the inverter for faults

close to its terminal reaches its hardware current limit. To find faults, the proposed method calculates the harmonic components of the currents. If the harmonic current (I_H) is above a threshold, a fault is found. The proposed method is described in detail in Algorithm 2 and the method of implementation are discussed in the following sub-section.

$$Case(a) : I_1 = \frac{V_1}{j_{Xfmr} + Z_{line1} + Z_{load1} + Z_{inv1}} \tag{6.1}$$

$$I_2 = \frac{V_2}{j_{Xfmr} + Z_{line2} + Z_{load2} + Z_{inv2}} \tag{6.2}$$

$$V_{1R} = V_1 - [I_1 \times (Z_{inv1} + jxfmr + Z_{line1})] \tag{6.3}$$

$$V_{2R} = V_2 - [I_2 \times (Z_{inv2} + jxfmr + Z_{line2})] \tag{6.4}$$

$$Case(b) : Z_0 = (Z_{xfmr0} + Z_{line0}) || (Z_{load0} + 3Z_n) \tag{6.5}$$

$$Z_1 = (Z_{inv1} + Z_{xfmr1} + Z_{line1}) || Z_{load1} \tag{6.6}$$

$$Z_2 = (Z_{inv2} + Z_{xfmr2} + Z_{line2}) || Z_{load2} \tag{6.7}$$

$$I_{1f} = I_{2f} = I_{0f} = \frac{V_1 + V_2}{j_{Xfmr} + Z_{line1} + Z_{load1} + Z_{inv1}} \tag{6.8}$$

$$Case(c) : I_1 = \frac{V_1}{j_{Xfmr} + Z_{line1} + Z_{load1} + Z_{inv1}} \tag{6.9}$$

$$I_{1f} = \frac{Z_1 \times I_1}{Z_1 + Z_f} \quad I_2 = 0 \quad I_0 = 0 \tag{6.10}$$

6.3.2   Implementation of Proposed Protection Method

The proposed method's practical application is depicted in the Figure 6.4 flowchart. The values of the protection settings, which are based on the operating conditions, configurations, relay locations, and other factors of the system, are dependent on all of the protection elements. In addition, the proposed method necessitates a number of settings, $3I_2^{limit}, 3I_0^{limit}, 3V_0^{limit}, H^{limit}$, which are described in Algorithm 2. Power flow and short circuit studies on the system under investigation are required to ob-

---

Algorithm 2 Proposed Microgrid Fault Detection Method [7]

Step: 1 Calculate phase voltages (V_{abc}) and currents (I_{abc}) at protection device locations using CTs and PTs.

Step: 2 Calculate sequence voltages and currents.

$$
\begin{bmatrix} I_0^{"} \\ I_1^{"} \\ I_2^{"} \end{bmatrix} = \frac{1}{3} * \begin{bmatrix} 1 & 1 & 1 \\ 1 & a^2 & a \\ 1 & a & a^2 \end{bmatrix} * \begin{bmatrix} I_a^{"} \\ I_b^{"} \\ I_c^{"} \end{bmatrix}
$$
$$
\begin{bmatrix} V_0^{"} \\ V_1^{"} \\ V_2^{"} \end{bmatrix} = \frac{1}{3} * \begin{bmatrix} 1 & 1 & 1 \\ 1 & a^2 & a \\ 1 & a & a^2 \end{bmatrix} * \begin{bmatrix} V_a^{"} \\ V_b^{"} \\ V_c^{"} \end{bmatrix}
$$
(6.11)

Step: 3 Extract current harmonics components (I_n).

Step: 4 Determine thresholds for protection elements: $3I_2^{limit}, 3I_0^{limit}, 3V_0^{limit}, H^{limit}$.

Step: 5 Calculate $\frac{3I_2}{I_1}, \frac{3I_0}{I_1}, \frac{3V_2}{V_1}, I_H$ where $I_H = \frac{\sqrt{\sum_{n=1}^{7} I_n^2}}{n}$.

Step: 6 If $(\frac{3I_2}{I_1} \geq 3I_2^{limit})$ || $(\frac{3I_0}{I_1} \geq 3I_0^{limit})$ || $(\frac{3V_2}{V_1} \geq 3V_0^{limit})$ || $(I_H \geq H^{limit})$, $T_{Trip} = start$.

Step: 7 TRIP$=\begin{cases} 1, & \text{If } T_{Trip} > R_{TimeDelay}. \\ 0, & \text{otherwise.} \end{cases}$
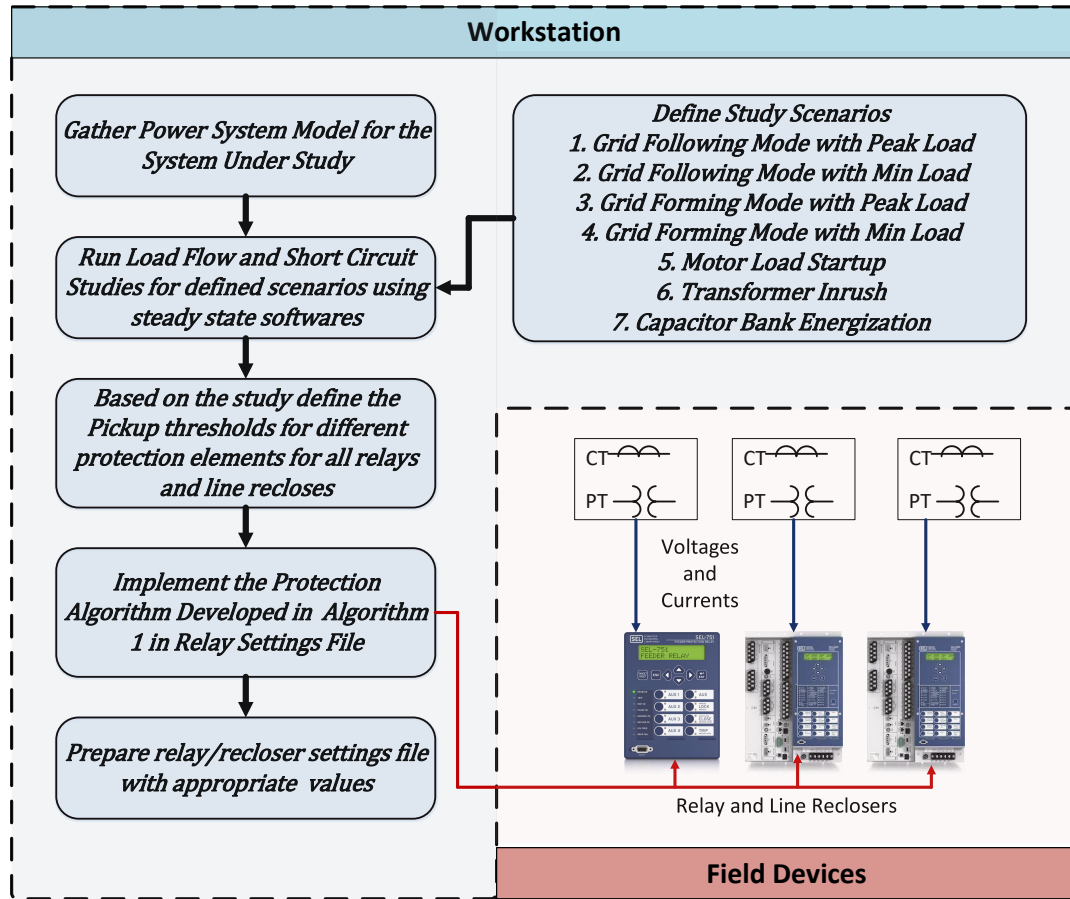
Figure 6.4: Implementation framework for the Proposed Protection Architecture.

tain these values. To ensure that the settings chosen will produce accurate results for all possible scenarios, a variety of scenarios must be examined. The study of transformer energization, capacitor bank switching, motor start, and cold load pick up requires particular attention. It is necessary to select settings to ensure that the proposed method is accurate in detecting faults but does not produce false alarms for typical distribution switching events. Custom math variables are used in the relay and recloser settings file to implement Algorithm 2, and the settings values from the studies are assigned to each PD. Each PD uses the values of its corresponding current transformer (CT) and potential transformer (PT) to determine the TRIP conditions because the settings are local to that PD.

6.4   Simulation Results and Discussion

6.4.1   Distribution Protection Issues with the Integration of IDGs

The effects of IDG integration on distribution system protection in grid following and grid forming modes of operation are examined in three scenarios.

6.4.1.1   Case 1

In this case, the loads are only served by the substation, and the IDG is disconnected (recloser DR open). On node 846, an LLG fault is applied at 1s for 0.5s. Figure 6.5a demonstrates that the fault current reached 0.4kA and that the nearby protection device R1 cleared the fault in $1.055s$.

6.4.1.2   Case 2

Both the substation and the inverter are connected and serving the load in this scenario. The fault is in the same place as before. Figure 6.5b demonstrates that the fault current exceeded case 2's value of 0.48kA. The fault current is higher because the fault is fed by both the substation and the inverter, and the R1 recloser trips faster, at $1.045s$. However, the substation's contribution to the fault current is lower than in Case 1, and it may desensitize the R3 feeder breaker relay.

6.4.1.3   Case 3

The islanding recloser (IR) is open in this instance. This results in the creation of a local microgrid with IDG serving as the sole source in a circuit downstream of IR. In grid-forming mode, the inverter serves the loads. The fault is applied at node 846, just like in the previous two instances. Figure 6.5c demonstrates that the fault current is significantly lower than in the previous two instances, reaching 0.2 kA. The protection device $R1$ is unable to clear the fault due to a lack of fault current. Additionally, neither the R2 $northe DR$ backup protection devices within the microgrid area function. This clearly demonstrates IBMG's lack of conventional OC

protection.
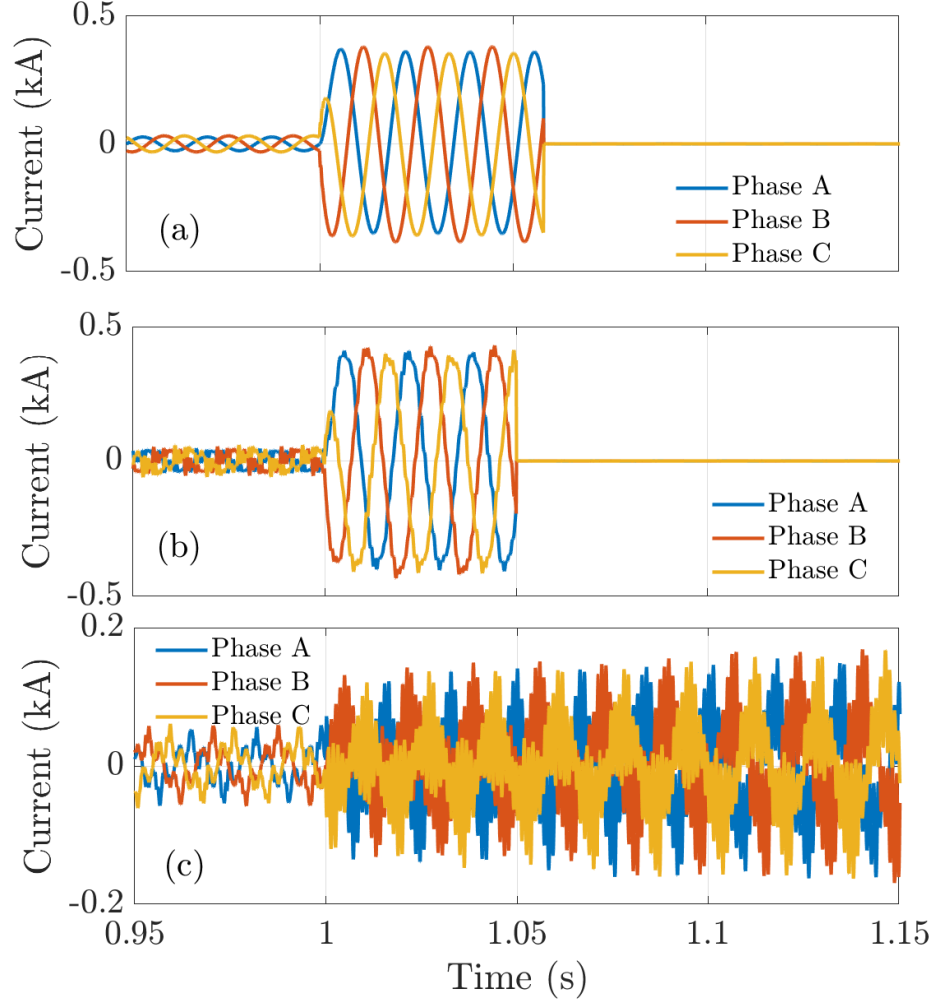
Figure 6.5: R1 Fault currents for fault at Node 846 (a) Case 1, (b) Case 2, (c) Case 3 [7].

6.4.2   Application of Proposed Protection Method

Faults at Node 846 are used to evaluate the proposed protection scheme's performance. All of the relays and reclosers depicted in Figure 6.1 are equipped with the protection schemes. The same location is exposed with both balanced (LLLG) and unbalanced (LG) faults. The summary of the results is displayed in Figure 6.7. The active power, reactive power, and voltages observed at recloser location R1 during a LLLG fault are depicted in Figure 6.7a to 6.7d. Figure 6.7e demonstrates that the proposed algorithm quickly operates the recloser R1 to isolate the fault when the
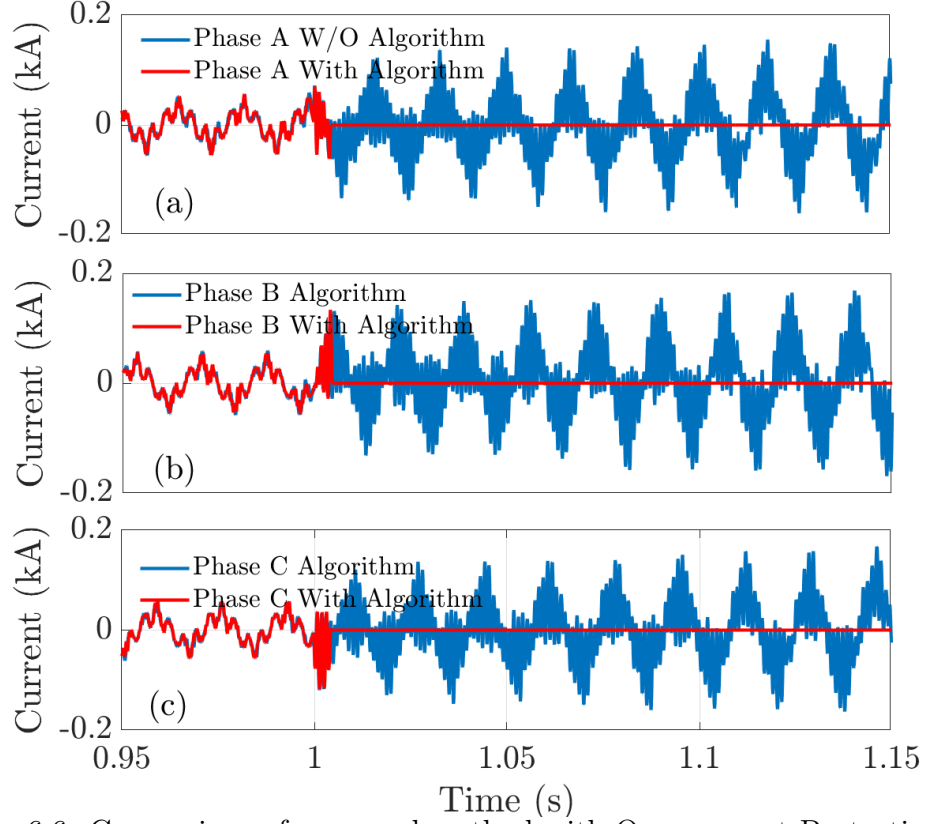
Figure 6.6: Comparison of proposed method with Over current Protection [7].
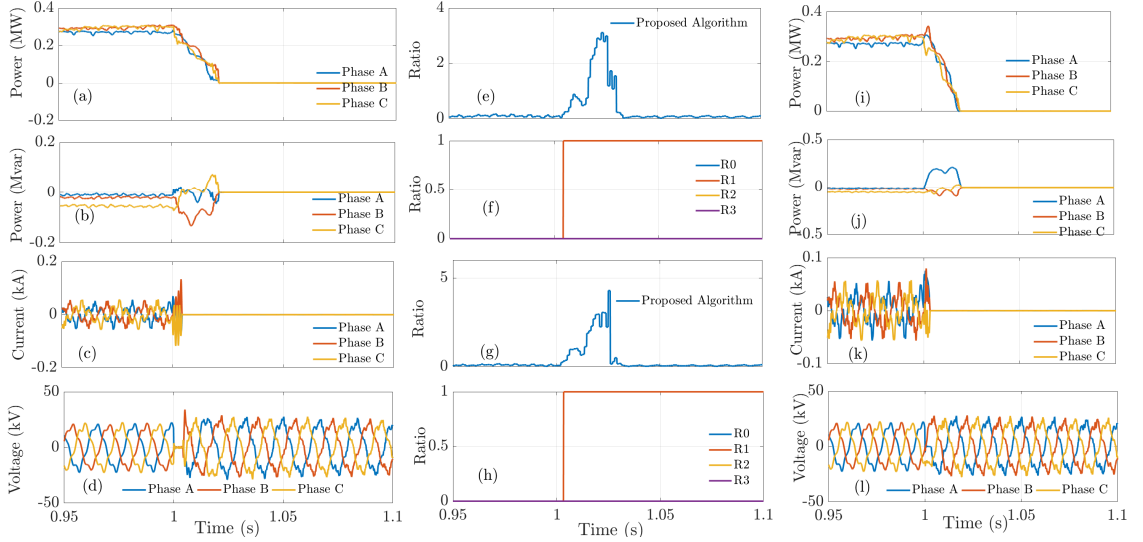
Figure 6.7: Proposed Method results at Recolser location R1 for fault at Node 846 [7].

fault is applied for one second. Due to the absence of fault current in the islanded

mode of operation, the fuse F1 does not operate. Figure 6.7f exemplifies how recloser
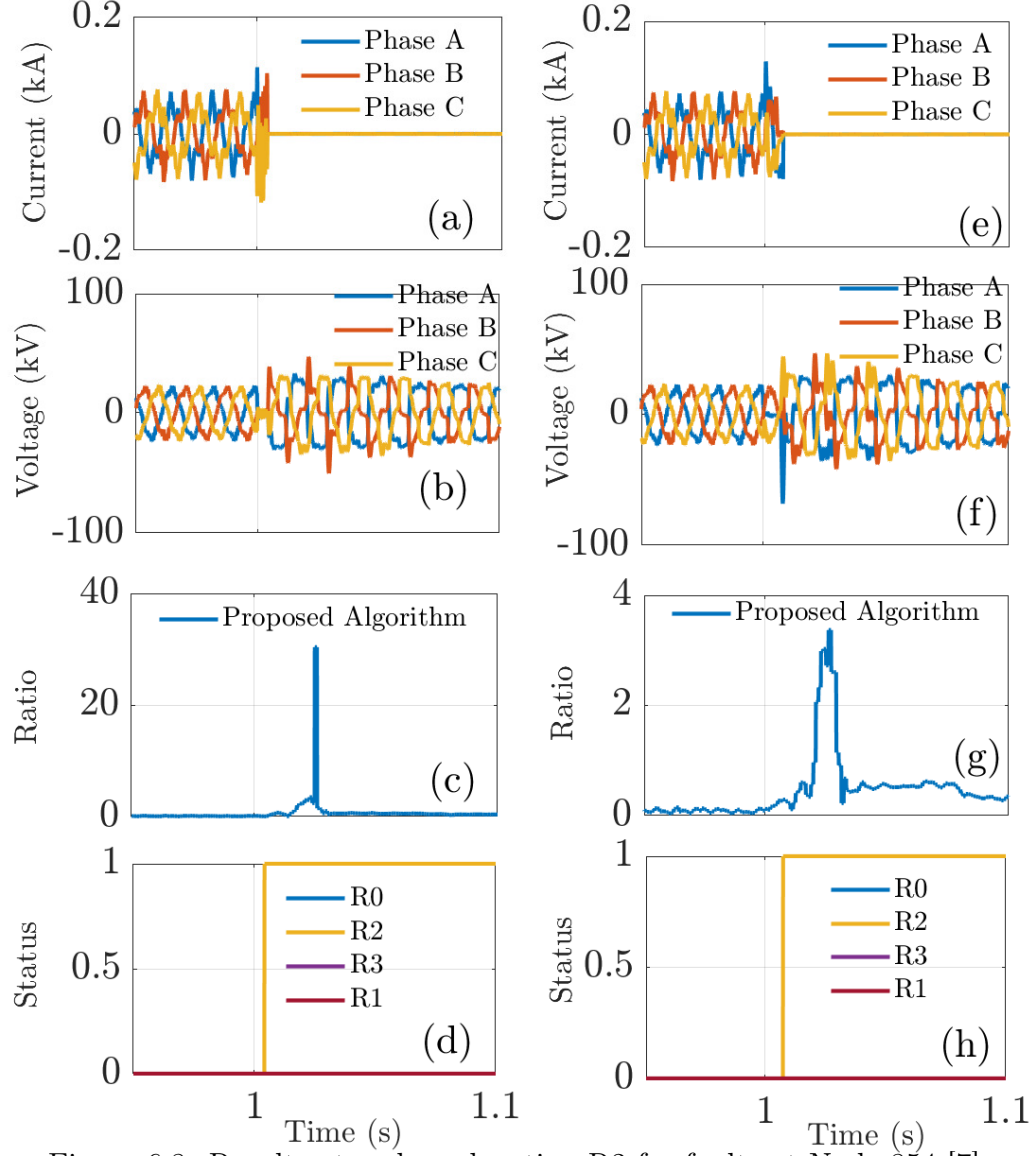
Figure 6.8: Results at recloser location R2 for faults at Node 854 [7].

R1 functions in the vicinity of the fault. The proposed and existing overcurrent protection schemes are contrasted in Figure 6.6. When compared to the overcurrent element, the outcomes demonstrate that the proposed method can accurately and reliably identify and isolate faults. During a LG fault, the voltages, currents, and active power at recloser location R1 are depicted in Figure 6.7g to 6.7j. The proposed method is reliable for LG fault cases as well, as it is for the LLLG fault case.

To demonstrate the approach's robustness, faults are applied to various locations. The summary of the results is displayed in Figure 6.8. During a LLLG fault, the

voltages and currents seen at recloser location R2 are depicted in Figure 6.8a and 6.8b. Figure 6.8c demonstrates that the proposed algorithm quickly operates the recloser R2 to isolate the fault when the fault is applied for one second. Figure 6.8d shows that recloser R2 works best when it is near the fault. The voltages and currents observed at recloser location R2 during a LG fault are depicted in Figure 6.8e and Figure 6.8f. As shown in Figure 6.8g and Figure 6.8h, the proposed method is dependable for LG fault cases as well as the LLLG fault case. Table 6.2 presents a summary of the various faults and a comparison of the proposed approach to the existing OC approach. For microgrid fault protection, the proposed method improves fault detection and sensitivity.

Table 6.2: Comparison of Proposed Method with Existing OC Method

Fault Location	Fault Type	PD	Conventional OC (s)	Proposed Method (s)
Node 840	LLLG	R0	$\geq$1s	0.003
	LG	R0	$\geq$1s	0.003
Node 846	LLLG	R1	$\geq$1s	0.001
	LG	R1	$\geq$1s	0.001
Node 854	LLLG	R2	$\geq$1s	0.221
	LG	R2	$\geq$1s	0.425
Node 826	LLLG	DR	$\geq$1s	0.181
	LG	DR	$\geq$1s	0.449

6.4.3   Performance of Proposed Method for Different Fault location

In this section, fault locations are varied to validate the effectiveness of the proposed microgrid protection scheme. Proposed method needs to work for all faults within the microgrid. First a LLLG fault is applied at node 840. Figure 6.9a and Figure 6.9b show the active and reactive power observed at recloser location $R0$. Figure 6.9c and Figure 6.9d show the current and voltage at recloser location $R0$. Figure 6.9e shows the value of proposed protection element. It shows that following the fault there is a

big change in the element value and it crosses the pre-programmed threshold, which cause $R0$ recloser to operate. Figure 6.9f shows that $R0$ which is the closest recloser to the fault operates first and isolates the fault.

Figure 6.9: Fault Location 1: Results at recloser location R0 for faults at Node 840 (a) Active Power, (b) Reactive Power, (c) Current, (d) Voltage, (e) Proposed algorithm pickup values, and (f) Recloser Status.

Then, a similar LLLG fault is applied at node 860. Figure 6.10a and Figure 6.10b shows the active and reactive power observed at recloser location $R1$. Figure 6.10c and Figure 6.10d show the current and voltage at recloser location $R1$. Figure 6.10e shows the value of proposed protection element. It shows that following the fault there is a big change in the element value and it crosses the pre-programmed threshold,

which cause $R1$ recloser to operate. Figure 6.10f shows that $R1$ which is the closest recloser to the fault operates first and isolates the fault.
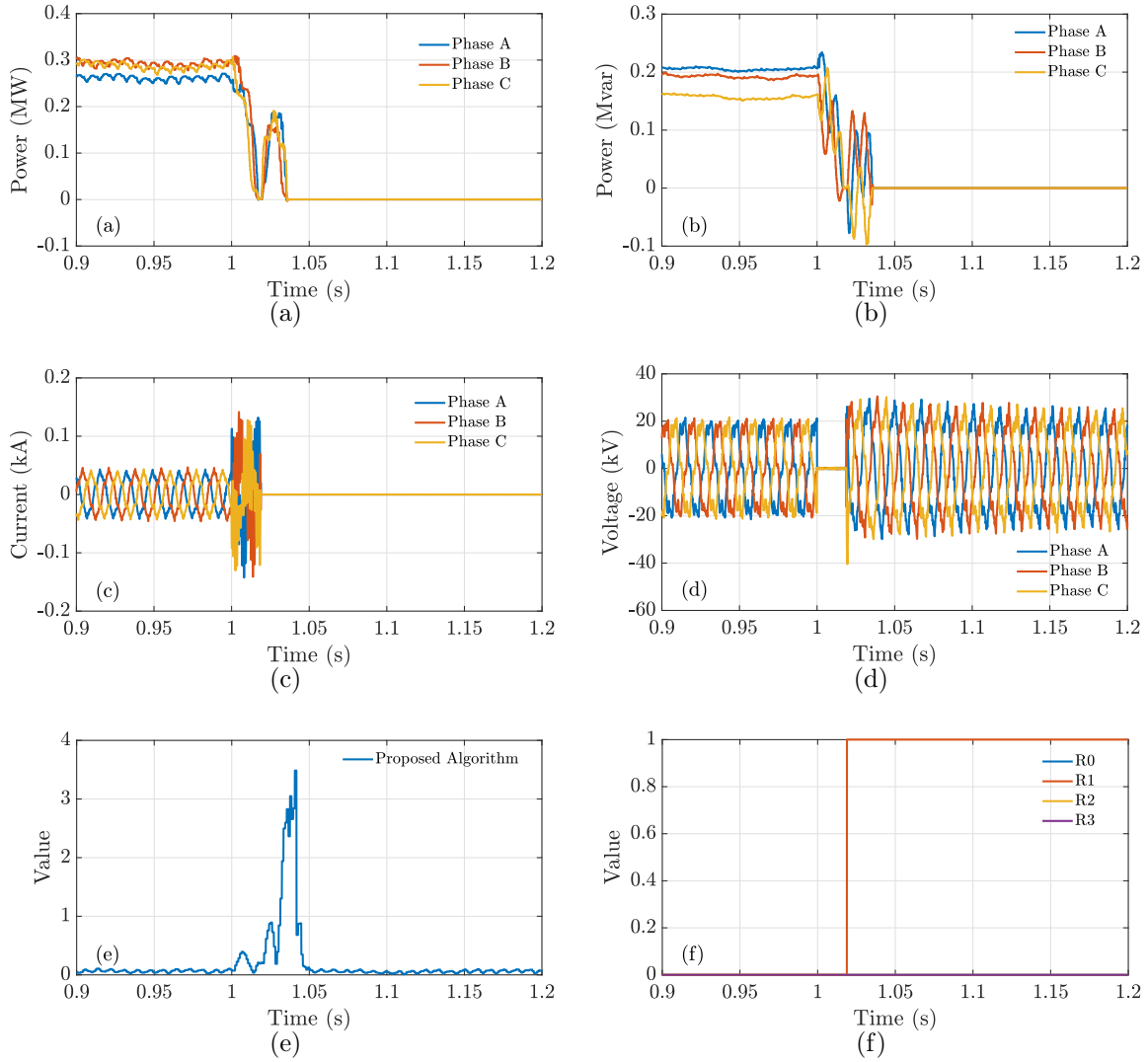
Figure 6.10: Fault Location 2: Results at recloser location R1 for faults at Node 860 (a) Active Power, (b) Reactive Power, (c) Current, (d) Voltage, (e) Proposed algorithm pickup values, and (f) Recloser Status.

Then, a similar LLLG fault is applied at node 854. Figure 6.11a and Figure 6.11b show the active and reactive power observed at recloser location $R2$. Figure 6.11c and Figure 6.11d show the current and voltage at the recloser location $R2$. Figure 6.11e shows the value of proposed protection element. It shows that following the fault there is a big change in the element value and it crosses the pre-programmed threshold,

which cause $R2$ recloser to operate. Figure 6.11f shows that $R2$, which is the closest recloser to the fault, operates first and isolates the fault.

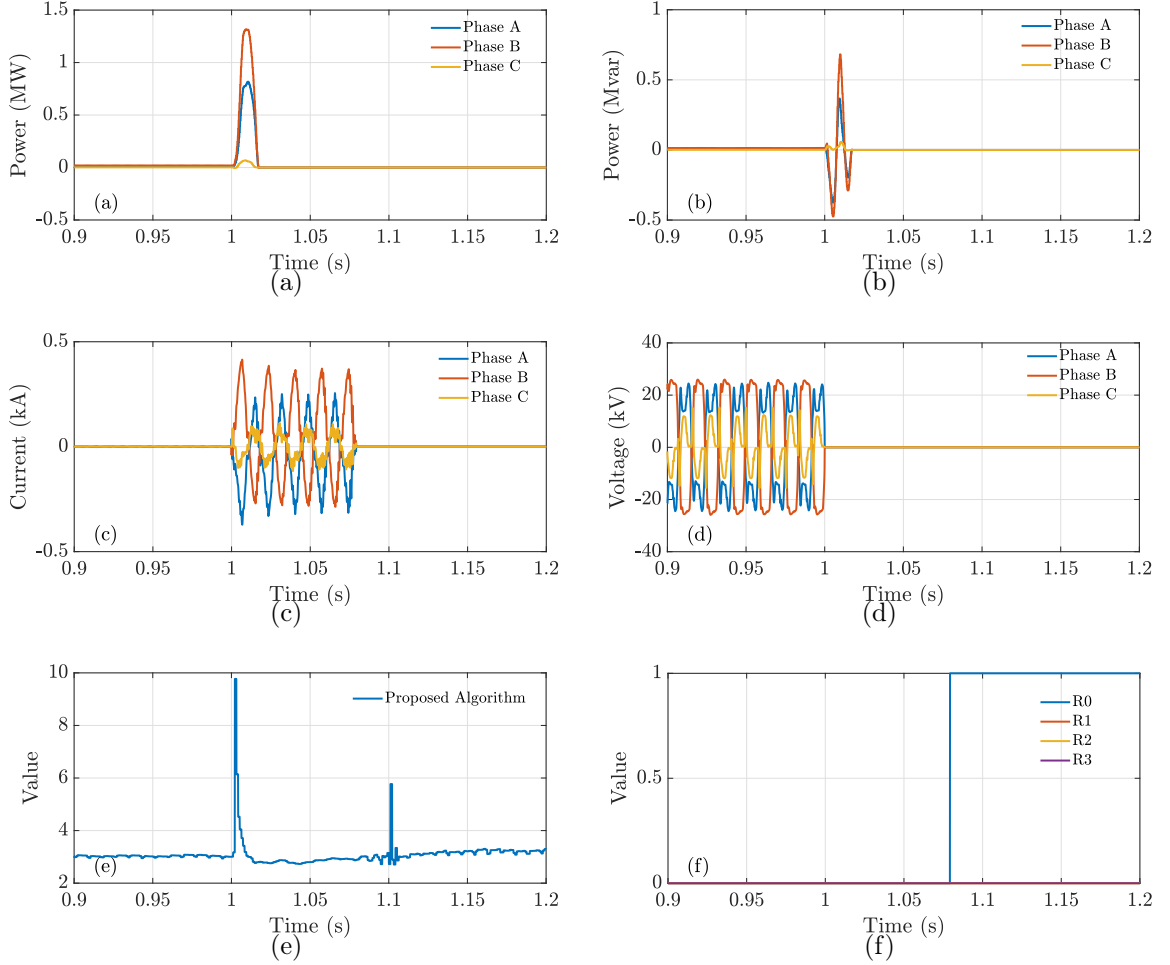Figure 6.11: Fault Location 3: Results at recloser location R2 for faults at Node 854 (a) Active Power, (b) Reactive Power, (c) Current, (d) Voltage, (e) Proposed algorithm pickup values, and (f) Recloser Status.

6.4.4   Performance of Proposed Method for Different DER Size and Location

Effectiveness of the proposed algorithm is tested for different microgrid topology by moving the DER locations and changing DER size.

6.4.4.1   Case 1- Different DER location

For different location of DER proposed algorithm need to effectively identify fault and nearest protection device must response for any type of fault in the distribution system. First location of the DER is node 824, then the second location is node 836. Additionally, fault location is fixed at node 854 for both cases. LLLG and LG faults are applied in both cases. Figure 6.12f shows that recloser $R2$ operates for a fault in node 854 and DER location 824. This is the right operation as the current flows in forward direction through the $R2$ recloser. Figure 6.12a to Figure 6.12e show the other parameters active power, reactive power , voltage, currents and proposed algorithm value respectively.

Figure 6.13f shows that recloser $R1$ operates for a fault in node 854 and DER location 836. This is the right operation as the current flows in reverse direction through the $R1$ recloser and closest to the fault location. Figure 6.13a to Figure 6.13e show the other parameters active power, reactive power , voltage, currents and proposed algorithm value respectively. In all the cases, fault was detected and nearby protection device operated for the particular fault.

6.4.4.2   Case 2: Different DER sizes

For different Size of DERs ($3MVA, 4MVA, 5MVA and 6MVA$), proposed algorithm need to effectively identify all types fault and maintain coordination between protection devices. To validate this, LLLG and LG fault applied at node 854. In all the cases fault was detected and nearby protection device operate for that fault. In this particular test case, A thorough investigation performed for fixed generation to variable load ratio. Load and generation highest ratio is 1. To perform this test this ratio varied between 0.5 to 1. Total load of this microgrid is 2.8MVA.
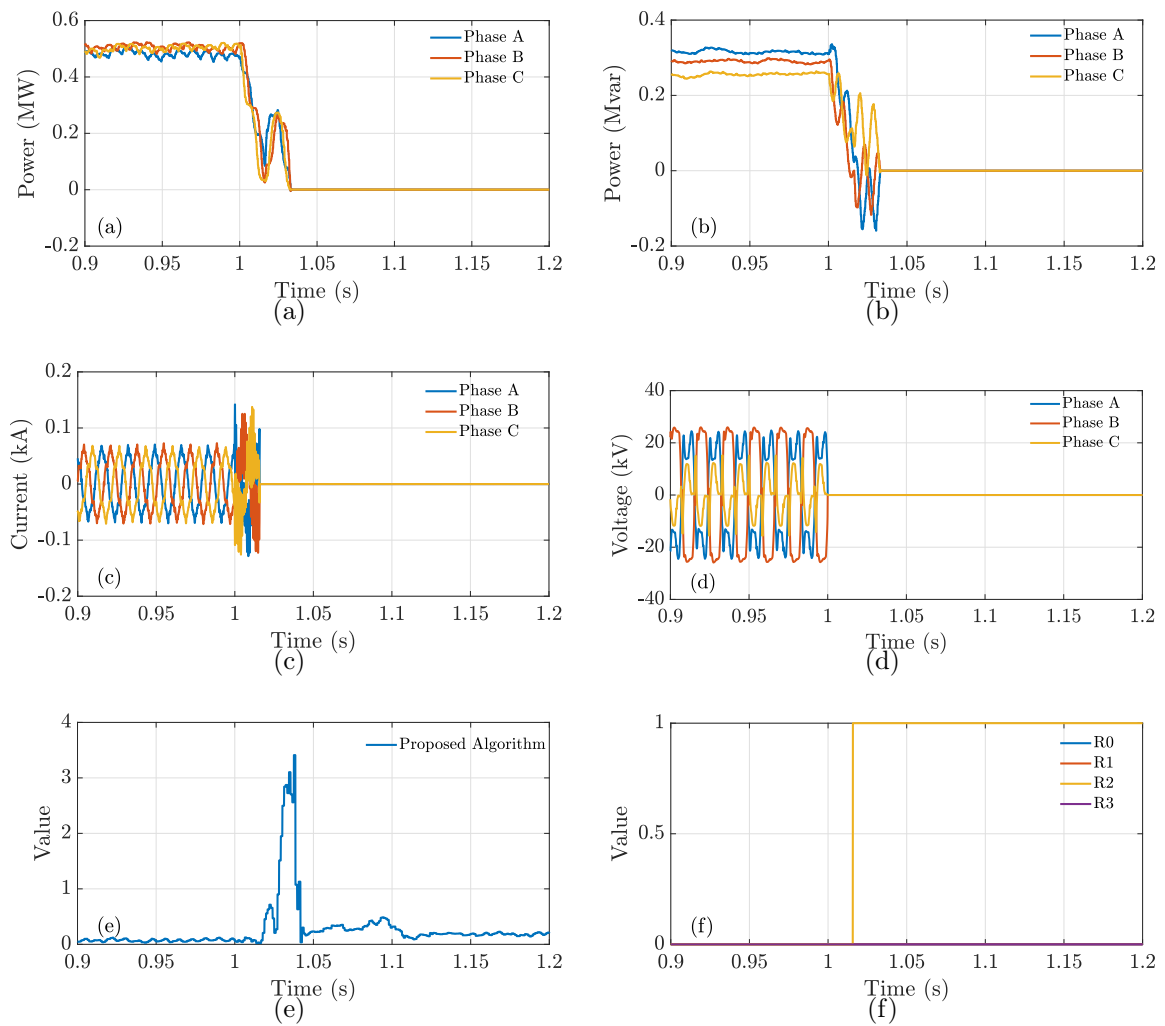
Figure 6.12: DER Location 1: Results at recloser location R2 for faults at Node 854 and DER at Node 824 (a) Active Power, (b) Reactive Power, (c) Current, (d) Voltage, (e) Proposed algorithm pickup values, and (f) Recloser Status.
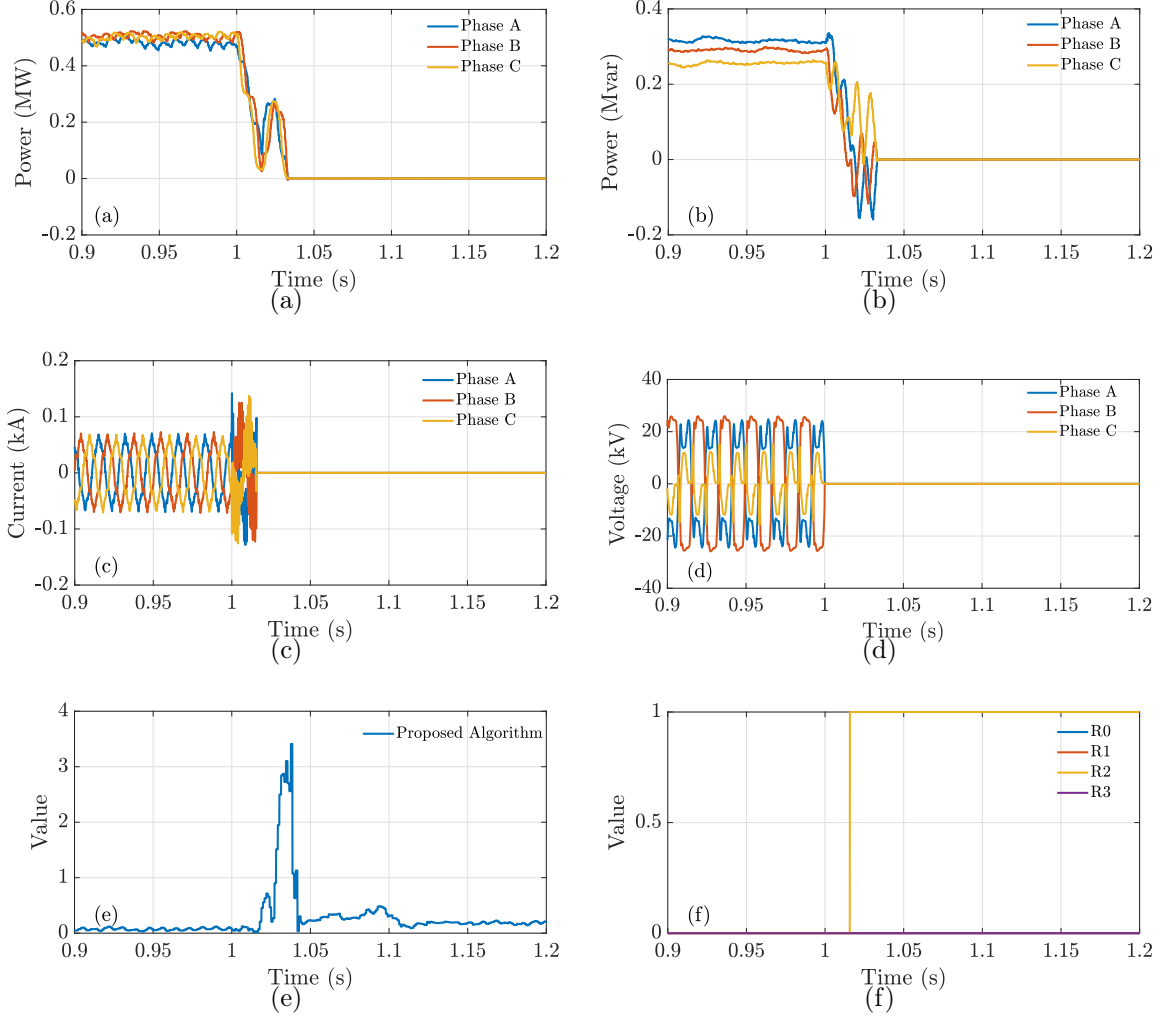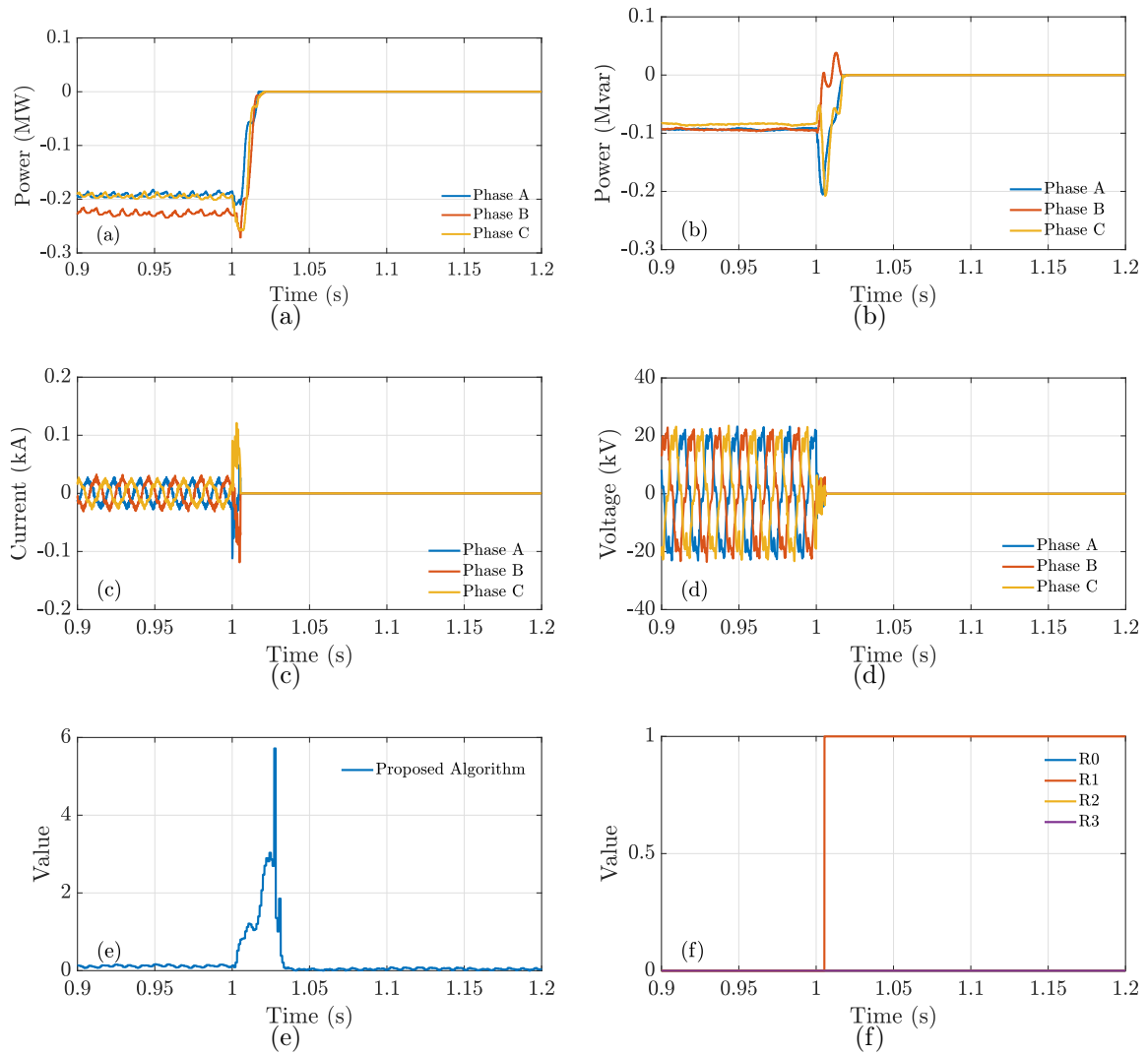
Figure 6.13: DER Location 2: Results at recloser location R1 for faults at Node 854 and DER at Node 836 (a) Active Power, (b) Reactive Power, (c) Current, (d) Voltage, (e) Proposed algorithm pickup values, and (f) Recloser Status.

6.4.5   Sensitivity of Proposed Method for Typical Distribution Switching Events

Any new protection schemes needs to prove it's reliability and show that the chances of false alarms are negligible . There is a lot of very common switching events that happen in a distribution circuit like transformer energization, capacitor bank switching and motors starts. In this section, the proposed algorithm is tested for these scenarios and the effectiveness of proposed protection scheme is tested.

6.4.5.1   Case 1: Transformer Energization

This section Verifies the effectiveness of proposed method for transformer energization event. There are distribution transformer which draws a large inrush current following an outage, during a startup. Any protection scheme should be able to detect that phenomenon and should not operate the protection devices as it is not a fault. Figure 6.14(a)-(d) show the active power, reactive power, currents and voltages observed at location $R2$ during transformer energization at node 888. Figure 6.14e shows that although there is a little increase in the proposed algorithm value but it does not cross the threshold for fault detection. Figure 6.14f confirms that none of the reclosers operate during the transformer energization event.

6.4.5.2   Case 2: Capacitor Bank Start-Up

This section Verifies the effectiveness of proposed method for capacitor bank start up event. There are distribution cap banks which draws a large current during a startup. Any protection scheme should be able to detect that phenomenon and should not operate the protection devices as it is not a fault.Figure 6.15a- 6.15d show the active power, reactive power, currents and voltages observed at location $R2$ during transformer energization at node 888. Figure 6.15e shows that although there is a little increase in the proposed algorithm value but it does not cross the threshold for fault detection. Figure 6.15f confirms that none of the reclosers operate during the capacitor bank start up event. So algorithm was able to differentiate between typical
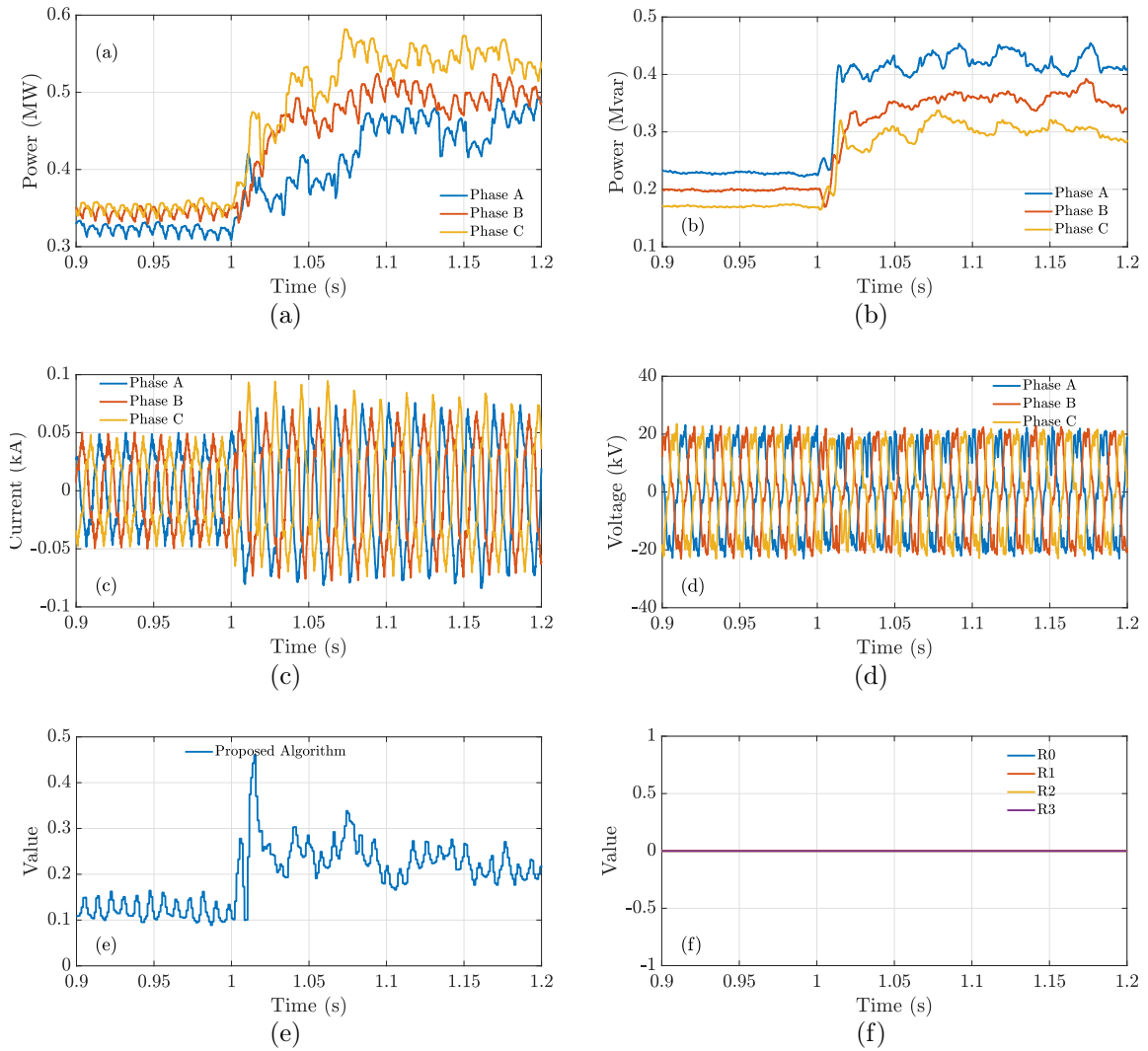
Figure 6.14: Transformer energization at Node 888 at 1 second (a) Active Power, (b) Reactive Power, (c) Current, (d) Voltage, (e) Proposed algorithm pickup values, and (f) Recloser Status.

distribution operation scenario due to capacitor bank energization and fault in the system.
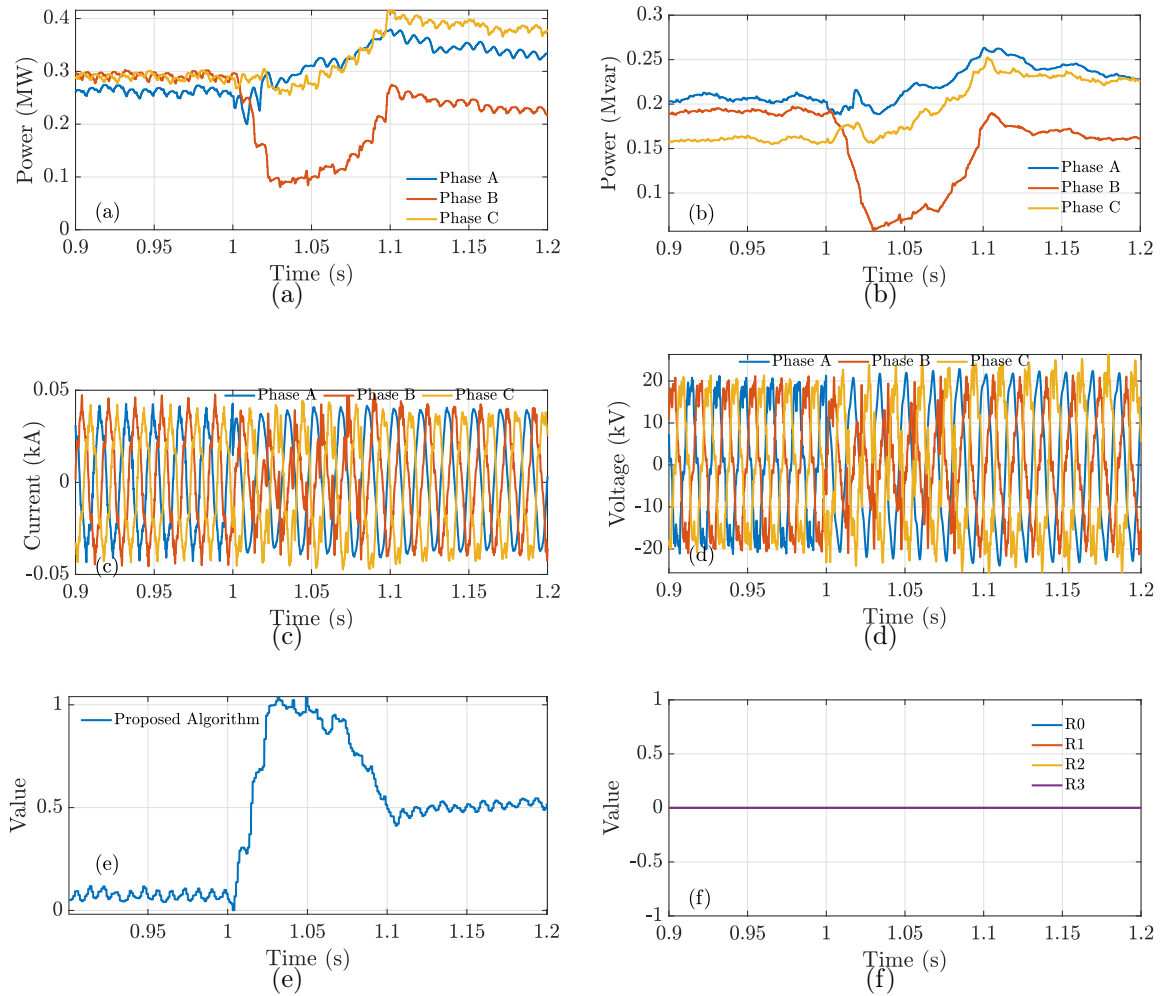
Figure 6.15: Capacitor Bank start up at Node 864 at 1 second (a) Active Power, (b) Reactive Power, (c) Current, (d) Voltage, (e) Proposed algorithm pickup values, and (f) Recloser Status.

6.4.5.3   Case 3: Motor Start-up

A motor started up at node 888 at 1 sec 6.16. There was an increase in current when motor started up however, the amount of current due to motor start did not exceed the limit. Therefore, the algorithm was able to differentiate between typical distribution operation, resulting from motor start up, and a fault in the system.
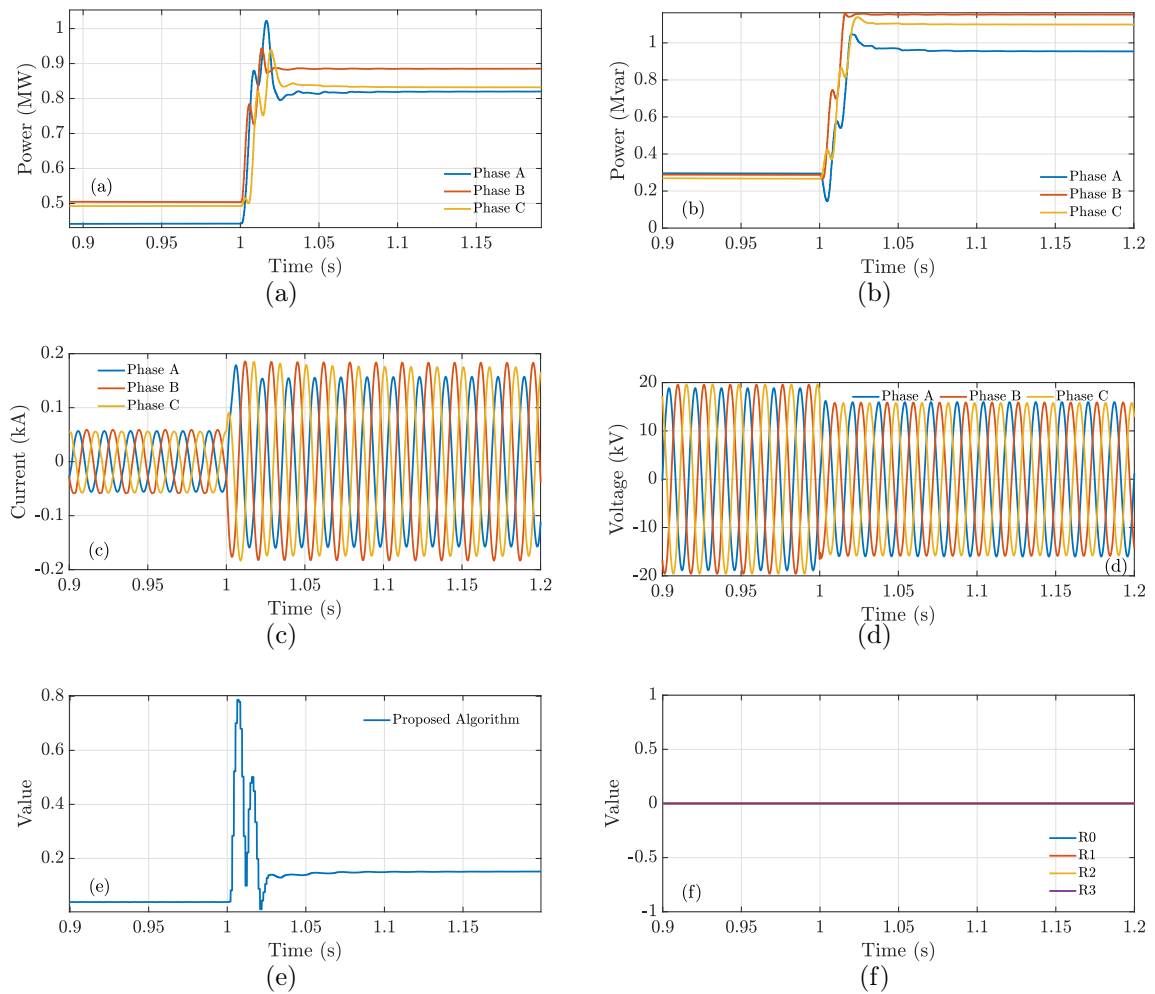
Figure 6.16: 1 MW Motor start up at Node 888 at 1s (a) Active Power, (b) Reactive Power, (c) Current, (d) Voltage, (e) Proposed algorithm pickup values, and (f) Recloser Status.

6.4.6   Computational Burden of Proposed Algorithm

The proposed algorithm is implemented in electro-magnetic transient (EMT) simulation software PSCAD®. PSCAD® software does not perform real-time simulation. To compute the computational burden of the proposed algorithm signals have been recorded in PSCAD and then the recorded data is exported in MATLAB to calculate the execution time of the algorithm. Figure 6.17 shows the computation time of the algorithm for fault at node 854. The results show that in a Intel Core I5 windows machine with a clock speed of 2.3 GHz it takes around 15 ms to execute the algorithm. The algorithm execution time can be faster with more powerful machines.
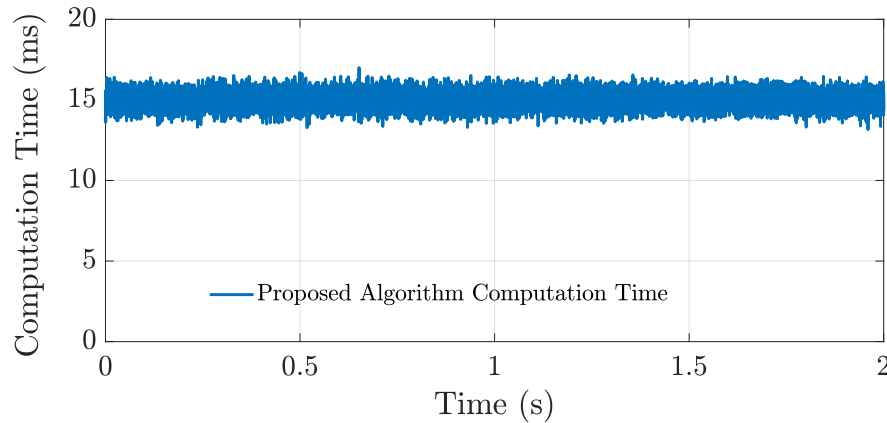
Figure 6.17: Computational time of the proposed algorithm for fault at Node 854.

6.5   Chapter Summary

For both grid-following and grid-forming modes of operation, the impact of inverter-based distributed generation on distribution protection has been investigated in this chapter. The chapter begins by highlighting the drawbacks of the current overcurrent-based protection for microgrids that are entirely inverter-based. Then, in contrast to more conventional approaches, proposes a novel protection scheme that can effectively identify IBMG flaws and produces promising results. The proposed method's robustness will be evaluated for various IDG sizes, locations, and numbers in future work. In a hardware-in-the-loop (HIL) setup, the performance of the proposed method will also be compared to that of other adaptive protection techniques.

CHAPTER 7: CONCLUSIONS AND FUTURE WORK

In this work, new methods are presented to effectively address the challenges related with integrating a fully inverter-based generation resource microgrid with a power distribution system.

Main contributions of the dissertation are as follows:

- This dissertation presents the theoretical background of fully inverter-based microgrids and describes how the short circuit behavior varies for different inverter modes of operation.

- This work investigates the transient overvoltage for a fully inverter-based distribution system microgrids. The results show that the ground fault overvoltage mechanism of inverter-based resources is different than that of synchronous machine-based resources.

- The addition of a grounding transformer does not necessarily guarantee the mitigation of overvoltage. The work also shows the necessity of a ground reference for the steady-state operation of microgrids with unbalanced loads. A negative sequence impedance control method is proposed to reduce the negative sequence voltage and decrease the phase overvoltage and unbalance. The proposed methods are validated and the performance evaluated via several test cases performed on different size IEEE test systems. Test results validate the proposed methods and show that these approaches can improve the inverter-based microgrid system design and increase the reliability of such systems.

- Also, the impact of inverter-based distributed generation on distribution protection has been studied for both grid-following and grid-forming modes of op-

eration. First, the limitations of existing overcurrent-based protection for fully inverter-based microgrids discussed. Then, a novel protection scheme is proposed that can effectively detect faults for inverter-based microgrids. Based on the test results, the proposed methods shows promising performance improvements in comparison with conventional methods.

The work proposed in this dissertation leads to an number of future research plans for developing analytical tools that can help the design and integration of microgrids. Suggestions of future work areas are detailed below:

- In the future, the robustness of the proposed method will be tested for different inverter-based distributed generation sizes, locations, and numbers. The proposed method's performance will also be compared with other adaptive protection methods.

- The current work does not consider inverter protection settings in the study. In future work, scenarios can be considered with inverter protection settings and the findings can be validated using hardware in the loop simulations.

- The negative sequence impedance reference selection in the transient overvoltage mitigation work can be automated in the future, where the current work provides a basis to address this enhancement. This will help to make the developed method more robust and effective without necessitating any system prior knowledge.

- The proposed method for fault detection can be enhanced for different microgrid topologies, sizes, and locations. The robustness of the proposed method can be further evaluated and adjusted accordingly.

- The sequence network models developed here for different inverter control modes will be compared with positive sequence models used in commercial software

to perform short circuit studies. The deficiencies of positive sequence models used in steady state short circuit studies will be demonstrated and a method for representing inverter dynamics in such software will be presented.

REFERENCES

[1] EPRI, "Grid considerations for microgrids." [Online]. Available: https://www.epri.com/research/products/000000003002020344

[2] A. Aram, "Hitachi review - global innovation report: Microgrid market in the usa," 2017. [Online]. Available: https://www.hitachi.com/rev/archive/2017/r2017_05/pdf/P26-30_Global.pdf

[3] Bloom Energy, "California power outage map." [Online]. Available: https://www.bloomenergy.com/bloom-energy-outage-map/

[4] Y. Lin, J. H. Eto, B. B. Johnson, J. D. Flicker, R. H. Lasseter, H. N. Villegas Pico, G.-S. Seo, B. J. Pierre, and A. Ellis, "Research roadmap on grid-forming inverters," 11 2020. [Online]. Available: https://www.osti.gov/biblio/1721727

[5] B. Banu, M. Smith, and S. Kamalasadan, "Control of transient overvoltage for inverter only based microgrids in power distribution system," in *2021 IEEE Power & Energy Society General Meeting (PESGM)*, 2021, pp. 1–5.

[6] W. H. Kersting and G. Shirek, "Short circuit analysis of IEEE test feeders," in *PES T D 2012*, 2012, pp. 1–9.

[7] B. Banu, M. Smith, and S. Kamalasadan, "Novel protection method for fully inverter-based distribution system microgrid," in *2021 North American Power Symposium (NAPS)*, 2021, pp. 01–06.

[8] B. Singh, G. Pathak, and B. K. Panigrahi, "Seamless transfer of renewable-based microgrid between utility grid and diesel generator," *IEEE Transactions on Power Electronics*, vol. 33, no. 10, pp. 8427–8437, 2018.

[9] O. P. Jaga and S. G. Choudhuri, "Seamless transition between grid-connected and islanded operation modes for hybrid pv-bess combination used in single-phase, critical load applications," in *2021 International Conference on Sustainable Energy and Future Electric Transportation (SEFET)*, 2021, pp. 1–6.

[10] M. Kalantar-Neyestanaki and R. Cherkaoui, "Coordinating distributed energy resources and utility-scale battery energy storage system for power flexibility provision under uncertainty," *IEEE Transactions on Sustainable Energy*, vol. 12, no. 4, pp. 1853–1863, 2021.

[11] Z. Ye, C. Chen, B. Chen, and K. Wu, "Resilient service restoration for unbalanced distribution systems with distributed energy resources by leveraging mobile generators," *IEEE Transactions on Industrial Informatics*, vol. 17, no. 2, pp. 1386–1396, 2021.

[12] A. Schatz and P. Musilek, "Implications of microgrids, economic autonomy and renewable energy systems for remote indigenous communities," in *2020 IEEE Electric Power and Energy Conference (EPEC)*, 2020, pp. 1–4.

[13] H.-C. Jo, J.-Y. Kim, G. Byeon, and S.-K. Kim, "Optimal scheduling method of community microgrid with customer-owned distributed energy storage system," in *2019 International Conference on Smart Energy Systems and Technologies (SEST)*, 2019, pp. 1–6.

[14] A. K. Jain, A. Nagarajan, I. Chernyakhovskiy, T. Bowen, B. Mather, and J. Cochran, "Evolution of distributed energy resource grid interconnection standards for integrating emerging storage technologies," in *2019 North American Power Symposium (NAPS)*, 2019, pp. 1–6.

[15] M. H. Saeed, W. Fangzong, B. A. Kalwar, and S. Iqbal, "A review on microgrids' challenges & perspectives," *IEEE Access*, vol. 9, pp. 166 502–166 517, 2021.

[16] J. W. Zapata, G. Postiglione, and F. Pezet, "Supervision based smart microgrid systems: Grid connected, island mode and seamless transition," in *2020 International Symposium on Power Electronics, Electrical Drives, Automation and Motion (SPEEDAM)*, 2020, pp. 336–341.

[17] "Approved draft guide to using IEEE ieee p 1547 for interconnection of energy storage distributed energy resources with electric power systems," *IEEE P1547.9/D5.6, May 2022 (Approved Draft)*, pp. 1–83, 2022.

[18] T. Ye, L. Jin, and R. Xue, "Influence of grid-connection photovoltaic on power quality and relay protection of distribution network," in *2019 IEEE 8th International Conference on Advanced Power System Automation and Protection (APAP)*, 2019, pp. 940–944.

[19] National Renewable Energy Laboratory, "Increasing resiliency through renewable energy microgrids." [Online]. Available: https://www.nrel.gov/docs/fy17osti/69034.pdf

[20] R. Bisht, S. Subramaniam, R. Bhattarai, and S. Kamalasadan, "Active and reactive power control of single phase inverter with seamless transfer between grid-connected and islanded mode," in *2018 IEEE Power and Energy Conference at Illinois (PECI)*, 2018, pp. 1–8.

[21] A. Muhtadi, D. Pandit, N. Nguyen, and J. Mitra, "Distributed energy resources based microgrid: Review of architecture, control, and reliability," *IEEE Transactions on Industry Applications*, vol. 57, no. 3, pp. 2223–2235, 2021.

[22] J. Shiles, E. Wong, S. Rao, C. Sanden, M. A. Zamani, M. Davari, and F. Katiraei, "Microgrid protection: An overview of protection strategies in north american microgrid projects," in *2017 IEEE Power & Energy Society General Meeting*, 2017, pp. 1–5.

[23] W. Zhao, X. Bi, W. Wang, and X. Sun, "Microgrid relay protection scheme based on harmonic footprint of short-circuit fault," *Chinese Journal of Electrical Engineering*, vol. 4, no. 4, pp. 64–70, 2018.

[24] L. He, S. Rong, and C. Liu, "An intelligent overcurrent protection algorithm of distribution systems with inverter based distributed energy resources," in *2020 IEEE Energy Conversion Congress and Exposition (ECCE)*, 2020, pp. 2746–2751.

[25] J. Shiles, E. Wong, S. Rao, C. Sanden, M. A. Zamani, M. Davari, and F. Katiraei, "Microgrid protection: An overview of protection strategies in north american microgrid projects," in *2017 IEEE Power Energy Society General Meeting*, 2017, pp. 1–5.

[26] N. L. Soultanis, S. A. Papathanasiou, and N. D. Hatziargyriou, "A stability algorithm for the dynamic analysis of inverter dominated unbalanced lv microgrids," *IEEE Transactions on Power Systems*, vol. 22, no. 1, pp. 294–304, 2007.

[27] H. Cai, G. Hu, F. L. Lewis, and A. Davoudi, "A distributed feedforward approach to cooperative control of ac microgrids," *IEEE Transactions on Power Systems*, vol. 31, no. 5, pp. 4057–4067, 2016.

[28] A. K. Soni, R. K. Panda, A. Kumar, A. Mohapatra, S. N. Singh, and S. C. Srivastava, "Impact of control parameters on short-circuit capacity of inverter based sources," in *2022 IEEE IAS Global Conference on Emerging Technologies (GlobConET)*, 2022, pp. 1113–1118.

[29] J. Rocabert, A. Luna, F. Blaabjerg, and P. RodrÃguez, "Control of power converters in ac microgrids," *IEEE Transactions on Power Electronics*, vol. 27, no. 11, pp. 4734–4749, 2012.

[30] P. J. Hart, R. H. Lasseter, and T. M. Jahns, "Coherency identification and aggregation in grid-forming droop-controlled inverter networks," *IEEE Transactions on Industry Applications*, vol. 55, no. 3, pp. 2219–2231, 2019.

[31] Z. Li, C. Zang, P. Zeng, H. Yu, S. Li, and J. Bian, "Control of a grid-forming inverter based on sliding-mode and mixed H_2/H_∞ control," *IEEE Transactions on Industrial Electronics*, vol. 64, no. 5, pp. 3862–3872, 2017.

[32] H. Juan Carlos Quispe, "Analysis of directional protections in distributed generation system with synchronous generators and inverter-based resources," in *2022 IEEE XXIX International Conference on Electronics, Electrical Engineering and Computing (INTERCON)*, 2022, pp. 1–4.

[33] S. Hemavathi and M. Singh, "Microgrid short circuit studies," in *2018 IEEE 8th Power India International Conference (PIICON)*, 2018, pp. 1–6.

[34] Z. Fu, F. Zhang, S. Li, W. Meng, and C. Zhang, "Research on short circuit operation mechanism and current limiting strategy of single phase inverter," in *2018 IEEE Applied Power Electronics Conference and Exposition (APEC)*, 2018, pp. 205–209.

[35] I. Kim, "Short-circuit analysis models for unbalanced inverter-based distributed generation sources and loads," *IEEE Transactions on Power Systems*, vol. 34, no. 5, pp. 3515–3526, 2019.

[36] Q. Zhang, D. Liu, Z. Liu, and Z. Chen, "Fault modeling and analysis of grid-connected inverters with decoupled sequence control," *IEEE Transactions on Industrial Electronics*, vol. 69, no. 6, pp. 5782–5792, 2022.

[37] M. Baran and I. El-Markaby, "Fault analysis on distribution feeders with distributed generators," *IEEE Transactions on Power Systems*, vol. 20, no. 4, pp. 1757–1764, 2005.

[38] A. Hooshyar, E. F. El-Saadany, and M. Sanaye-Pasand, "Fault type classification in microgrids including photovoltaic dgs," *IEEE Transactions on Smart Grid*, vol. 7, no. 5, pp. 2218–2229, 2016.

[39] S. Buso, T. Caldognetto, and Q. Liu, "Analysis and experimental characterization of a large-bandwidth triple-loop controller for grid-tied inverters," *IEEE Transactions on Power Electronics*, vol. 34, no. 2, pp. 1936–1949, 2019.

[40] J. A. Mueller, M. Rasheduzzaman, and J. W. Kimball, "A model modification process for grid-connected inverters used in islanded microgrids," *IEEE Transactions on Energy Conversion*, vol. 31, no. 1, pp. 240–250, 2016.

[41] F. Wang, H. Zuo, Y. Xu, W. Xiao, X. Liang, and Y. Zhou, "Modeling and simulation of electromagnetic transient parameter identification method based on photovoltaic power station," in *2018 10th International Conference on Measuring Technology and Mechatronics Automation (ICMTMA)*, 2018, pp. 135–138.

[42] Z. Xie, Y. Chen, W. Wu, Y. Xu, H. Wang, J. Guo, and A. Luo, "Modeling and control parameters design for grid-connected inverter system considering the effect of pll and grid impedance," *IEEE Access*, vol. 8, pp. 40 474–40 484, 2020.

[43] K. Jia, Q. Liu, B. Yang, L. Zheng, Y. Fang, and T. Bi, "Transient fault current analysis of IIRESs considering controller saturation," *IEEE Transactions on Smart Grid*, vol. 13, no. 1, pp. 496–504, 2022.

[44] J. A. Mueller and J. W. Kimball, "An efficient method of determining operating points of droop-controlled microgrids," *IEEE Transactions on Energy Conversion*, vol. 32, no. 4, pp. 1432–1446, 2017.

[45] D. Ramasubramanian and V. Vittal, "Positive sequence model for converter-interfaced synchronous generation with finite dc capacitance," *IEEE Transactions on Power Systems*, vol. 33, no. 3, pp. 3172–3180, 2018.

[46] D. Ramasubramanian, P. Pourbeik, E. Farantatos, and A. Gaikwad, "Simulation of 100*IEEE Electrification Magazine*, vol. 9, no. 2, pp. 62–71, 2021.

[47] D. Shin, K.-J. Lee, J.-P. Lee, D.-W. Yoo, and H.-J. Kim, "Implementation of fault ride-through techniques of grid-connected inverter for distributed energy resources with adaptive low-pass notch pll," *IEEE Transactions on Power Electronics*, vol. 30, no. 5, pp. 2859–2871, 2015.

[48] S. A. Saleh, A. S. Aljankawey, B. Alsayid, and M. S. Abu-Khaizaran, "Influences of power electronic converters on voltage-current behaviors during faults in dgus-part ii: Photovoltaic systems," *IEEE Transactions on Industry Applications*, vol. 51, no. 4, pp. 2832–2845, 2015.

[49] M. Brucoli, T. C. Green, and J. D. F. McDonald, "Modelling and analysis of fault behaviour of inverter microgrids to aid future fault detection," in *2007 IEEE International Conference on System of Systems Engineering*, 2007, pp. 1–6.

[50] Q.-C. Zhong and Y. Zeng, "Control of inverters via a virtual capacitor to achieve capacitive output impedance," *IEEE Transactions on Power Electronics*, vol. 29, no. 10, pp. 5568–5578, 2014.

[51] Z. Shuai, C. Shen, X. Yin, X. Liu, and Z. J. Shen, "Fault analysis of inverter-interfaced distributed generators with different control schemes," *IEEE Transactions on Power Delivery*, vol. 33, no. 3, pp. 1223–1235, 2018.

[52] W.-M. Guo, L.-H. Mu, and X. Zhang, "Fault models of inverter-interfaced distributed generators within a low-voltage microgrid," *IEEE Transactions on Power Delivery*, vol. 32, no. 1, pp. 453–461, 2017.

[53] M. A. Haj-ahmed and M. S. Illindala, "The influence of inverter-based dgs and their controllers on distribution network protection," *IEEE Transactions on Industry Applications*, vol. 50, no. 4, pp. 2928–2937, 2014.

[54] H. Hooshyar and M. E. Baran, "Fault analysis on distribution feeders with high penetration of pv systems," *IEEE Transactions on Power Systems*, vol. 28, no. 3, pp. 2890–2896, 2013.

[55] T. Kauffmann, U. Karaagac, I. Kocar, S. Jensen, E. Farantatos, A. Haddadi, and J. Mahseredjian, "Short-circuit model for type-iv wind turbine generators with decoupled sequence control," *IEEE Transactions on Power Delivery*, vol. 34, no. 5, pp. 1998–2007, 2019.

[56] T. Kauffmann, U. Karaagac, I. Kocar, S. Jensen, J. Mahseredjian, and E. Farantatos, "An accurate type iii wind turbine generator short circuit model for protection applications," *IEEE Transactions on Power Delivery*, vol. 32, no. 6, pp. 2370–2379, 2017.

[57] K. Visscher and S. De Haan, "Virtual synchronous machines (vsg's) for frequency stabilisation in future grids with a significant share of decentralized generation," in *CIRED Seminar 2008: SmartGrids for Distribution*, 2008, pp. 1–4.

[58] A. Engler *et al.*, "Control of parallel operating battery inverters," in *Photovoltaic Hybrid Power Systems Conference*, 2000, pp. 1–4.

[59] F. Gonzalez-Longatt, J. L. Rueda, P. Palensky, H. R. Chamorro, and V. Sood, "Frequency support provided by inverted based-generation using grid-forming controllers: A comparison during islanded operation," in *2021 IEEE Electrical Power and Energy Conference (EPEC)*, 2021, pp. 113–118.

[60] S. Alzahrani, K. Sinjari, and J. Mitra, "An integrated control and protection scheme for microgrids," in *2021 International Conference on Smart Energy Systems and Technologies (SEST)*, 2021, pp. 1–6.

[61] T. Kawabata and S. Higashino, "Parallel operation of voltage source inverters," *IEEE Transactions on Industry Applications*, vol. 24, no. 2, pp. 281–287, 1988.

[62] B. Wang, R. Burgos, Y. Tang, and B. Wen, "Fault characteristics analysis on 56-bus distribution system with penetration of utility-scale pv generation," in *2021 6th IEEE Workshop on the Electronic Grid (eGRID)*, 2021, pp. 01–08.

[63] K. Jia, Z. Yang, T. Bi, and Y. Li, "Impact of inverter-interfaced renewable energy generators on distance protection and an improved scheme," in *2019 IEEE Power & Energy Society General Meeting (PESGM)*, 2019, pp. 1–1.

[64] M. Shahidehpour and J. F. Clair, "A functional microgrid for enhancing reliability, sustainability, and energy efficiency," *The Electricity Journal*, vol. 25, no. 8, pp. 21 – 28, 2012.

[65] Y. Xu, C. Liu, K. P. Schneider, F. K. Tuffner, and D. T. Ton, "Microgrids for service restoration to critical load in a resilient distribution system," *IEEE Transactions on Smart Grid*, vol. 9, no. 1, pp. 426–437, 2018.

[66] T&D World, "Improving grid resiliency one microgrid at a time." [Online]. Available: https://www.tdworld.com/distributed-energy-resources/article/21118745/improving-grid-resiliency-one-microgrid-at-a-time#

[67] P. P. et al., "Grounding and ground fault protection of multiple generator installations on medium-voltage industrial and commercial power systems - part 1: The problem defined working group report," *IEEE Transactions on Industry Applications*, vol. 40, no. 1, pp. 11–16, 2004.

[68] "IEEE guide for the application of neutral grounding in electrical utility systems–part i: Introduction," *IEEE Std C62.92.1-2016 (Revision of IEEE Std C62.92.1-2000)*, pp. 1–38, 2017.

[69] "IEEE guide for the application of neutral grounding in electrical utility systems, part ii–synchronous generator systems," *IEEE Std C62.92.2-2017 (Revision of IEEE Std C62.92.2-1989)*, pp. 1–38, 2017.

[70] "IEEE draft guide for the application of neutral grounding in electrical utility systems, part vi - systems supplied by current-regulated sources," *IEEE Std C62.92.6-2017*, pp. 1–36, 2017.

[71] S. C. Vegunta, M. J. Higginson, Y. E. Kenarangui, G. T. Li, D. W. Zabel, M. Tasdighi, and A. Shadman, "Ac microgrid protection system design challenges-a practical experience," *Energies*, vol. 14, no. 7, 2021. [Online]. Available: https://www.mdpi.com/1996-1073/14/7/2016

[72] "Microgrid protection systems," *PES-TR71,Power System Relaying and Control Committee*, pp. 1–58, 2019.

[73] P. Tatro and J. Gardell, "Power plant and transmission system protection coordination-phase distance (21) and voltage-controlled or voltage-restrained overcurrent protection (51v)-nerc protection coordination webinar series," *The North American Electric Reliability Corporation (NERC): Atlanta, GA, USA*, pp. 1–55, 2010.

[74] J. Ciufo and A. Cooperberg, *What Is Power System Protection, Why Is It Required and Some Basics?* Wiley, 2022, pp. 1–12.

[75] "IEEE guide for protection system redundancy for power system reliability," *IEEE Std C37.120-2021*, pp. 1–72, 2022.

[76] O. Gomis-Bellmunt, J. Liang, J. Ekanayake, R. King, and N. Jenkins, "Topologies of multiterminal hvdc-vsc transmission for large offshore wind farms," *Electric Power Systems Research*, vol. 81, no. 2, pp. 271–281, 2011. [Online]. Available: https://www.sciencedirect.com/science/article/pii/S0378779610002166

[77] Y. N. Velaga, R. Jain, and J. Sawant, "Modeling distributed energy resources for analyzing distribution systems with high renewable penetration," in *2022 IEEE Rural Electric Power Conference (REPC)*, 2022, pp. 11–17.

[78] C. K. Sao and P. W. Lehn, "Control and power management of converter fed microgrids," *IEEE Transactions on Power Systems*, vol. 23, no. 3, pp. 1088–1098, 2008.

[79] V. Blasko and V. Kaura, "A new mathematical model and control of a three-phase ac-dc voltage source converter," *IEEE Transactions on Power Electronics*, vol. 12, no. 1, pp. 116–123, 1997.

[80] J. Morren and S. de Haan, "Ridethrough of wind turbines with doubly-fed induction generator during a voltage dip," *IEEE Transactions on Energy Conversion*, vol. 20, no. 2, pp. 435–441, 2005.

[81] C. Feltes, H. Wrede, F. W. Koch, and I. Erlich, "Enhanced fault ride-through method for wind farms connected to the grid through vsc-based hvdc transmission," *IEEE Transactions on Power Systems*, vol. 24, no. 3, pp. 1537–1546, 2009.

[82] L. Xu, "Coordinated control of dfig's rotor and grid side converters during network unbalance," *IEEE Transactions on Power Electronics*, vol. 23, no. 3, pp. 1041–1049, 2008.

[83] H.-S. Song and K. Nam, "Dual current control scheme for pwm converter under unbalanced input voltage conditions," *IEEE Transactions on Industrial Electronics*, vol. 46, no. 5, pp. 953–959, 1999.

[84] P. Rioual, H. Pouliquen, and J.-P. Louis, "Regulation of a pwm rectifier in the unbalanced network state using a generalized model," *IEEE Transactions on Power Electronics*, vol. 11, no. 3, pp. 495–502, 1996.

[85] O. Gomis-Bellmunt, A. Junyent-FerrE, A. Sumper, and J. Bergas-JanE, "Ride-through control of a doubly fed induction generator under unbalanced voltage sags," *IEEE Transactions on Energy Conversion*, vol. 23, no. 4, pp. 1036–1045, 2008.

[86] S. Alepuz, S. Busquets-Monge, J. Bordonau, J. A. Martinez-Velasco, C. A. Silva, J. Pontt, and J. Rodriguez, "Control strategies based on symmetrical components for grid-connected converters under voltage dips," *IEEE Transactions on Industrial Electronics*, vol. 56, no. 6, pp. 2162–2173, 2009.

[87] Y. Zhou, P. Bauer, J. A. Ferreira, and J. Pierik, "Operation of grid-connected dfig under unbalanced grid voltage condition," *IEEE Transactions on Energy Conversion*, vol. 24, no. 1, pp. 240–246, 2009.

[88] J. Hu, Y. He, L. Xu, and B. W. Williams, "Improved control of dfig systems during network unbalance using pi-r current regulators," *IEEE Transactions on Industrial Electronics*, vol. 56, no. 2, pp. 439–451, 2009.

[89] Z. Li, Y. Li, P. Wang, H. Zhu, C. Liu, and W. Xu, "Control of three-phase boost-type pwm rectifier in stationary frame under unbalanced input voltage," *IEEE Transactions on Power Electronics*, vol. 25, no. 10, pp. 2521–2530, 2010.

[90] M. Graungaard Taul, X. Wang, P. Davari, and F. Blaabjerg, "Current reference generation based on next-generation grid code requirements of grid-tied converters during asymmetrical faults," *IEEE Journal of Emerging and Selected Topics in Power Electronics*, vol. 8, no. 4, pp. 3784–3797, 2020.

[91] M. W. Altaf, M. T. Arif, S. N. Islam, and M. E. Haque, "Microgrid protection challenges and mitigation approaches-a comprehensive review," *IEEE Access*, vol. 10, pp. 38 895–38 922, 2022.

[92] D. Liu, D. Tzelepis, and A. Dysko, "Protection of microgrids with high amounts of renewables: Challenges and solutions," in *2019 54th International Universities Power Engineering Conference (UPEC)*, 2019, pp. 1–6.

[93] A. Srivastava, R. Mohanty, M. A. F. Ghazvini, L. A. Tuan, D. Steen, and O. Carlson, "A review on challenges and solutions in microgrid protection," in *2021 IEEE Madrid PowerTech*, 2021, pp. 1–6.

[94] E. Gairola and M. S. Rawat, "An extensive review on microgrid protection issues, techniques and solutions," in *2021 9th IEEE International Conference on Power Systems (ICPS)*, 2021, pp. 1–6.

[95] R. W. Kenyon, B. Wang, A. Hoke, J. Tan, C. Antonio, and B.-M. Hodge, "Validation of maui pscad model: Motivation, methodology, and lessons learned," in *2020 52nd North American Power Symposium (NAPS)*, 2021, pp. 1–6.

[96] Department of Energy's Grid Modernization Lab Call, "Grid modernization initiative." [Online]. Available: https://www.energy.gov/sites/prod/files/2019/05/f63/GMI-National-Lab-Call-2019-05-29.pdf

[97] A. B. Nassif, "Assessment and mitigation of temporary overvoltages on distribution feeders with high penetration of distributed energy resources," in *2021 IEEE PES Innovative Smart Grid Technologies Conference - Latin America (ISGT Latin America)*, 2021, pp. 1–5.

[98] A. B. Nassif, E. Loi, K. A. Wheeler, and S. Bahramirad, "Impact of ibr negative-sequence current injection on ground fault temporary overvoltage and ground overcurrent protection," in *2022 IEEE/PES Transmission and Distribution Conference and Exposition (T&D)*, 2022, pp. 1–5.

[99] J. A. X. Prabhu, J. S. Jha, R. Chelluri, and N. Somidi, "Importance of negative phase sequence overcurrent protection for solidly grounded delta-wye transformer," in *2019 3rd International Conference on Recent Developments in Control, Automation & Power Engineering (RDCAPE)*, 2019, pp. 12–16.

[100] A. Castro and D. Zaninelli, "Introduction of current limiting impedance for a previously solid grounded medium voltage distribution network," in *2019 IEEE Milan PowerTech*, 2019, pp. 1–6.

[101] B. Rittong and S. Sirisumrannukul, "Assessment of voltage sag and temporary overvoltage for neutral grounding resistance in distribution system," in *2019 IEEE PES GTD Grand International Conference and Exposition Asia (GTD Asia)*, 2019, pp. 796–801.

[102] Solectra Renewables, "Effective grounding for PV plants." [Online]. Available: https://www.solectria.com//site/assets/files/1484/solectria_effective_grounding_for_pv_plants.pdf

[103] Y. Zhang, "Performances of different grounding methods on mmc-based bipolar dc grids," in *2019 4th IEEE Workshop on the Electronic Grid (eGRID)*, 2019, pp. 1–7.

[104] H. B. . Lee, S. E. Chase, and R. C. Dugan, "Overvoltage considerations for interconnecting dispersed generators with wye-grounded distribution feeders," *IEEE Transactions on Power Apparatus and Systems*, vol. PAS-103, no. 12, pp. 3587–3594, 1984.

[105] A. Nelson, A. Hoke, S. Chakraborty, M. Ropp, J. Chebahtah, T. Wang, and M. McCarty, "Inverter ground fault overvoltage testing," in *2015 IEEE 42nd Photovoltaic Specialist Conference (PVSC)*, 2015, pp. 1–6.

[106] A. Nelson, A. Hoke, S. Chakraborty, M. Ropp, J. Chebahtah, T. Wang, and B. Zimmerly, "Experimental evaluation of load rejection over-voltage from grid-tied solar inverters," in *2015 IEEE 42nd Photovoltaic Specialist Conference (PVSC)*, 2015, pp. 1–6.

[107] M. Ropp, A. Hoke, S. Chakraborty, D. Schutz, C. Mouw, A. Nelson, M. McCarty, T. Wang, and A. Sorenson, "Ground fault overvoltage with inverter-interfaced distributed energy resources," *IEEE Transactions on Power Delivery*, vol. 32, no. 2, pp. 890–899, 2017.

[108] W. Wang, X. Shi, A. Huque, and T. Key, "Impact of interconnection transformer configuration on operation of inverter-based der," in *2021 IEEE 48th Photovoltaic Specialists Conference (PVSC)*, 2021, pp. 2149–2154.

[109] H. Zeng, P. Yang, H. Cheng, J. Xin, W. Lin, W. Hu, M. Wan, Y. Li, and H. Wu, "Research on single-phase to ground fault simulation base on a new type neutral point flexible grounding mode," *IEEE Access*, vol. 7, pp. 82 563–82 570, 2019.

[110] N. Smotrov, A. Okhlopkov, and V. Bitney, "Analysis of overvoltage processes under single-phase-to-earth fault conditions in tpp 6-10 kv switchgear," in *2022 4th International Youth Conference on Radio Electronics, Electrical and Power Engineering (REEPE)*, 2022, pp. 1–6.

[111] "IEEE guide for the application of neutral grounding in electrical utility systems–part iv: Distribution," *IEEE Std C62.92.4-2014 (Revision of IEEE Std C62.92.4-1991)*, pp. 1–44, 2015.

[112] J. Mohammadi, F. Badrkhani Ajaei, and G. Stevens, "Grounding the dc microgrid," *IEEE Transactions on Industry Applications*, vol. 55, no. 5, pp. 4490–4499, 2019.

[113] L. Chen, J. Zhao, R. Liu, F. Velez-Cedeno, H. Liu, and Y. Liu, "Distributed energy resource overvoltage during un-intentional islanding," in *2019 IEEE Industry Applications Society Annual Meeting*, 2019, pp. 1–6.

[114] Y. Zhou, X. Zhao, X. Cui, R. Yang, and J. Lai, "Transient analysis and simulation of a single-phase grounding fault in 20kv small resistance grounding system," in *2019 IEEE 3rd International Electrical and Energy Conference (CIEEC)*, 2019, pp. 1101–1105.

[115] N. El-Sherif and S. P. Kennedy, "A design guide to neutral grounding of industrial power systems: The pros and cons of various methods," *IEEE Industry Applications Magazine*, vol. 25, no. 1, pp. 25–36, 2019.

[116] "IEEE guide for protective relay applications to power system buses," *IEEE Std C37.234-2021 (Revision of IEEE Std C37.234-2009)*, pp. 1–144, 2022.

[117] S. A. Abdelrazek and S. Kamalasadan, "Integrated pv capacity firming and energy time shift battery energy storage management using energy-oriented optimization," *IEEE Transactions on Industry Applications*, vol. 52, no. 3, pp. 2607–2617, 2016.

[118] M. Ahmed, R. Bhattarai, S. J. Hossain, S. Abdelrazek, and S. Kamalasadan, "Coordinated voltage control strategy for voltage regulators and voltage source converters integrated distribution system," *PES GM Meeting, 2017 IEEE*, pp. 1–6, 2017.

[119] T. G. Paul, S. J. Hossain, S. Ghosh, P. Mandal, and S. Kamalasadan, "A quadratic programming based optimal power and battery dispatch for grid connected micro grid," *IEEE Transactions on Industry Applications*, vol. 53, no. 99, pp. 1–12, 2017.

[120] H.-E. H. Soloot, E. Agheb, A. H. Soloot, and S. Moghadam, "A swot analysis of two protection strategies due to the expansion of renewable distributed generation on distribution network," in *2020 15th International Conference on Protection and Automation of Power Systems (IPAPS)*, 2020, pp. 49–52.

[121] P. Mahat, Z. Chen, B. Bak-Jensen, and C. L. Bak, "A simple adaptive overcurrent protection of distribution systems with distributed generation," *IEEE Transactions on Smart Grid*, vol. 2, no. 3, pp. 428–437, Sep. 2011.

[122] S. M. Brahma and A. A. Girgis, "Development of adaptive protection scheme for distribution systems with high penetration of distributed generation," in *2003 IEEE Power Engineering Society General Meeting (IEEE Cat. No.03CH37491)*, vol. 4, July 2003, pp. 2083–2083.

[123] T. Sun, H. Liu, X. Ling, Q. Tu, C. Chao, and X. Zheng, "Adaptability analysis of directional overcurrent protection in the distribution network with photovoltaic," in *2021 6th International Conference on Power and Renewable Energy (ICPRE)*, 2021, pp. 1079–1083.

[124] I. Kiaei, S. Lotfifard, and M. Ghanaatian, "Current-only directional overcurrent protection using postfault current," in *2019 IEEE Texas Power and Energy Conference (TPEC)*, 2019, pp. 1–5.

[125] M. Bello and A. Maitra, "Lessons learned on protection coordination considerations within inverter-based microgrids," in *2018 IEEE PES/IAS PowerAfrica*, 2018, pp. 539–544.

[126] G. P. Bierals, *Overcurrent Protection - Questions.* River Publishers, 2021, pp. 85–96.

[127] L. Che, M. E. Khodayar, and M. Shahidehpour, "Adaptive protection system for microgrids: Protection practices of a functional microgrid system." *IEEE Electrification Magazine*, vol. 2, no. 1, pp. 66–80, March 2014.

[128] N. Kumar and D. K. Jain, "An adaptive inverse-time overcurrent protection method for low voltage microgrid," in *2020 IEEE 9th Power India International Conference (PIICON)*, 2020, pp. 1–5.

[129] P. Gupta, R. S. Bhatia, and D. K. Jain, "Adaptive protection schemes for the microgrid in a smart grid scenario: Technical challenges," in *2013 IEEE Innovative Smart Grid Technologies-Asia (ISGT Asia)*, Nov 2013, pp. 1–5.

[130] G. P. Bierals, *Overcurrent Protection NEC Article 240 and Beyond.* River Publishers, 2021, pp. i–x.

[131] "Ieee standard for the specification of microgrid controllers," *IEEE Std 2030.7-2017*, pp. 1–43, 2018.

[132] T. Patel, S. Brahma, J. Hernandez-Alvidrez, and M. J. Reno, "Adaptive protection scheme for a real-world microgrid with 100resources," in *2020 IEEE Kansas Power and Energy Conference (KPEC)*, 2020.

[133] E. Casagrande, W. L. Woon, H. H. Zeineldin, and D. Svetinovic, "A differential sequence component protection scheme for microgrids with inverter-based distributed generators," *IEEE Transactions on Smart Grid*, vol. 5, no. 1, pp. 29–37, 2014.

[134] B. Wang and L. Jing, "A protection method for inverter-based microgrid using current-only polarity comparison," *Journal of Modern Power Systems and Clean Energy*, vol. 8, no. 3, pp. 446–453, 2020.

[135] S. F. Zarei, H. Mokhtari, and F. Blaabjerg, "Fault detection and protection strategy for islanded inverter-based microgrids," *IEEE Journal of Emerging and Selected Topics in Power Electronics*, vol. 9, no. 1, pp. 472–484, 2021.

[136] M. E. Ropp and M. J. Reno, "Influence of inverter-based resources on microgrid protection: Part 2: Secondary networks and microgrid protection," *IEEE Power and Energy Magazine*, vol. 19, no. 3, pp. 47–57, 2021.

[137] A. Hooshyar and R. Iravani, "Microgrid protection," *Proceedings of the IEEE*, vol. 105, no. 7, pp. 1332–1353, 2017.

[138] "IEEE guide for protective relay applications to distribution lines," *IEEE Std C37.230-2007*, pp. 1–100, 2008.